A STUDY OF MECHANISMS FOR DISCOMFORT GLARE

Yingxin Jia

A thesis submitted

For the degree of

Doctor of Philosophy

City University London

School of Health Sciences

Division of Optometry and Visual Science

September 2014

Table of Contents

List of Figures and Tables

Acknowledgements

I would like to express my sincere gratitude to my supervisors, Prof. John L Barbur and Dr. Gary Bargary both from City University London, for their advice, support, patience and encouragement throughout my PhD study.

I would like to acknowledge that my PhD work is part of a large Engineering and Physical Sciences Research Council (EPSRC) (EPSRC Reference: EP/G044538/1) funded project. I am grateful for the financial support I received from the research council. My sincere thanks also go to Prof. Peter Raynham, Dr. Navaz Davoudian and Dr. Edward Barratt all from University College London for their collaboration and recruitment of participants.

I would also like to thank Mr. Alister Harlow for technical support during my experimental setting-up and programming. I also wish to thank all my colleagues for sharing the brilliant knowledge about vision science.

My families also receive my deepest love and gratitude for their dedication during my PhD study.

Declaration

This thesis has been completed solely by the PhD candidate, Yingxin Jia. The research work contained in the thesis was done by the candidate, unless otherwise stated. It has not been submitted for any other degrees. All sources of information have been acknowledged and references have been provided.

The University librarian of City University London has the powers of discretion to allow the thesis to be copied in whole or in part without further reference to the author. This permission is subject to normal conditions of acknowledgement and only for study purposes.

Abstract

The presence of a bright light source in the visual field, particularly when viewed against a dark background, can generate a form of discomfort, which is often described as 'discomfort glare'. The mechanisms for discomfort glare remain poorly understood, even after 50 years of multidisciplinary research in this field. The aim of this investigation was to investigate a number of relevant parameters that can affect discomfort glare in order to gain insights into the corresponding mechanisms. We measured retinal illuminance levels for discomfort glare at threshold as a function of source size, eccentricity and surrounding background luminance. In addition, the pupil size was measured throughout and related to the measured thresholds for discomfort glare.

A group of 50 subjects with normal visual acuity and no clinical signs of eye disease took part in the primary study that measured discomfort glare thresholds as a function of source size. A light 'homogenizer' was used to integrate the concentrated light output from a quad LED light source. Pulse frequency modulation was used to control the intensity of the source and continuous pupil size measurements made it possible to calculate retinal illuminance. Discomfort glare thresholds were estimated by measuring the retinal illuminance of the glare source at threshold using a staircase procedure.

Discomfort glare thresholds were measured as a function of glare source area, eccentricity and background luminance. The amplitude of pupil constriction was also measured both below and above the discomfort glare threshold. A model of contrast vision with the filtering of a photoreceptor signal through centre-surround ganglion cells was developed to account for the small size dependence of discomfort glare thresholds that was observed experimentally. Another model for scattered light was applied to compute the corresponding pupil constriction amplitude caused by the integrated photoreceptor signals generated by the glare source both within and outside the stimulus area.

The threshold for discomfort glare decreased gradually with glare source size and increased with background luminance and showed little dependence on glare source eccentricity. The effect of forward light scatter in the eye was also investigated and a model was developed to account for the continued increase in pupil response amplitude well above the discomfort glare threshold. The effect of glare source size on discomfort glare thresholds could be predicted by a model involving photoreceptor saturation and edge response. When the scattered light outside the stimulus area was also taken into account, the pupil constriction amplitude increased log-linearly with stimulus retinal illuminance both below and above discomfort glare thresholds. These findings suggest that discomfort glare depended largely on the localised retinal illuminance and could be accounted for by the saturation of photoreceptor signals in the retina. The results and the pupil modeling work also suggest that the pupil response to light flux increments continued well above the discomfort glare threshold, largely as a result of light scattered outside the area of the glare source.

List of Abbreviations

2AFC	Two-Alternative Forced Choice
CAA	Contrast Acuity Assessment
DG	Discomfort Glare
fMRI	Functional Magnetic Resonance Imaging
ipRGCs	Intrinsically Photosensitive Retinal Ganglion Cells
LGN	Lateral Geniculate Nucleus
L-cones	Long Wavelength Sensitive Cones
M-cones	Medium Wavelength Sensitive Cones
mm	Millimeter
ms	Millisecond
PLR	Pupil Light Reflex
S-cones	Short Wavelength Sensitive Cones

1 Introduction

When one views a light source, such as a car headlamp or a residential streetlight, one may experience a feeling of visual discomfort, particularly when the luminance of the light source is appreciably greater than the adapted background luminance. This is known as 'discomfort glare'. A number of explanations to account for discomfort glare have been proposed, but the mechanisms for discomfort glare remain poorly understood (Wordenweber et al., 2010, Mainster and Turner, 2012). The lighting industry, in an attempt to minimize glare, has promoted the development of a number of metrics to quantify discomfort glare (Binder, 2003, Vos, 1999). In spite of such efforts, the progress has been slow and often hindered by the lack of consistent definitions of what one means by discomfort glare and clear-cut experimental findings.

1.1 Human visual system

In order to examine the properties of the mechanisms that cause discomfort glare, it is useful to review some of the stages involved in phototransduction and the processing of retinal signals. The first stage of visual processing involves image formation in the eye followed by extraction of information carried as spatial modulations of intensity and/or spectral contents in the retinal image (Palmer, 1999). The eye, like a pinhole camera, captures object space information that is then converted to electrical signals by the photoreceptors in the eye. This information is then transmitted to the primary visual cortex via the optic nerve. The visual cortex is located at the back of the brain, as shown in Figure 1-1. Despite of the existence of auditory

cortex and other cortices, it is estimated that more than 50% of cortex in the macaque monkey is involved in processing visual information (DeYoe and Van Essen, 1988). This is similar to human cortex, although the percentage of visual cortex is slightly lower.

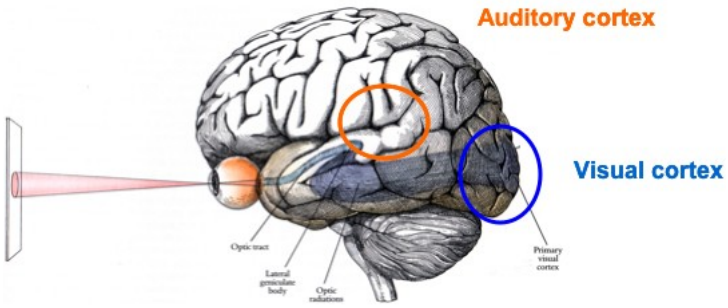

Figure 1-1 The human visual system. Both eye and brain play an important role in processing visual information. It begins in the eyes, and then goes from the lateral geniculate nucleus (LGN) to cortex via the optic radiations (Saenz, 2007).

Damage to the eyes or the visual cortex can cause loss of conscious vision, but the subjects can still make use of visual signals via subcortical pathways. Residual visual responses in the absence of conscious vision are often labeled as 'blindsight' (Cowey and Stoerig, 1995).

1.1.1 The human eye

The visual system begins with the eye which functions like a camera. The optics of the eye are shown in Figure 1-2. The light captured by the eye passes through the cornea and is limited by the size of the iris before it passes through the lens, a transparent structure, whose shape is manipulated by ciliary body. The light then travels through the vitreous humour and finally ends up on the retina to form an inverted image of the visual world. The retina is a complex structure that will be discussed in detail in Section 1.1.2. The photoreceptors are densely packed in the retina and convert light

into electrical signals. The signals generated are then transmitted to the striate cortex via the optic nerve with some fibres projecting to midbrain nuclei.

The total amount of light entering the eye depends on size of the pupil (i.e., the image of the iris as seen through the cornea). If the light level is low, the pupil tends to be large. In contrast, the pupil will constrict at higher levels of ambient illumination. Other factors also affect the size of pupil, thus having an influence on the amount of light entering the eye. For instance, mental efforts that result in focused attention also cause the dilation of pupil (Hahnemann and Beatty, 1967). An increase in pupil size is observed when people pay particular attention to objects of interest.

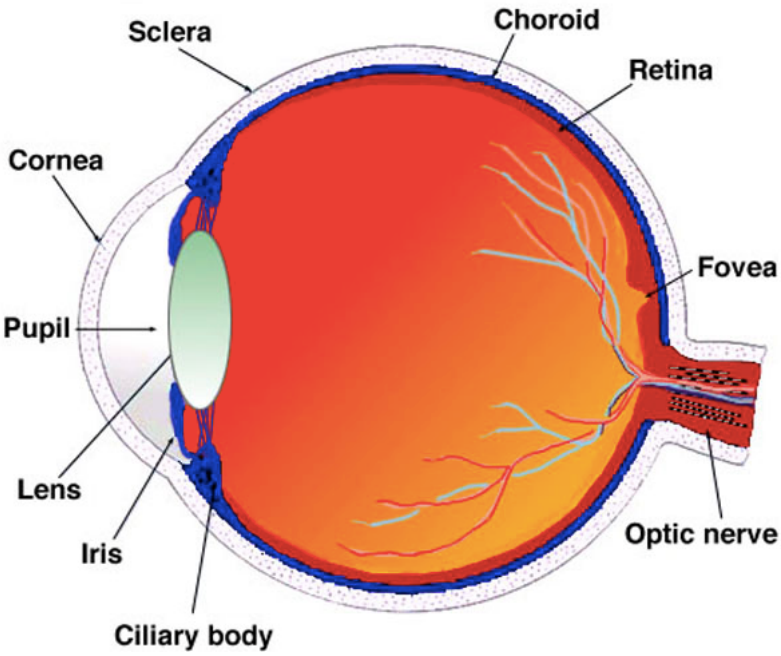

Figure 1-2 Cross section of the human eye (Kolb).

As illustrated in Figure 1-2, the human eye can be described as consisting of two regions. The front portion of the eye is known as the anterior chamber, while the rear portion is called the posterior chamber.

The structures contained in the anterior chamber include:

Cornea: Transparent layer that forms the front of the eye

Iris: A structure containing the back surface full of heavy pigmentation that greatly limits light passing through with the exception of the pupil

Pupil: A variably sized opening in the opaque iris

Sclera: The white outer coating of the eye, continuous with the cornea

The structures contained in the posterior chamber include:

Lens: Gradient index lens that can change shape to alter focus

Ciliary body: Tissue that connects the iris to the choroid and controls the shape of lens

Choroid: Tough layer with the pigmented vessels between the retina and the sclera

Retina: Photosensitive inner lining of the eye consisting of photoreceptors and neural layers

Fovea: Central region of retina with sharpest vision

Optic Nerve: Bundle of nerve fibres that carry information to the brain

1.1.2 Retina

In order to process the collected optical information, one of the most critical functions in the human visual system is the conversion of the light energy into electrical signals. The light flux captured by the eye is first converted to

electrical signals that are then processed and coded into a form suitable for transmission along the optic nerve. It is the photoreceptors in the retina that respond to light and transform light energy into electrical signals. There are several typical neurons in the retina, such as horizontal, bipolar, amacrine and ganglion cells (see Figure 1-3). Photoreceptors synapse on bipolar cells that feed into ganglion cells. The long axons of the ganglion cells leave the eye and synapse in the LGN (see Figure 1-1). This arrangement is called feedforward and reflects the nature of retinal organization. Besides the feedforward nature, there are also lateral interconnections that produce the horizontal transmission of retinal information. Some of this lateral transmission is thought to be pre-ganglion cells including horizontal and amacrine cells, as illustrated in Figure 1-3. In addition to the feedforward and lateral transmission of information, another one is feedback transmission. In this pathway, retinal information is transmitted from the ganglion cells back towards the photoreceptors (Linberg and Fisher, 1986).

Some of the light that travels through the pupil is absorbed by intraocular structures including lens, vitreous humour and blood vessels. Remaining light that passes photoreceptors is absorbed by the retinal pigment epithelium, minimizing intraretinal scatter. However, most of the light is absorbed by the photoreceptors in the retina. The photoreceptors contain a kind of protein called opsin that plays an important part in converting the energy of absorbed photons into electrical signals. It is worth noting that the incident light travels from the inner side to the outer retina whereas the electrical signals travel in the opposite direction. That means the light hits

the ganglion cells first and then travels towards the outer segments of the photoreceptors.

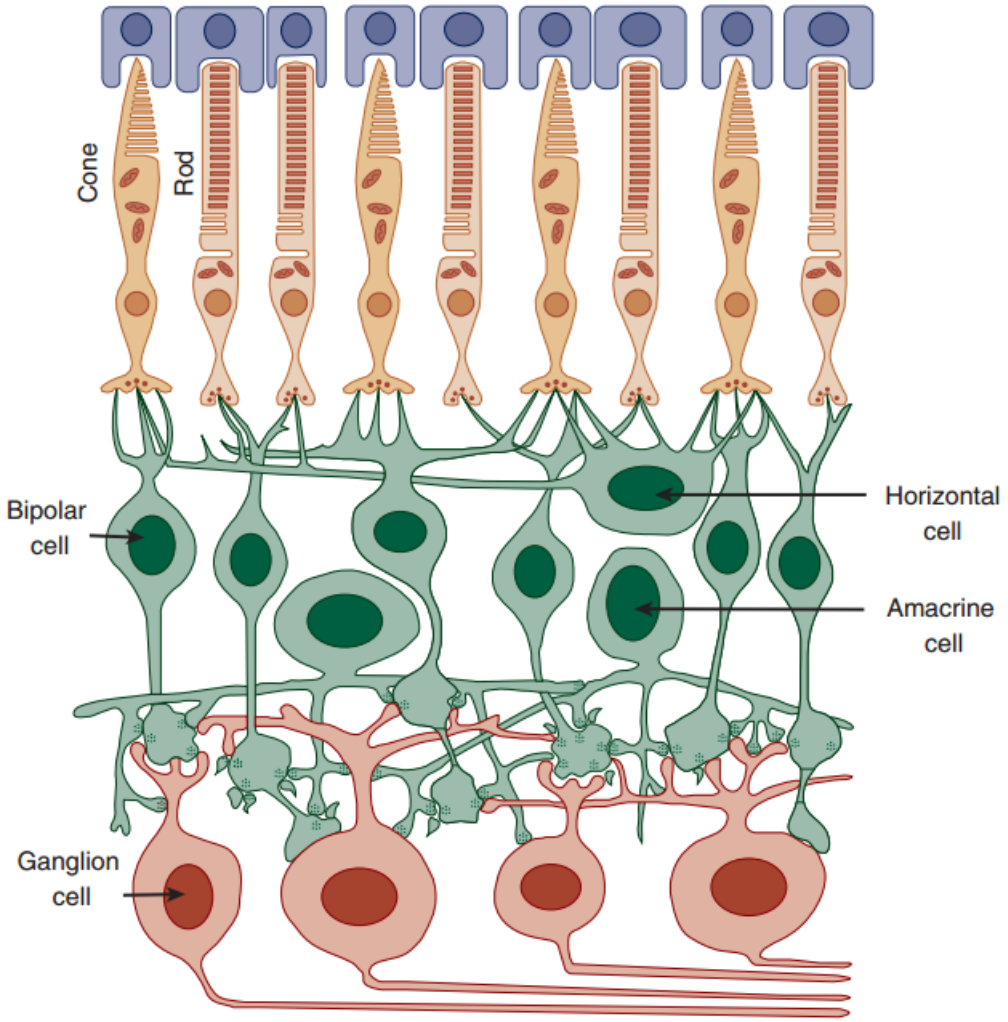

Figure 1-3 Human retina organization (Schwartz, 2010).

Cones and rods are two kinds of photoreceptor cells in the retina. There are about 6 million cones, most of which concentrated in the centre of the retina (fovea), shown in Figure 1-4 (Osterberg, 1935). Cones are not as sensitive to light as rods, but in general can generate faster responses to light. Cones produce rapid biphasic photocurrent responses with short onset latency and significant undershoot (Schnapf et al., 1987). In contrast, rods are more numerous (120 million in the human eye), but are absent at the fovea (see

Figure 1-4). Rods are extremely light sensitive, but have slow responses to light and exhibit very large spatial summation. Isolated rod photoreceptor signals increase in amplitude and exhibit shorter latencies with increasing flash intensities. The blind spot region does not contain photoreceptors and is located approximately 18 degrees in the nasal retina.

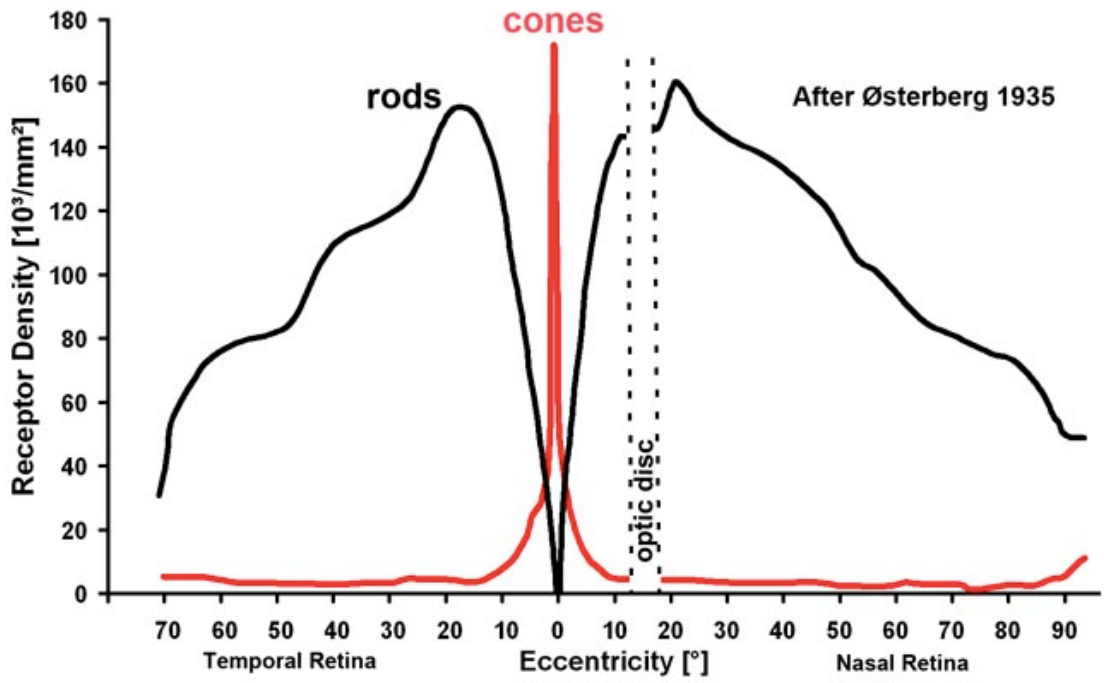

Figure 1-4 Densities of rods and cones in the retina (Osterberg, 1935).

If we pay more attention to the cones and rods, it can be seen that there are four primary functional layers: outer segment, inner segment, external limiting membrane and outer nuclear layer, as shown in Figure 1-5. The visual pigments are carried in the layer of outer segments in the form of the stack of membrane discs. The light is converted into electrochemical energy by those visual pigments. This process is known as visual phototransduction. A number of studies have focused on phototransduction in rods (Baylor et al., 1984) since they are extremely sensitive to the light in comparison with

cones. When a rhodopsin molecule absorbs a photon of light, the molecule changes its shape, thus altering the flow of electric current. These electrical changes are produced in the outer membrane of the photoreceptor and are then propagated to its next neuron in order to enable the transmission of electrical signals.

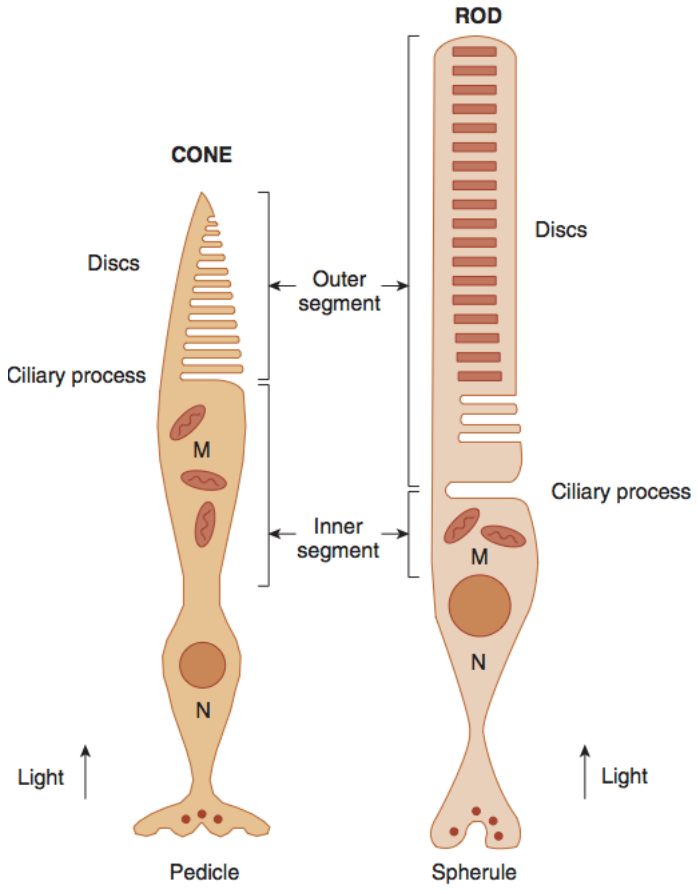

Figure 1-5 Schematic graph of a cone and a rod. Nucleus is designated by 'N' and is located in the outer nuclear layer (Schwartz, 2010).

Retinal ganglion cells are of great interest to the study of glare. As described, a ganglion cell is a type of neuron located near the inner surface of the retina. It receives electrical signals from photoreceptors via other intermediate neurons, and then transmits visual information from the retina to the regions

in midbrain. There are about 1.2 to 1.5 million ganglion cells in the human retina. On average, each ganglion cell receives inputs from about 100 cones and rods since the number of cone and rod photoreceptors is about 125 million. However, the distribution of retinal ganglion cells is uneven. In the fovea, a single ganglion cell will receive information from about 5 photoreceptors, while in the periphery, a single ganglion cell will communicate with many thousands of photoreceptors (Curcio and Allen, 1990).

1.1.2.1 Photoreceptor adaptation

Besides the simple response to light, photoreceptors can also adapt to the surrounding light level so as to extend the operating range.

When light is imaged on the retina, the eye adapts to the current light level, and this is often described as adaptation. In general, visual 'adaptation' is used to describe both adjustment to higher light levels after exposure to a dimmer light level, as well as adjustment to lower light levels after exposure to a brighter light level.

The most powerful feat of adaption of visual system is that the human eye can adapt to a vast range of illumination levels (Barbur and Stockman, 2010). The full range of light levels over which vision is possible is shown in Figure 1-6 and extends from 10^{-6} to about 10^{4} cd/m^2. Although the light detection still exists when the light level is above 10^{4} cd/m^2, glare effects and after-images can significantly impair visual performance (Schreuder, 2008). When the light level is reduced to 10^{3} cd/m^2, visual performance improves with excellent vision down to 3 cd/m^2. When the background luminance level

continues to fall down to about 1 cd/m^2, such as candlelight, it makes the reading difficult. At -3 log cd/m^2 one can only detect very low spatial frequencies at high contrast whilst at -5 log cd/m^2 the detection of light becomes a challenge. That ability of human visual system to operate over a large range of adapting light levels is known as adaptation, mediated by photoreceptors in the retina.

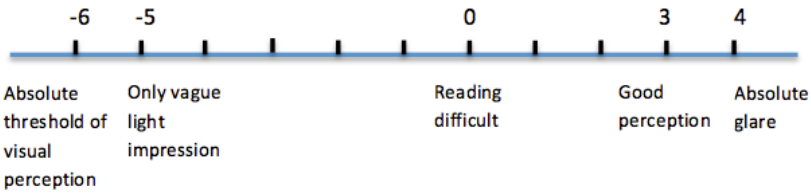

Figure 1-6 Adapted background luminance levels in log cd/m^2.

As mentioned, dark adaptation is the improvement in vision after exposure to a bright-adapting light, because rods and cones start to recover sensitivity when dark adaptation begins. However, it is worth noting that rod adaptation and cone adaptation have different time courses, which is illustrated in Figure 1-7.

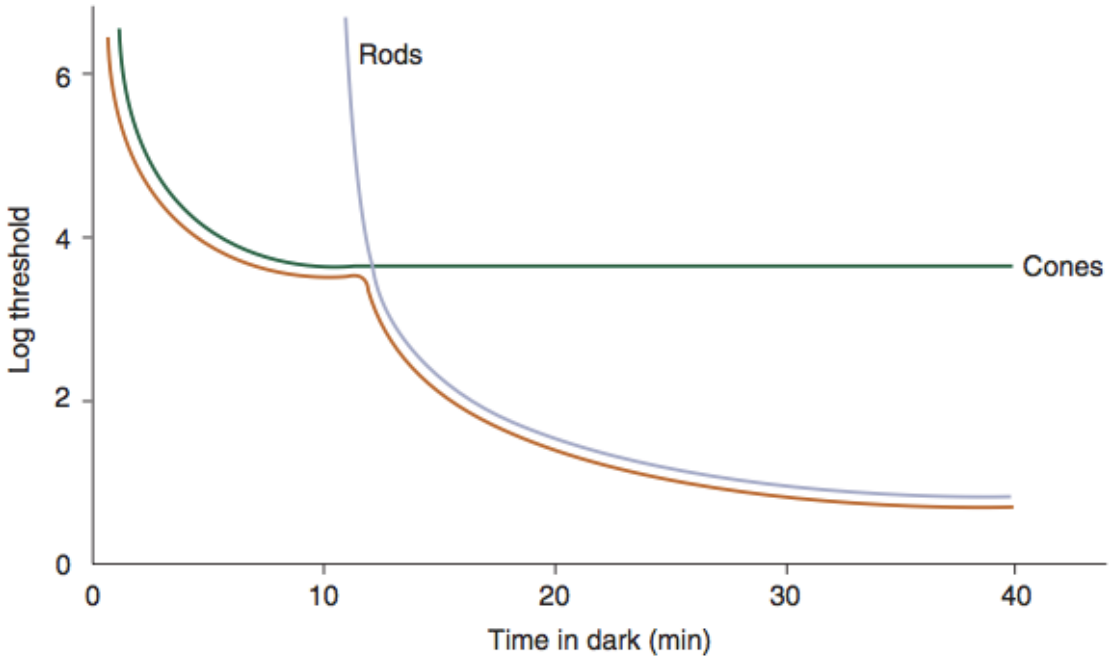

Figure 1-7 Absolute thresholds for both rods and cones over the duration of dark adaptation (Schwartz, 2010).

Figure 1-7 depicts an idealised dark adaptation curve that can be measured experimentally in the following way. The subject is adapted to a bright light level. The adapting light is then turned off and measurements of absolute detection thresholds are then made in a number of experimental ways throughout the recovery period. The bright-adapting light in the very beginning is usually intense to ensure that most of the visual pigments are bleached. The absolute threshold measured in dark adaptation is the dimmest light that can be detected after exposure to the bright light. For a period of time, the threshold decreases, which means the lowest possible retinal illuminance needed to detect light is reduced. Therefore, the photoreceptor becomes increasingly sensitive to that stimulus light until adaptation is complete after about 40 minutes in the dark.

Part of the basic mechanisms responsible for controlling dark adaptation is the switchover between rods and cones. It is noticed that the threshold for cones decreases dramatically within the first 5 minutes and then reaches a plateau. Cone adaptation is virtually complete at about 10 minutes when the rods begin to adapt. The rate of change in sensitivity as shown in Figure 1-7, suggests that the cones recover much faster than rods, but the latter are more sensitive to light. As the photoreceptors adapt to darkness, most of the visual pigment in the photoreceptors is regenerated. The bleached pigments in the very beginning are transferred to unbleached ones by the action of enzymes generated in the pigment epithelium located behind the retina (Hollins and Alpern, 1973, Rushton, 1972).

The bleaching of rod pigment during light adaptation is an exponential curve that increases as function of duration (Binder, 2003). The rate of increment of the proportion of pigment in the bleached state slows down with time course. If the photoreceptors adapt to different adapting light intensities, the rate of pigment bleaching changes. In addition, more and more visual pigment is bleached as the adapting intensity is increased.

1.1.2.2 Photoreceptor responses

As described in the previous section, the photoreceptors can adapt so as to operate over a large range of light levels. However, the range of adaptation is limited since almost all pigments are bleached at a sufficiently high light level. It is generally accepted that the response of photoreceptors in the retina increases with the increasing intensity of a uniform flash of light. Naka and Rushton fitted an exponential saturation function to describe photoreceptor

saturation (Naka and Rushton, 1966). As described by Hood, Finkelstein and Buckingham (Hood et al., 1979), this function is denoted by:

$$\frac{R}{R_{max}} = \frac{I^n}{I^n + \sigma^n}$$

where R is the photoreceptor response amplitude triggered by a flash of light with intensity I and R_{max} is the maximum response. σ is the intensity of the flash that triggers the $\frac{1}{2}R_{max}$. This function is also called Michaelis-Menton equation. An example of retinal illuminance-response curve is shown in Figure 1-8. In this case, the half-maximal response is at 3.5 log Td and response range is about 3 log units.

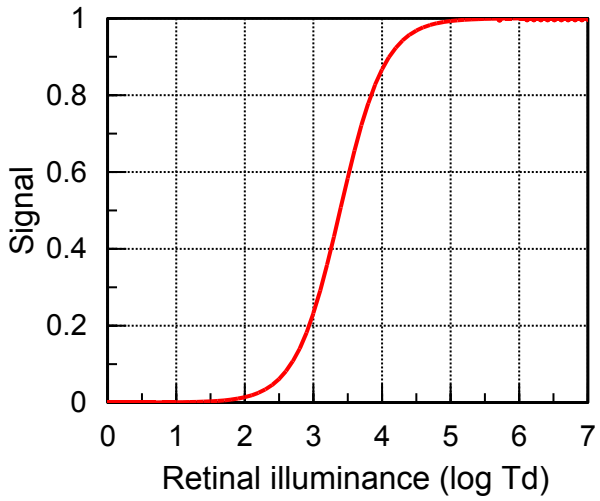

Figure 1-8 Retinal illuminance-response curve with half-maximal response at 3.5 log Td and a response range of 3 log units.

It can be seen from the retinal illuminance-response curve, photoreceptors saturate beyond a certain light level. This has also been illustrated in Figure 1-8 and Figure 1-9. The photoreceptor signals increase with the increasing flash intensity until saturation occurs.

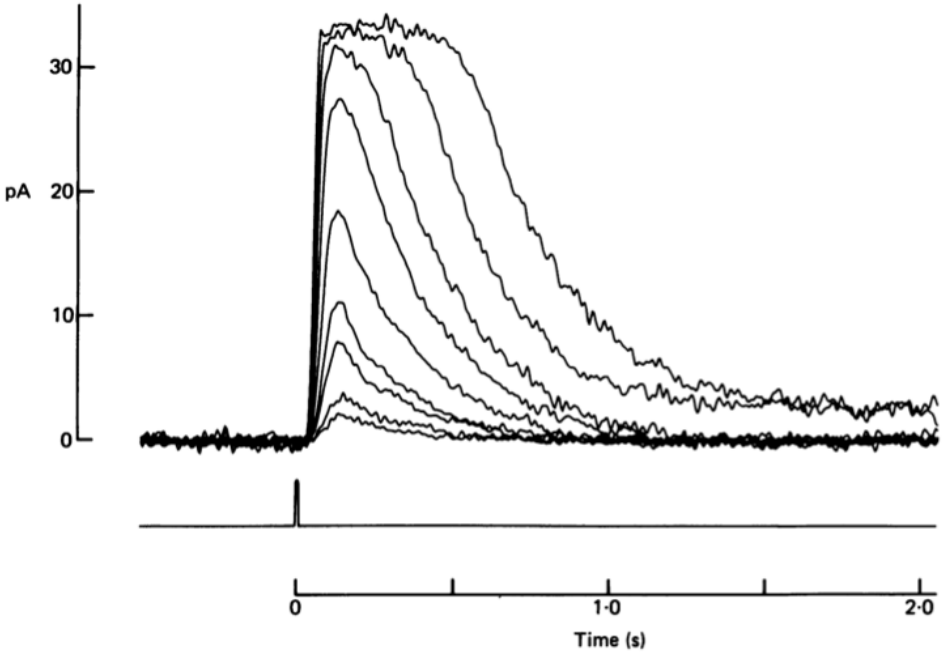

Figure 1-9 Rods respond to various flash stimuli with varying intensities. This plot shows the membrane current of the outer segment in pA against the level in darkness. (Baylor et al., 1984).

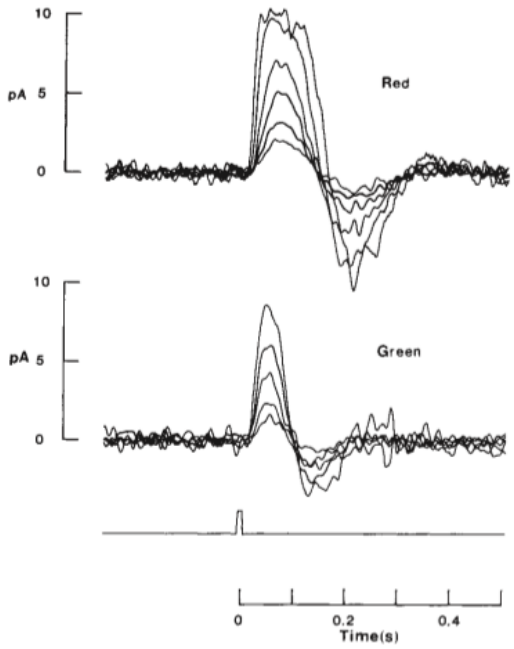

Figure 1-10 L-Cones (Top) and M-Cones (Bottom) respond to flash stimuli with different intensity strength (Schnapf et al., 1987).

When the photoreceptors are triggered by a flash stimulus, the flash stimulus evokes a reduction in the influx of sodium ions into the outer segment of rods

caused by the corresponded channel closure, which results in the membrane hyperpolarisation. The inward current of sodium ions becomes less and less as the flash intensity becomes greater, which leads to the increase of membrane potential, i.e. the amplitude of hyperpolarisation (Binder, 2003). When the flash intensity is sufficiently high to suppress completely the steady inward current, peak response amplitude is achieved and the signal saturates.

1.1.3 Visual cortex

Areas in the visual cortex are responsible for processing the information received from the retina. Cerebral cortex consists of a number of surface areas which are folded into a small volume. When unfolded, the neurons in the cerebral cortex form a layered sheet. The reason why the cerebral cortex is convoluted and folded is to ensure efficient packing into the human skull. The size of human brain is the size of two fists. However, if the cerebral cortex were not folded the size of brain would be the size of a basketball. It is also worth noting that the cerebral cortex consists of two cerebral hemispheres which are similar to each other, but may differ in functional roles.

Visual cortex is located in the occipital lobe, one of the four lobes in the cerebral cortex, which is at the back of the brain. The primary visual cortex, also known as V1, is part of the occipital lobe. Neurons in the LGN pass the information to the primary visual cortex, where the first steps in cortical processing occur. On each hemisphere of the brain, there is one visual cortex. The visual input to the primary visual cortex is transmitted in a crossed way.

The left hemisphere visual cortex receives signals from the right visual field and the right visual cortex from the left visual field, shown in Figure 1-11.

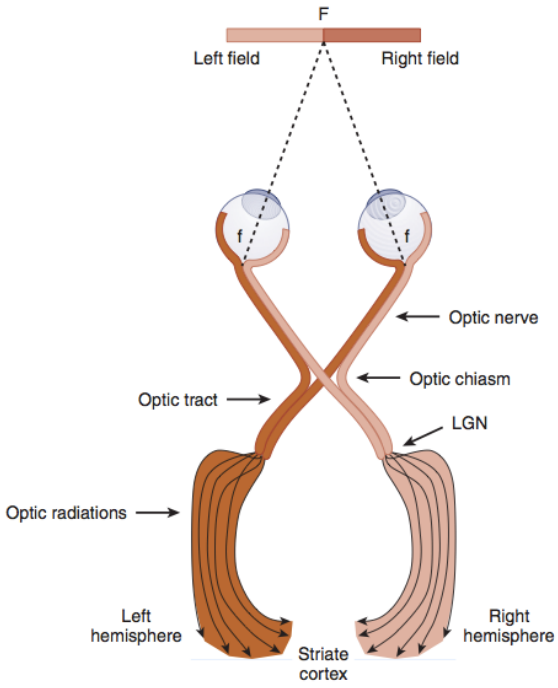

Figure 1-11 A typical visual pathway carries information from retina to the primary visual cortex. The visual information in the right visual field is processed in left hemisphere visual cortex, and the information involved in the left visual field is processed in right hemisphere (Schwartz, 2010).

1.2 The perception of glare in human vision

The word 'glare', in common use, describes the visual experience when very bright objects or sources of light are present in the visual field. In order to define this terminology more accurately, one needs to understand the mechanisms that account for glare. The word, glare, appearing in the scientific literature for the first time dated back to the early 20th century, when Sir Herbert Parsons addressed the conference for the newly founded Illuminating Engineering Society of London (Parsons, 1910). Thereupon, there was a stirring of interest in glare studies around the world. Holladay then proposed that the negative effects of glare could be attributed to

impairment of vision as a result of scatter light. Although scattered light may well contribute to the overall discomfort caused by glare sources, it does not account fully for the perceptual effects that are normally linked to the phenomenon of glare.

1.2.1 Attributes and classification of glare

In order to investigate glare, it is useful to distinguish two separate categories (Rea, 2000, Stiles, 1929b). Discomfort glare (which is the principal topic of this thesis), the glare that causes annoyance, distraction and discomfort, also known as psychological glare cannot be accounted for entirely in terms of scattered light (Luckiesh and Holladay, 1925). The second one is disability glare, also known as physiological glare, which is the glare that impairs human vision by reducing the contrast of the retinal image, primarily through the role of scattered light (Stiles, 1929c, van den Berg et al., 2013, Vos, 2003a). It was Stiles who first distinguished discomfort glare from disability glare (Stiles, 1929b). Disability glare is a light scatter effect and of great importance in terms of affecting the contrast of the retinal image (Holladay, 1926, Stiles, 1929a), whereas discomfort glare cannot be solely attributed to light scatter. By its nature disability glare has been more straightforward to define and study (Vos, 2003b), whereas discomfort glare has proved to be more elusive in both definition and study (Mainster and Turner, 2012).

Disability glare is the effect of straylight on the eye (van den Berg et al., 2010). In elucidating the underlying mechanisms, the study of disability glare has been more straightforward. It is generally accepted that one of the

mechanisms for disability glare is the intraocular forward scatter that acts as a veiling luminance, lowering the contrast of the retinal image (Vos, 2003a) and thus reducing visual performance (De Waard et al., 1992, Fisher and Christie, 1965). When a person looks at a glare source, some of the light will be scattered by the optics of the eye, but excessive, localised amounts of light will remain at the location of the glare source. As a result of scattered light in the eye, the contrast of the retinal image is reduced, even in the absence of any external glare sources. When the external glaring source exists, people can get either disability glare or discomfort glare or both in their eyes.

The luminance of a light source needs to be significantly larger than the surrounding background in order to cause discomfort glare. When the source is sufficiently bright to cause discomfort glare, the subject responds pre-attentively by saccading away from the glare source. Unlike disability glare, even after 50 years of multidisciplinary research very little is understood about the mechanisms or physiological underpinnings of discomfort glare (Mainster and Turner, 2012). In this study the threshold for discomfort glare will be measured to investigate the mechanisms underlying discomfort glare. The threshold for discomfort glare varies somewhat from one individual to another and this may reflect the relative input of a number of factors that contribute to discomfort glare (Mainster and Turner, 2012). Discomfort glare is common in daily life. It could be the unfavourable headlamp or streetlight for the drivers and pedestrians in the street illumination. It could also be the adverse light for office workers in the working environments.

Other labels such as ‘dazzling glare’ and ‘scotomatic glare’ have also been introduced (Mainster and Turner, 2012). The dazzling glare is the glare that produces squinting, aversion and visual disability, while the scotomatic glare is the one that raises the afterimages and visual disability. Both the dazzling and scotomatic glare can be recognised as special forms of discomfort glare since both can cause physical discomfort. Dazzling glare, as an extreme form of discomfort glare, occurs in the situations where the higher light level is perceived by comparison with normal discomfort glare, causing both the physical discomfort and visual disability. The scotomatic glare occurs when the highest retinal illuminance is spread over the retina, causing the excruciating unbearable discomfort.

1.2.2 Contributing variables relevant to discomfort glare

Previous studies on discomfort glare have focused mostly on the impact that different properties of the glare source may have on particular aspects of discomfort. The effect of glare source luminance (Hopkinson, 1957, Luckiesh and Holladay, 1925), angular subtense (Luckiesh and Guth, 1949), eccentricity from line of sight (Clear, 2013, Holladay, 1926, Holladay, 1927, Luckiesh and Guth, 1946), arrangement of the glare source/sources and illuminance level at the observers’ eye have all been investigated (Rubiño et al., 1994, Bullough et al., 2008, Guth and McNelis, 1961). Background adaptation luminance has also been investigated and found to be a contributing factor to discomfort glare (Clear, 2013). In brief, the relative importance of these factors can be summarised as follows:

- The luminance of the glare source is one of the most significant factors that affects the level of discomfort the subject reports. The visual sensation of glare is greater with light sources of very high luminance.
- The size of glare sources also plays some role in affecting discomfort glare. In general, for fixed background luminances, the sensation of glare increases with source size (Vos, 2003b). The study by Vos also shows that for the same light source intensity, subjects feel more comfortable with extended light sources, rather than with concentrated sources.
- In addition, the position of glare sources in the visual field is another factor that affects discomfort glare. Findings from earlier studies (Guth, 1961) suggest that the sensation of discomfort is reduced as the angle from the line of sight to the glare source becomes larger.
- The spatial arrangement of multiple glare sources can also affect discomfort glare (Rubiño et al., 1994). If the glare sources are arranged longitudinally with regard to the line of vision, less glare can be caused in comparison to that arranged transversely.
- With regard to the adaptation luminance, it was found that the amount of discomfort glare one perceived could be reduced when the background luminance level was higher. This may explain why drivers suffer from less discomfort in daytime while they may report much more discomfort glare at night, even when the same light sources are involved.
- Other factors which can also influence the sensitivity to discomfort glare include the macular pigment optical density (Stringham et al.,

2011). The findings from this study suggest that an increase in macular pigment density can reduce visual discomfort, as well as photostress and visual disability.

In summary, the principal parameters that can affect discomfort glare are the luminance of the light source, its size and eccentricity and the background light adaptation level (Theeuwes et al., 2002)

1.2.3 Pupil responses to discomfort glare

The investigation of pupil responses to discomfort glare is of great interest since the pupil activity might be a candidate for the physiological origin of discomfort. When the eye is exposed to a bright light source and a low luminance background simultaneously, the pupil responds to ambiguous signals that may involve different pathways. Hopkinson claimed that it is not the change in pupil size that determines the sensation of discomfort glare, but the opposing actions of the dilator and sphincter muscles (Hopkinson, 1956). Furthermore, Fry and King found that under discomfort glare conditions the pupil becomes significantly unstable. Therefore, they speculated that it might be the involuntary pupillary fluctuation under steady lighting conditions that affects the origin of discomfort glare (Fry and King, 1975). The dynamic characteristics of pupillary hippus (an involuntary spasm of the pupil) was further investigated by Howarth and his colleagues. The authors ruled out the role of the pupil by showing no differences in fluctuation of pupil size with and without glare (Howarth et al., 1993). They concluded that the pupillary hippus is unlikely to contribute significantly to discomfort glare.

1.2.4 Brain activity linked to discomfort glare

In addition to pupil/retinal mechanisms that may be involved in discomfort glare, one cannot rule out the involvement of higher level mechanisms in extrastriate regions of the visual cortex. The primary function of these areas is to extract and process the useful information from the retinal image and to enable perceptual processes. Therefore, the perception of discomfort glare cannot be separated completely from activity in higher visual areas of the brain. It has therefore become of great interest to establish whether the presence of discomfort glare causes selective activation of cortical areas (Raynham et al., 2007).

Functional magnetic resonance imaging (fMRI) is a widely used neuroimaging procedure both in research and clinical areas. Through the detection of change in blood flow, the mapping of active brain areas can be achieved, and this provides a measure of cortical specialisation. The oxygenated blood is more likely to flow to the brain area that is responding to a sensory input (Roy and Sherrington, 1890). In an fMRI study, the area of brain activity is normally located by examining the difference between two brain images collected in the presence and absence of the stimulus. The inspected difference is in terms of blood-oxygenation-level-dependent (BOLD) contrast (Ogawa et al., 1990), which has been widely used. Some studies have investigated the effect of the luminance of the presented stimulus in comparison with the background luminance on BOLD fMRI response (Goodyear and Menon, 1998). The result showed that within the visual cortex

BOLD signal activation levels increased with increasing stimulus luminance contrast.

1.2.5 Subjective and objective measurements of discomfort glare

In order to investigate the mechanisms for discomfort glare, several measurements have been proposed. Some of these tests rely on the measurement of perceived glare using visual psychophysical techniques whilst others rely on the measurement of some parameters (such as blink rate) that is thought to correlate with the level of discomfort glare.

1.2.5.1 Borderline between comfort and discomfort

Early investigations into discomfort glare focused on the borderline between comfort and discomfort (BCD). BCD is a single, subjective label that provides a method to assess the threshold by asking the subjects to adjust the intensity of a glare source to the borderline between comfort and discomfort (Guth, 1951, Guth, 1952). Through this method of adjustment, the discomfort level was obtained and the relationships between the source brightness and the properties of glare source were found. However, this measurement failed to take into account the multifaceted and progressive nature of discomfort glare. Some potential problems exist with the use of BCD measurement. The most important is the large inter-subject and within subject variability since there is no clear definition of what the subject has to look for and this leads to large differences in criteria. In order to improve on the assessment of discomfort from a glare stimulus, de Boer employed a multi-label scale system that is known as de Boer glare rating system.

1.2.5.2 De Boer glare scale

The current state-of-the-art assessment for discomfort glare is the de Boer glare rating scale that was proposed by de Boer in 1967. Measures of discomfort are typically obtained using the de Boer scale(De Boer, 1967), a rating system on a 9-point scale. Albeit this subjective rating scale was found less effective (Gellatly and Weintraub, 1990), this is a significant reference when appraising discomfort glare. With de Boer glare rating scale, the discomfort glare is assessed using a multi-label scale including 9 numbered points with 5 different verbal descriptors. The de Boer glare rating system is numbered in the way that the smallest numerical value represents the most amount of discomfort perceived and the largest numerical value indicates the least amount of discomfort perceived by the subjects (see Table 1-1). In 1973, de Boer changed the last verbal descriptor from 'Unnoticeable' to 'Just Noticeable' to improve the effectiveness of his multi-label scale system. With the wide use of de Boer glare rating system, many other versions have followed based on the version of 1967 by changing the verbal descriptors somewhat. The cross-study comparisons of these different rating scale versions (Gellatly and Weintraub, 1990) witnessed some noise in the results because of the versatility of the understanding of the verbal descriptive words, which means there is still space to improve the effectiveness of the de Boer glare rating scale system.

1)	Unbearable
2)	
3)	Disturbing
4)	
5)	Just Admissible
6)	
7)	Satisfactory
8)	
9)	~~Unnoticeable~~ → Just Noticeable

Table 1-1 de Boer glare scale.

1.2.5.3 Glare index systems

The majority of the studies on discomfort glare have been concerned with road lighting or interior lighting, and they have led to the introduction by the CIE of a number of glare-index metrics, which attempt to quantify the level of discomfort for a given lighting installation (CIE, 1983, CIE, 1994). The metrics involve a weighting between glare source luminance, glare source size and surrounding or background luminance.

The research interests in glare in different countries have been divided into varying glare evaluation systems, which are based on the original work of Stiles and Holladay. In the UK, Hopkinson and Petherbridge in the 1950s developed the British Glare Index system which was based on Stiles' work on

glare in the late 1920s. In America, Holladay's work on glare provided the foundation for Guth's studies of discomfort glare in the 1950s, and subsequently Guth proposed the Visual Comfort Probability in 1971 which was adopted officially in America.

Besides the British and American glare researchers, researchers from other countries also made contributions to evaluation models of discomfort glare. German researcher, Sollner, put forward the German Glare Limiting system in the 1960s. Australian and South African systems (Einhorn, 1969) also emerged during that period.

A number of features of existing glare systems were combined into a simple method to evaluate discomfort glare by CIE. Therefore, the CIE Glare Index was proposed by Einhorn (Einhorn, 1979).

Note that all the above mentioned glare index systems reveal empirical relationships between the subjective evaluation of discomfort glare sensation by an average observer and various factors in the lighted environment. The predictions of the subsequent models show large differences and poor agreement with measured experimental data (Clear, 2013). The proposed models may therefore not capture sufficiently well the properties of the mechanisms involved in discomfort glare.

1.2.5.4 Facial muscle EMG activity

It is well known that an obvious reflex in the facial muscles around the eye can often accompany discomfort glare. Those facial muscles generate the electrical activity labeled as the EMG (electromyogram). The observation of

EMG activity has been widely used in many fields of ergonomics. It can be employed in visual perception of discomfort glare as well. EMG activity of facial muscles surrounding the eyes could be an objective measure of discomfort glare sensation (Berman et al., 1994). EMG recordings from a subject were obtained in a measurement session and a glare stimulus was introduced halfway through the recording session which triggered an increase in EMG amplitude. In general the amplitudes of the EMG signals increased in the presence of a discomfort glare source.

Although the facial muscle activity is not the origin of discomfort, the study showed that EMG signals can be used to provide an objective measure of response to discomfort glare.

Another objective measure of discomfort glare using EMG was introduced by Murray *et al* (Murray et al., 2002). They developed a portable device for measuring the generated muscular activity of the contraction muscles around the ocular orbit. That muscle spasm was activated by the exposure to a glare stimulus. These findings suggest that the measured signal amplitude is directly proportional to the illuminance level at the eye. Therefore, the signal amplitude may be a candidate for an index of discomfort glare. In comparison with the subjective evaluation of discomfort glare, this objective assessment was found to be in a good agreement with the subjective rating system.

1.3 Mechanisms for discomfort glare

In order to find effective approaches to reduce the side effects of discomfort glare, some physiological underpinnings of discomfort glare have to be found and investigated. The few studies that investigated the physiological

mechanism for discomfort glare were mostly concerned with efferent displays of visual discomfort. For instance, some studies, as mentioned above, showed that it is pupil activity that plays a role in determining the physiological origin of discomfort (Fugate and Fry, 1956). Fry and King speculated that it might be related to the involuntary pupillary fluctuation under steady lighting conditions (Fry and King, 1975). However, in 1993 Howarth ruled out the role of pupil by showing no differences in fluctuation of pupil size with and without glare (Howarth et al., 1993). In addition, more recent studies confirm that the use of facial muscle activity can provide information on discomfort glare (see Section 1.2.5.4) (Berman et al., 1994). Although this measurement could be used as an objective test of discomfort glare, the specific origin is yet to be determined. Facial muscle activity may well relate to pain, rather than the visual discomfort. The efferent manifestations that can be observed under conditions of discomfort glare do not necessarily reflect the properties of the mechanism that cause discomfort glare.

Among a number of investigations into the association between pupillary function and discomfort glare response, some studies aimed to provide some test of this discomfort glare-pupillary function hypothesis by examining the spectral sensitivity of the pupil constriction in the presence of discomfort glare. The results showed that the spectral response to discomfort glare in terms of pupil constriction is more like the scotopic spectral sensitivity function V'(λ) with more pupil constriction in the blue part of the visible spectrum. This finding was used to suggest that rods play an important role

in relation to the discomfort glare response, even during daytime (Berman et al., 1996, Kooi, 2004). This may not however be the full story. Adrian (Adrian, 2003) reported that the greater spectral sensitivity of pupillary mechanism in the blue part is an artifact since the original study considering the spectral sensitivity of pupil constriction was limited to a two-degree field. He, therefore, compared the spectral sensitivity of a ten-degree field with that of a two-degree field. Rather than a rod input to pupil response, it is more likely that S-cones or even melanopsin may make a contribution to the pupil response (Kooi, 2004). In addition, another hypothesis might be the difference between luminance and brightness in the blue part of the spectrum. It was found that discomfort glare might be linked with brightness perception. Berman et al. suggested for lower light levels, less discomfort was produced in comparison with higher light levels under the condition of equal photopic luminance (Berman et al., 1996). Based on all these three hypotheses, Kooi made use of a laboratory filter set to distinguish between the different proposed hypotheses. He found that short-wavelength sensitive cone played a determinate role in revealing the discomfort glare mechanisms since the more S-cone stimulation was found to lead to greater visual discomfort (Kooi, 2004).

Some other studies showed that there is a long-standing paradox regarding the mechanism of discomfort glare. The studies suggest that there is a relationship between visual distraction and detectability of glare source (Lynes, 1977). But whether the glare and distraction share a common cause within the visual system is still not clear.

This critical review reveals our poor understanding of the mechanisms that mediate discomfort glare. Also, there is no consistency about the definition of discomfort glare and this makes measurements difficult. The purpose of this study was to describe less ambiguously the properties of discomfort glare and to produce a more accurate method of measuring discomfort glare thresholds. The aim was also to propose and describe mechanisms for discomfort glare.

1.4 Evaluations of discomfort glare

As described in Chapter 1.1, the human eye and brain form a complex system with regard to detection and processing of light. It can work effectively at a given level of light adaptation to process spatially structured patterns within the visual field. The human eye is adapted to a number of diverse lighting conditions, since it is capable of processing visual information over some ~ 9 log units change in ambient lighting (Lindsay and Norman, 1977). Nevertheless, the human visual system has limitations. Some lighting levels are associated with an adverse effect that results in visual discomfort. Such adverse phenomena include glare, which is often defined as a sensation caused by bright areas compared with the dimmer background area within the visual field. Two main kinds of glare are mentioned in Chapter 1.2: disability glare and discomfort glare. Of the two, discomfort glare is of greater interest, because it may trigger distraction, annoyance and irritation. Despite the extensive studies of both types of glare, mechanisms underlying disability glare have been described satisfactorily, whereas the mechanisms that mediate discomfort glare are less well understood.

Significant effort has been made to establish the evaluation of discomfort glare since the use of term 'glare' in scientific research. One of the empirical prediction systems established in North America is called the Visual Comfort Probability (VCP) system (Guth, 1963). A number of variables were considered to assess discomfort glare based on VCP system, including the sizes, luminances and numbers of glare sources, the position in the field of view and the background luminance which the observers were adapted to. The evaluation criterion used in this system is a threshold one, termed as borderline between comfort and discomfort (BCD) (Luckiesh and Guth, 1949), described in Section 1.2.5.1. The VCP system evaluates a lighting system and its surrounding environment in terms of the percentage of the observer populations who consider the observed lighting system as a comfortable one. If VCP is equal to or greater than 70, then the lighting system being evaluated is regarded as comfortable. Almost during the same period, the British Glare Index (BGI) system, another evaluation system, was established and developed in Britain (Hopkinson, 1963). The BGI system involved the same variables as those in the assessment of discomfort glare with the VCP system. The basic factors concerned in the empirical prediction systems are luminance of the glare source, luminance of the background, source size and source position, unless otherwise stated. These basic factors can be combined in one general formula to reveal the relationship between the sensation of glare and the concerned factors (Boyce, 2003). It is formulated as

$$G = \frac{L^m \times \omega^n}{{L_b}^x \times d^y}$$

where the L is the luminance of glare source, L_b is the luminance of background, ω is the angular substance of glare source at eye, d is the deviation of glare source from line of sight and G is the sensation of glare. Depending on different evaluation methods, the exponents m, n, x and y are somewhat different. A third prediction system was put forward by Sollner in Germany (Bodmann et al., 1966). It was originally called the Luminance Curve Method and also known as the European Glare Limiting Method. Although some modifications on this method have been taken, this evaluation system witnessed poor performance with current lighting technology.

It is worth noting that there are two prediction systems for the evaluation of discomfort glare that have been proposed by the CIE (International Commission on Illumination). One is CIE Glare Index (CGI) (CIE, 1983) and the other is Unified Glare Rating (UGR) (CIE, 1995). Due to the lack of a unified formula on the evaluation of glare across different countries and the advance of lighting technology, a general method for discomfort glare assessment was required. It was found that the VCP system proposed in North America and the BGI system proposed in Britain have common features. Therefore, in 1979 Einhorn (Einhorn, 1979) from South Africa incorporated the formulae from different countries to establish one combined mathematical prediction system, known as CGI. However, the CGI system is a little bit complicated and less practical. Due to the complication of CGI, UGR was developed and adopted by CIE in 1995. The UGR system incorporated the Guth position index (Luckiesh and Guth, 1949), Hopkinson formulae and some features in Einhorn's study. According to the UGR

formula, the discomfort glare increases with the luminance of the glare source and with decreased background luminance. Through the calculation, if UGR is less than 10, the glare is negligible, but if UGR is greater than 30, strong discomfort glare is perceived.

On the other hand, discomfort glare could also be measured and predicted to some extent with a number of objective methods. Those studies concentrated on efferent manifestations of visual discomfort in an attempt to explore the physiological mechanisms underlying discomfort glare. Luckiesh and Moss in 1942 monitored the rate of blinking while reading, and found that the blink rate was increased significantly in the presence of glare. In addition, an increase of the intensity of the glare source varied the rate of blinking (Luckiesh and Moss, 1942). Some early research also focused on the fluctuation of pupil size, particularly pupillary hippus, which is an involuntary spasm of the pupil (Fugate and Fry, 1956, Fry and King, 1975, Hopkinson, 1956). Fry and King claimed that the pupil becomes unsteady in the presence of discomfort glare. However, later work revealed little correlation between pupillary hippus and discomfort glare (Howarth et al., 1993). More recent studies examined the activity of orbicularis oculi, the facial muscle surrounding the eye responsible for closing the eye under the conditions of discomfort glare (Berman et al., 1994). Berman's study in 1994 employed electromyographic (EMG) techniques since the EMG response of facial muscle is more obvious than the observable facial expressions. The results suggested that the measurement of EMG activity of the facial muscles could be used as an objective measurement of discomfort glare. When

subjected to discomfort glare, an increased EMG activity was witnessed. However, due to the non-portability of the device in Berman's study, the utility of the assessment of EMG activity of the facial muscles around the eye is restricted to the laboratory environment. Subsequently, a portable device that can be used to measure the electrical activity was developed (Murray et al., 2002). This new device is called the Ocular Stress Monitor (OSM), which can be used as an objective index of the discomfort glare since the generated signal amplitude is proportional to the illumination at the eye. The detection or characterization of discomfort glare might be achieved through the abovementioned objective measurements of discomfort glare. However, they provide little information with respect to the cause or origin of discomfort glare. Which properties of a glare source are key to trigger visual discomfort? What are the correlations between those key parameters and how would such correlations reveal the mechanism underlying discomfort glare? To answer such questions, discomfort glare thresholds (DGT) with a number of different variables were measured in this study. The aim of this study was to establish the relative importance of glare source intensity, size, location in the visual field and surrounding background adaptation luminance on the thresholds for discomfort glare.

1.5 Thesis outline

Chapter 1 introduces the project and provides essential background information on the visual perception of discomfort glare. Following the first chapter, the equipment and techniques involved in the glare study and the pupil study will be described in Chapter 2. The retinal mechanism for

discomfort glare will be discussed in Chapter 3 in terms of the measurements of discomfort glare threshold. Measured pupil responses over a wide range of light levels will be presented in Chapter 4. A specific hypothesis regarding pupil responses above the discomfort level threshold is tested and the findings are related to the results described in Chapter 3. Chapter 5 compares the findings from the measurement of discomfort glare thresholds presented in Chapter 3 with the related findings from a number of other experiments involved in a larger glare project. Another measure of discomfort glare thresholds from peripheral glare sources will be described so as to provide a measure of discomfort thresholds that could be used in an fMRI test. Chapter 5 also reviews the findings from an fMRI study designed to investigate cortical processes involved in discomfort glare. Both discomfort and disability glare will be compared to highlight the different mechanisms involved. The final chapter discusses the various findings and summarises the conclusions that emerge from this study.

2 Equipment and methods

2.1 Introduction

New apparatus and a number of measurement techniques have been designed and implemented to carry out the experiments described in this thesis. This chapter describes the equipment and calibration methods designed for the proposed research studies. The remaining chapters will only provide a short description of the visual stimuli employed in the various experiments.

2.2 Measurement of discomfort glare thresholds

A new test was developed to measure discomfort glare thresholds. Facilities were built in for automatic measurement of pupil size, control of retinal illuminance, glare source size and location in the visual field. In addition, one could also control the surrounding background luminance.

2.2.1 Glare stimuli

The glare source employed in this experiment was based on a quad LED (Light-emitting diode) cluster produced by Perkin Elmer. The LED cluster consisted of four LEDs selected to produce red, green, blue and amber light. The spectral radiance distribution of the component elements of the four LEDs and the combined output are shown in Figure 2-1 and 2-2, respectively. The four LEDs were driven equally to produce a pinkish glare source. The chromaticity of the glare source used in this experiment had CIE 1931 - (x, y) co-ordinates of 0.34 and 0.21, respectively. A spatially uniform source was

produced using a light homogeniser mounted in front of the LED cluster. The glare source was stable over time.

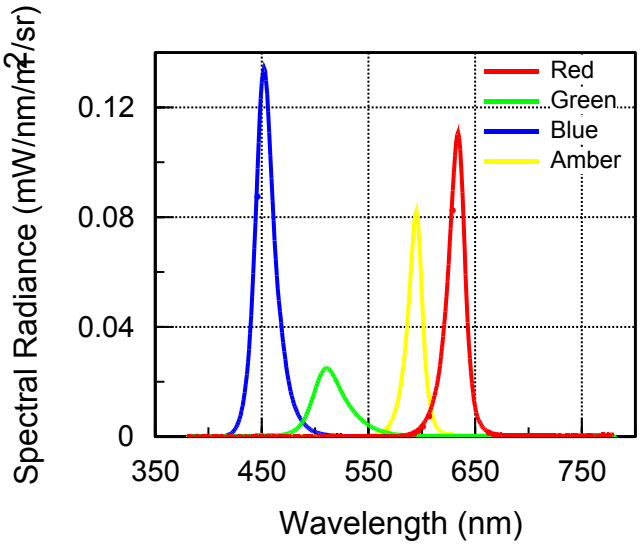

Figure 2-1 Spectral output of each LED emitter.

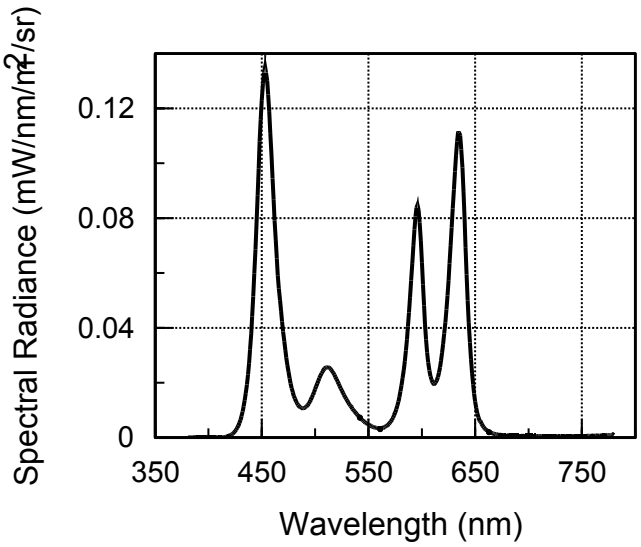

Figure 2-2 Relative spectral output of the combined four LEDs.

The light output of the glare source was controlled automatically and delivered to the eye at the desired intensity. The dependent variable was the retinal illuminance generated by the glare source. The latter takes into account the area of the pupil and is defined as $T = L \times A_p$, where T is the

retinal illuminance (in trolands), L is the luminance of the glare source (in cd/sq m) and A_p is the pupil area (in sq mm). The luminance of a glare source is the luminous intensity per unit area of an extended source. Therefore, it can be described as $L = I / A_s$, where I is the intensity of a glare source (in cd) and A_s is the source area (in sq m). The retinal illuminance can be expressed as $T = I \times A_p / A_s$ based on the two abovementioned equations. From this equation, it can be clearly seen that the retinal illuminance (T) depends on three variables: the intensity of the source (I), the area of the pupil (A_p) and the area of the source (A_s). A desired retinal illuminance can be achieved from a knowledge of source intensity, size and pupil area. The retinal illuminance is directly proportional to the amount of light per unit area reaching the retina and was therefore chosen as the measurement variable.

Figure 2-3 shows a single presentation of one glare stimulus. The fixation stimulus flickered rapidly for 0.25 s over the glare disc to prompt the subjects to attend to the target and to capture the point of regard. After 0.6 s, the glare stimulus was presented as a flash for about 0.3 s with a specific intensity. A video sensor was used to measure the pupil size just before, during and for some 1.5 s after the offset of the glare source. The measurement of pupil size prior to the onset of the glare stimulus was of great importance, since it determined the intensity of the glare stimulus to be presented to the eye. Typically, there were 60 frames collected by the camera within the period of 0.6 s since the temporal resolution of the camera was 100Hz (as described in Section 2.3). If less than 20 valid frames were

taken within the 0.6s, the glare stimulus would not be presented until more than 20 valid frames could be collected.

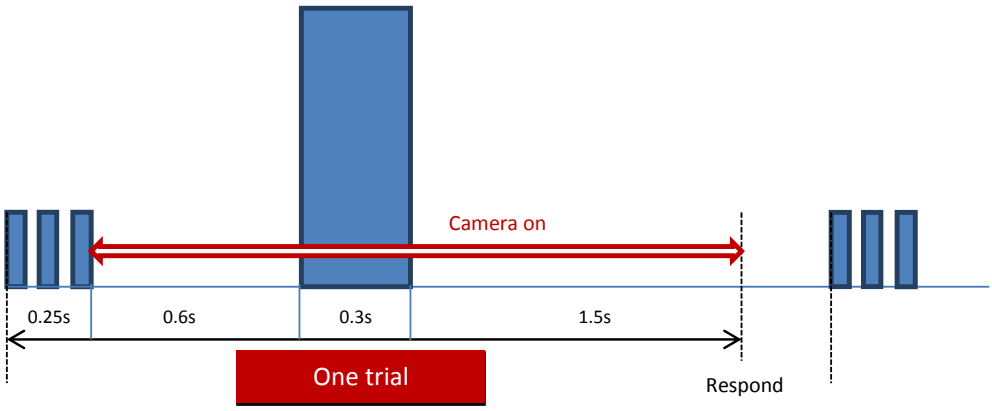

Figure 2-3 A typical timing profile employed to measure discomfort glare thresholds.

2.2.2 Apparatus

The glare source LED cluster described in Section 2.2.1 was mounted behind a large board that had a hole in the middle. The board displayed a photograph of a residential street background taken at night (as shown in Figure 2-4) and was positioned some 60 cm away from the subject's eye. The hole was placed along the road in the background image and was filled with the glare source. Between the large board and the glare source, a multi-aperture wheel was mounted to allow the variation in glare source size. The multi-aperture wheel with sixteen different sizes of apertures could be controlled by the program. The diameters of the sixteen apertures available for the study are listed in Table 2-1. Five out of sixteen apertures were employed in the primary test to investigate the effect of glare source size on discomfort glare thresholds. Before the test, the wheel was rotated so that the smallest aperture with label "0" was vertically at the top. Once the

vertical alignment was done, the starting wheel position was accepted by the program.

The ambient luminance of the surrounding area was varied through using a number of conventional lamps. The whole set-up was in a darkened room and for most of the tests we simulated a street scene at night.

Multi-aperture wheel calibration (16 sections)					
Viewing distance (mm):		600			
Slot No.	**Diameter (mm)**	**Diameter (deg)**	**Diameter (min)**	**Area (sq deg)**	**Log (Area)**
0	0.35	0.03	2.01	0.0009	-3.06
1	0.47	0.04	2.69	0.0016	-2.80
2	0.67	0.06	3.84	0.0032	-2.49
3	0.95	0.09	5.44	0.0065	-2.19
4	1.44	0.14	8.25	0.0149	-1.83
5	1.88	0.18	10.77	0.0253	-1.60
6	2.88	0.28	16.50	0.0594	-1.23
7	3.92	0.37	22.46	0.1101	-0.96
8	5.99	0.57	34.32	0.2570	-0.59
9	6.48	0.62	37.13	0.3007	-0.52
10	7.98	0.76	45.72	0.4561	-0.34
11	9.89	0.94	56.66	0.7005	-0.15
12	10.91	1.04	62.51	0.8524	-0.07
13	12.98	1.24	74.37	1.2066	0.08
14	13.93	1.33	79.81	1.3896	0.14
15	18.11	1.73	103.75	2.3486	0.37

Table 2-1 Specification of 16 apertures on a multi-aperture wheel. The highlighted ones are five apertures employed in the test investigating the effect of source size on discomfort glare thresholds.

Figure 2-4 The photograph used to provide the residential street background used in this experiment. The glare source was located in the middle of the board where the picture was pasted.

2.2.3 Intensity calibration

For each glare source size employed in the experiment, the relationship between drive voltage and the intensity of a glare source was obtained. This was done using the calibrated illuminance detector and the Vinculum photometer box. The illuminance detector was an LMT V (λ) corrected silicon photodiode detector. With the calibrated device placed at a certain distance, the illuminance level can be measured. The luminous intensity (I) of each LED cluster can be calculated from the measured illuminance level (E) generated at a distance (d) away from the source ($I = E * d^2$).

The intensity calibration prior to the experiment was carried out manually. The glare source was initially set to the largest aperture (1.73° in diameter). The calibrated detector was placed 24 cm away from the glare source. The range of drive voltage was from -10 to 10 V. The step sizes between -10 and -

9 V, between -9 and -8 V and between -8 to 10 V were 0.05, 0.1 and 1V, respectively. The luminous intensity of the glare source unit can be calculated from the measured illuminance level generated at 24 cm away from the source. For all the other source sizes (0.28°, 0.62°, 1.04° and 1.33° in diameter), the drive voltage was only set to 10 V. The readings for each glare source size were then compared with the one for the largest source size, and the scaling factors could be obtained which were used to produce the luminous intensities for all the other source sizes for a range of voltage from -10 to 10 V.

Figure 2-5 shows the relationship between drive voltage and the intensity for all the five source sizes used. This can be expressed in the form of a third-degree polynomial equation, and coded into the experimental program. Therefore, according to the relationship for each source size, the drive voltage can be altered once the luminous intensity is changed through the adjustment of the retinal illuminance.

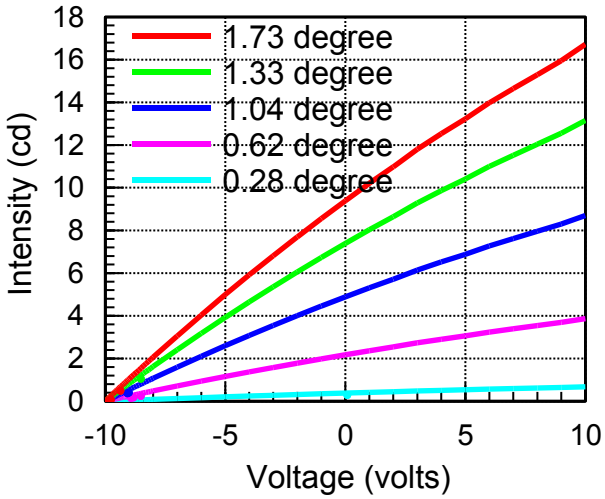

Figure 2-5 Relationships between drive voltage and the luminous intensity for each of five glare sources.

2.2.4 Criteria of discomfort glare judgment

It has been found that the inter-subject variability in discomfort glare thresholds is large (Luckiesh and Guth, 1949, Saur, 1969). In order to minimize inter-subject variability in thresholds for discomfort glare, the subjects were instructed to adhere to some criteria when they judged the presence or absence of discomfort glare. The principal perceptual effects that accompany or contribute to discomfort glare were explained to every subject before the test.

- The source appears too bright when compared to surrounding context
- The subject perceives expanded edges and boundaries that tend to spread out and glow because of scattered light.
- The 'glow' within the source leads to a complete loss of spatial detail within and around the glare source; this perceptual effect may reflect the saturation of photoreceptor responses.

- Once glimpsed, the subject experiences a pre-attentive reaction to look away quickly from the glare source.

Each subject had these criteria explained through preliminary presentations of the glare source at various intensities so as to help conceptualise a more stable definition of discomfort glare.

2.2.5 Procedure

Before the experiment started, some five minutes were taken to adapt to the surrounding background. This time also served to provide explanations and instruction for the test. Initially, the measurement variable, retinal illuminance was set to five log Td based on the result from a series of preliminary measurements of discomfort glare. The thresholds for discomfort glare were estimated using a two-alternative forced choice (2AFC) staircase procedure. The staircase procedure consisted of a number of stimulus presentations; each was described in Section 2.2.1. At the end of each stimulus presentation, the experimenter pointed out the end of pupil measurement. After viewing the glare stimulus, the subject was required to indicate the presence or absence of visual discomfort at the point of response, shown in Figure 2-3, by pressing the buttons Yes or No, respectively. This was judged by the appropriate criteria described in Section 2.3.4. The subjects were instructed to avoid blinks or saccades during the pupil measurement. At the end of each stimulus presentation, they could take the opportunity to shift fixation and blink before the next stimulus. When the observer was ready to continue with the test by looking steadily at the

fixation target, the experimenter would then start the next stimulus presentation until the measurements were completed.

The intensity of the stimulus was modulated according to a 1-up-1-down staircase with variable step sizes. To be precise, the two-alternative forced choices were “YES” and “NO” based on whether the discomfort was experienced by the subject or not. The varying step sizes in the staircase got smaller and smaller with the increasing number of reversals. The staircase employed nine reversals and the average of the last six reversals provided an estimate of discomfort glare threshold. As mentioned, the retinal illuminance on the log scale was chosen as the measurement variable for the staircase. In order to adjust the retinal illuminance in the staircase, the pupil measurement was taken prior to the onset of the glare stimulus. Once the pupil diameter was measured for a given source size, the stimulus intensity could be set to provide the corresponding retinal illuminance.

2.2.6 Parameters

The effects of three different variables on discomfort glare thresholds were investigated, including size, eccentricity of a glare source and background luminance.

To examine the effect of source size on discomfort glare thresholds, five different source sizes were used with the diameters of 0.28°, 0.62°, 1.04°, 1.33° and 1.73°, and the background was set to 2.6 cd/m^2; all glare stimuli were presented at the fovea. To investigate the effect of eccentricity of a glare source, four eccentricities were used, including 0°, 3°, 6° and 12° from the fovea; the source size was kept constant at 1.33° in diameter, and the

background luminance was set to 2.6 cd/m^2. Finally, three background luminances, 0.26 cd/m^2, 2.6 cd/m^2 and 26 cd/m^2, were examined using a constant source size of 1.33°, and again all were presented at the fovea.

2.3 Measurement of pupil constriction under discomfort glare

As mentioned in Section 2.2.1, in order to obtain the required luminous intensity of a glare source in one stimulus presentation, the pupil size in steady state was measured to adjust the corresponding retinal illuminance for the known source size. Therefore, a camera was an important device in the apparatus for the measurement of discomfort glare thresholds. A 100 Hz Pulnix camera was mounted on an optical bench to the left of the participant to record pupil size for the pupil measurement. Although the subjects were required to view the stimulus binocularly, the pupil sizes only from their left eyes were measured. The Pulnix camera is sensitive to infra-red light. A number of infra-red LEDs were placed under the subject's eye away from the line of sight to provide uniform illumination of the iris.

In the investigation of transient pupil responses to the onset of discomfort glare, the pupil diameter change caused by the glare stimulus was measured. The same camera at the same location was used in this experiment. However, not only the pupil size in steady state prior to the glare stimulus, but also the smallest constricted pupil size in the response to the discomfort glare was measured. Typically, a pupil response trace was recorded and the pupil constriction was calculated according to the pupil trace, in order to investigate the transient pupil responses to the onset of discomfort glare.

Figure 2-6 shows a typical pupil response trace to a 300-ms glare flash stimulus. The source size of the glare was 1.73° in diameter, and the retinal illuminance was set to 6.1 log Td.

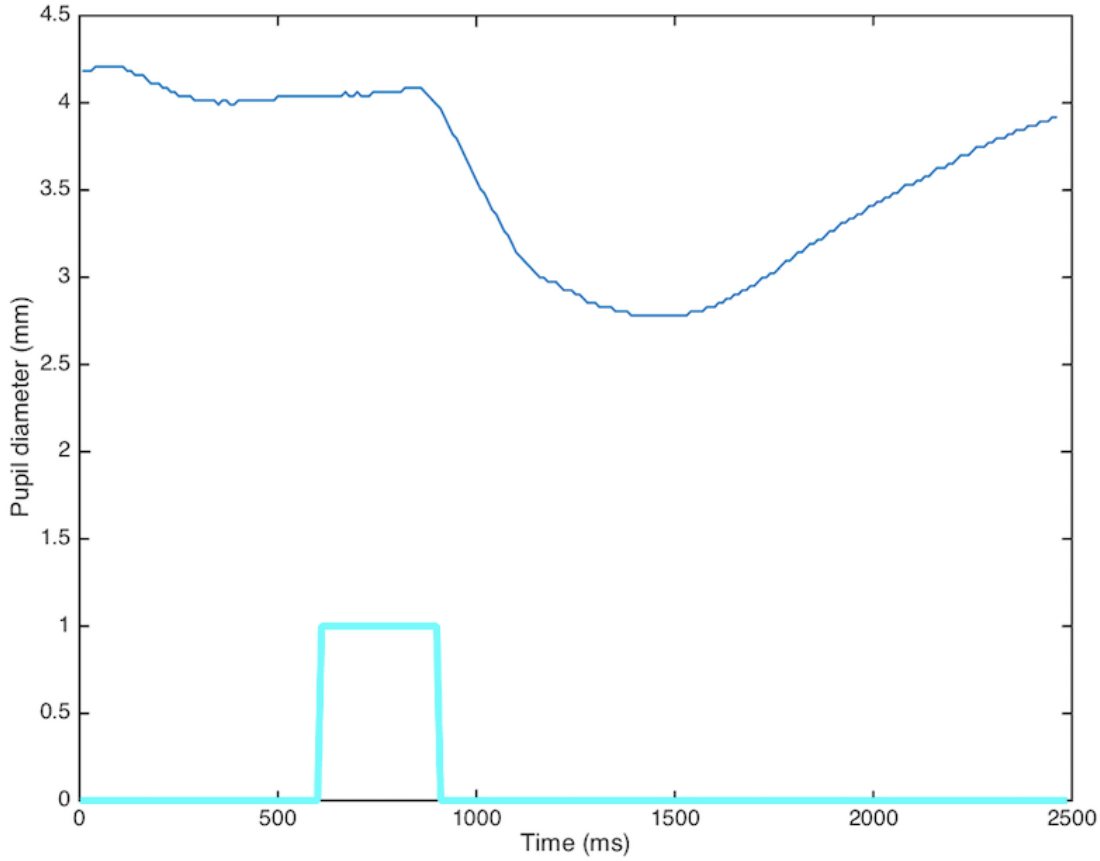

Figure 2-6 A typical pupil response trace to a 300-ms glare flash stimulus.

Once the pupil constriction was calculated for each retinal illuminance level, the pupil diameter change as a function of retinal illuminance was examined. In addition, a pupil model was put forward to establish the relationship between the pupil constriction caused by a glare flash stimulus and retinal illuminance. The measured experimental data were fitted into the model.

A number of assumptions were required to build up the pupil model. One of these is that the pupil diameter change caused by discomfort glare is directly proportional to the logarithm of total light flux entering the eye (log lm). To

validate this, another two pupillometry tests were carried out with a P-SCAN system (Barbur et al., 1987). One of them was to measure pupil constriction amplitude with varying area of the stimulus; the other was to measure pupil constriction with increasing target luminance for a stimulus of constant size.

The P-SCAN system allows the simultaneous binocular pupil measurements and eye movements. The pupil diameter is extracted through the calculation of the diameter of the circle that was fitted to the pupil. The results produce a solution for the measurement of pupil diameter. The P-SCAN system uses the customised hardware for the process of the video image and a computer based software for the extraction of pupil diameter, shown in Figure 2-7. Similar to the apparatus for the measurement of pupil size in the measurement of discomfort glare thresholds, the P-SCAN system also employs an infra-red sensitive CCD camera to capture the pupil image and uses some infra-red LEDs to illuminate the eye. The temporal resolution of the infra-red camera in the P-SCAN system is 50 Hz. In order to form a circle that is fitted to the pupil, a number of intersection points between a pattern of lines and the circumference of the pupil are obtained. The pupil diameter is then extracted based on the calculation of the coordinates of the centre from those intersection points.

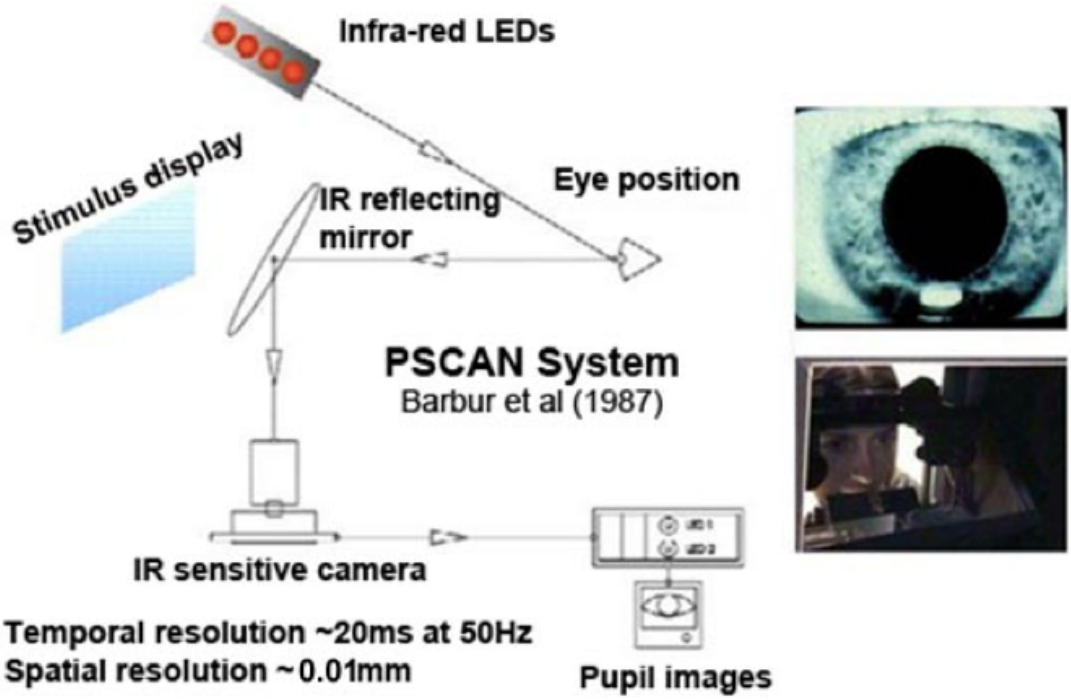

Figure 2-7 A schematic diagram illustrating the P-SCAN system. It is employed to produce a number of different stimulus conditions and measure the pupil responses to the stimulus (Adapted from Barbur 1987).

A number of different stimuli can be generated with the P-SCAN system, for instance, stimuli with different spatial structures, achromatic stimuli with different luminance contrasts and chromatic stimuli with different displacements. The achromatic stimuli with different luminance contrasts were of interest in the study of glare.

In order to examine a possible physiological correlate of visual discomfort, the pupil constriction response was measured over a large range of light levels. Based on the measured discomfort glare thresholds for individual subjects, the employed light levels can be obtained which included stimulus intensities above and below the subject's discomfort glare threshold.

The apparatus used in this study was the same as that used in the main experiment that measured discomfort glare thresholds with a number of

relevant parameters. A number of light levels were obtained to investigate the pupil constriction responses as a function of retinal illuminance. For each subject, the average discomfort glare threshold for five glare source sizes was measured. A range of light levels was employed to cover a range of two log units in retinal illuminance. For instance, if the measured average discomfort glare threshold was 5 log Td, then the range of light levels examined extended from 4 to 6 log Td with an interval of 0.1 log Td. Thus, 21 different light levels were presented in the experiment. There were eight repeats for each light level. Therefore, it was a total of 168 glare stimulus presentations that were presented randomly to avoid stimulus specific adaptation effects. All of the glare stimuli were presented at the fovea with a constant background luminance of 2.6 cd/m^2. Three glare source sizes (0.62°, 1.33° and 1.73° in diameter) were employed in this investigation.

The timing profile for each glare stimulus was the same as that employed for the measurement of discomfort glare thresholds (see Figure 2-3). A camera was used to measure the pupil diameters with a temporal frequency of 100 Hz; one frame was taken every 10 ms. For each subject, 168 pupil traces were recorded for each of the three source sizes employed. Some of the recorded pupil traces were excluded due to obvious blinks or unwanted saccades. The remaining pupil traces were used for final analyses.

The pupil constriction amplitude, Δd in mm, was obtained for each light level by working out the difference between the steady-state size of the pupil and the minimum pupil size measured in one pupil trace. Since the glare stimulus was presented as a brief flash only for about 0.3 s, the onset of pupil

constriction followed the onset of glare stimulus. In order to find the point on a pupil trace where the pupil started to constrict, a search algorithm was employed between 0.7 and 1.0 s (see the timing profile in Figure 2-3). The steady-state pupil size was obtained by averaging five pupil diameters just before the onset of pupil constriction. Another search algorithm was used from 1.0 to 1.85 s in order to find out the minimum pupil size measured in one pupil trace. Therefore, the dynamic pupil constriction was calculated in terms of pupil diameter as the difference between the steady-state pupil size and the minimum pupil size.

2.4 Subjects involved in the glare study

The whole glare study consisted of a number of different experiments. The experiments involved the measurement of discomfort glare thresholds with varying source sizes, source locations and background luminances. Experiments were also conducted to measure the pupil response to discomfort glare stimuli, to measure the discomfort thresholds from the peripheral glare, to investigate the fMRI neuroimaging under discomfort glare, to measure the scattered light in the eye and to assess the functional contrast sensitivity. The measurements of discomfort glare thresholds with a number of different variables and the investigation of transient pupil responses to the onset of glare stimulus were carried out by myself and represented the larger part of this thesis.

In the measurement of discomfort glare thresholds, 53 participants took part in the primary experiment designed to investigate the effect of source size. Prior to the test, the participants had an ocular examination on-site

conducted by a clinical optometrist. According to the exclusion criteria, three out of the 53 participants were excluded. Those exclusion criteria were based on the results from the eye test, including the presence of ocular disease, damage, intraocular lenses or surgery. The final sample was composed of 28 males and 22 females with an age range from 21 to 73 years. The 50 participants had normal best-corrected visual acuity of 6/9 or better. A separate sample for the two subtests examining the effects of eccentricity and background luminance on discomfort glare thresholds consisted of 12 participants. Five out of 12 participants also took part in the primary study that examined the effect of glare source size on discomfort glare thresholds. Those 12 subjects with normal or corrected-to-normal visual acuity had an age range of 25-35 years and consisted of six males and six females. The number of subjects for these tests is illustrated in Figure 2-8(a).

A subset of two participants, one male and one female, who completed the experiment for the measurement of discomfort glare thresholds took part in the establishment of pupil responses to discomfort glare. This additional experiment was carried out on a separate occasion, which examined the pupil constriction amplitude over a large range of light levels. The number of subjects that completed the element of pupil responses to the onset of discomfort glare is illustrated as a blue circle in Figure 2-8(a).

Another sample of 50 participants took part in the measurement of discomfort thresholds from the peripheral glare and a smaller subset of 28 participants took part in the investigation of fMRI neuroimaging under discomfort glare. This thesis will only concern 41 out of 50 participants

tested at City University, London in the comparison described in Chapter 5. All the subjects had normal or corrected-to-normal visual acuity, and all were screened according to the standard MRI exclusion criteria. In addition, no history of psychiatric or neurological disorders and no current use of psychoactive medication were reported by the participants. A portion of 35 out of 50 participants also took part in the primary experiment that investigated the effect of glare source size on discomfort glare thresholds. Therefore, that subset could be analysed in the comparison of the measured discomfort glare thresholds with thresholds from peripheral glare. The numbers of subjects involved in the investigation of the measurement of discomfort glare thresholds from the peripheral source and the fMRI test are illustrated in Figure 2-8(b).

A separate sample of 24 females and 29 males took part in the experiments for the measurement of scattered light in the eye and the assessment of functional contrast sensitivity. Similarly, all participants undertook an ocular test conducted by an optometrist on-site. The ocular examination included ophthalmoscopy and refraction. Moreover, the subjects also reported their general health, ocular health, use of medication and family ocular health history. All of the subjects had normal or corrected-to-normal vision. 10 participants were excluded based on the exclusion criteria, including the presence of ocular disease, damage, surgery or intraocular lenses in the eyes. 3 participants who experienced extreme difficulties performing either test were also excluded. The results from the remaining 40 observers with age range 21 to 68 (mean age = 42) were used in the final analysis. 36 out of 40

subjects also took part in the primary test for the measurement of discomfort glare thresholds. Therefore, the results from that portion could be compared with the findings from the measurement of discomfort glare thresholds. The numbers of subjects for the elements of scatter test and contrast sensitivity test are illustrated in Figure 2-8(c).

The entire glare study was non-invasive and the experiments carried out at City University London were approved by the School Research Ethics Committee at School of Health Science, City University London. The fMRI neuroimaging experiment carried out at Royal Holloway, University of London was approved by their ethics committee. The entire glare study also stuck to the principles of the Declaration of Helsinki. All of the subjects were required to provide written consent to participate the study.

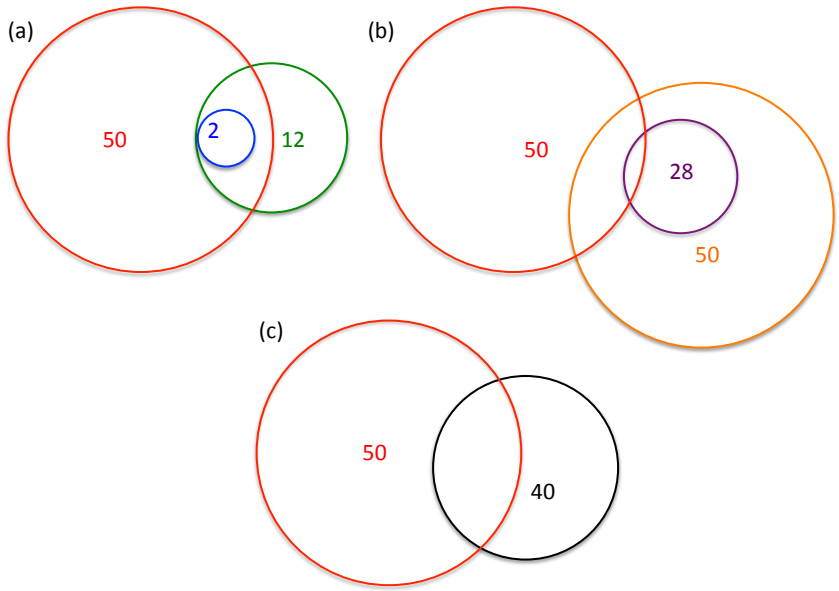

Figure 2-8 The red circle with a number, 50, represents the number of subjects that took part in the primary test measuring discomfort glare thresholds as a function of source size. (a) The green circle represents that 12 subjects took part in a test that examined eccentricity and background luminance. The blue circle represnts that 2 subjects completed the transient pupil responses to the onset of discomfort glare. (b) The orange circle represents another sample of 50 participants took part in the measurement of discomfort thresholds from peripheral glare. The purple circle represents that 28 participants took part in the fMRI test. (c) The black circle represents that 40 participants took part in the scatter test and contrast sensitivity threshold measurement.

3 Discomfort glare thresholds

3.1 Summary

As discussed in Chapter 1, the lack of an accepted standard variable and procedure to measure discomfort glare thresholds hinders the progress of glare research (Clear, 2013). Even though a number of different indices have been put forward to describe discomfort glare, the agreement between model predictions (Clear, 2013) and measured glare thresholds (Luckiesh and Guth, 1949) remains poor, particularly for the relationship between source luminance and size. The work reported in this chapter employed a subjective measure of discomfort glare in an attempt to simplify the measurement method, but also to discover something interesting in terms of mechanisms underlying discomfort glare. In the study of the measurement of discomfort glare thresholds, pupil diameter was measured throughout, allowing precise quantification of the amount of light reaching the retina. Discomfort glare thresholds were estimated with a staircase procedure. The size, eccentricity of a glare source and background luminance were varied systematically. To limit visual adaptation, the glare stimuli were presented as brief flashes. The methodology for discomfort glare work was detailed in Chapter 2.

3.2 Results

The discomfort glare thresholds were measured in this experiment. The relationship between the thresholds for discomfort glare and the relevant variables, the glare source size, eccentricity and background luminance, was

investigated. A possible mechanism and model was developed to account for discomfort glare.

3.2.1 Discomfort glare thresholds and target source size

Mean discomfort glare thresholds from a sample of 50 subjects are shown in Figure 3-1. The size of the glare source employed in the study varied over a forty-fold range in source area from 0.06 square degrees to 2.35 square degrees. The measured thresholds for discomfort glare are given in terms of retinal illuminance (log Td) and illuminance level at the plane of the pupil (log lx). It showed that the discomfort glare thresholds in terms of retinal illuminance were approximately constant at around 4.9 log Td with a standard deviation of 0.15 log Td, although a slight decrease with the increasing source size was observed. On the other hand, as the glare source size increased, there was a corresponding increase in discomfort glare thresholds when defined in terms of pupil plane illuminance.

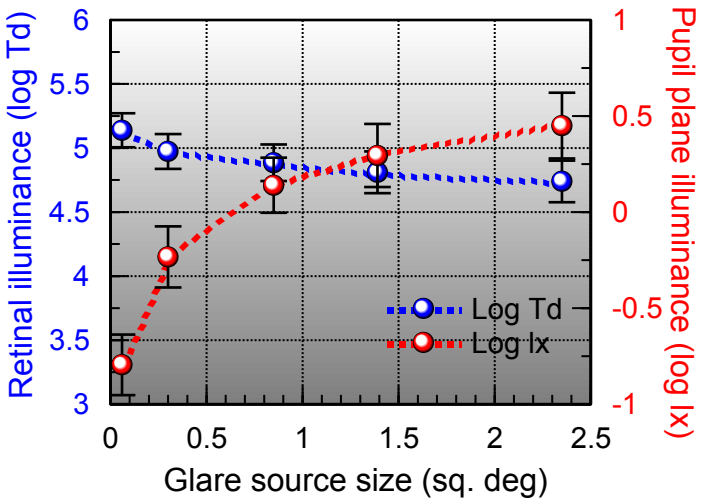

Figure 3-1 Mean discomfort glare thresholds for 50 observers. For each participant, thresholds were obtained at five different glare source sizes and each threshold was the average of four interleaved staircases. Thresholds were given in terms of retinal illuminance (log Td) and pupil plane illuminance (log lx). The retinal illuminance is amount needed to cause discomfort. The error bars represent ±2 SE.

A one-way repeated measures ANOVA, with source size as the factor, was carried out to compare 5 group mean thresholds for all 5 glare source sizes and 4 group mean thresholds for the glare source sizes excluding the smallest one. Both dependent variables, retinal illuminance in log Td and pupil plane illuminance in log lx, were considered for 5 group mean thresholds. Using the one-way repeated measures ANOVA, it was found that the main effect of glare source size was statistically significant. It gave $F(4, 196) = 13.262$, $p < 0.001$, and $F(4, 196) = 132.608$, $p < 0.001$ for retinal illuminance (log Td) and pupil plane illuminance (log lx) respectively. The dependent variable of retinal illuminance (log Td) was solely considered for 4 group mean thresholds. Again, the ANOVA result showed a significant main effect of source size even when only with 4 larger source sizes employed in the study, $F(3, 147) = 6.378$, $p < 0.001$.

In addition, since the measured average pupil sizes varied little for the five different glare source sizes, the thresholds for discomfort glare in terms of total light flux entering the eye had the same trend as the one shown in the results of pupil plane illuminance. The mean pupil diameters were 4.71, 4.56, 4.51, 4.41 and 4.41 mm for the glare source diameters of 0.28°, 0.62°, 1.04°, 1.33° and 1.73°, respectively.

Figure 3-2 shows the results for one subject tested repeatedly over a number of days, which showed a similar pattern to the results for a group of 50 subjects shown in Figure 3-1. The data points in Figure 3-2 represent the average thresholds for discomfort glare of six independent runs at five different glare source sizes. The reason why six repeat measurements were taken for one individual subject was to investigate the individual variability of discomfort glare thresholds. Again, for each glare source size used, both the retinal illuminance (log Td) and pupil plane illuminance (log lx) that corresponded to the discomfort glare thresholds were plotted. The thresholds for discomfort glare in terms of retinal illuminance (log Td) appeared relatively constant, although there was a trend of decrease as the glare source size increased; whereas the pupil plane illuminance increased with increasing source size. The mean retinal illuminance for all the five source sizes was 5.12 log Td with the standard deviation of 0.13 log Td.

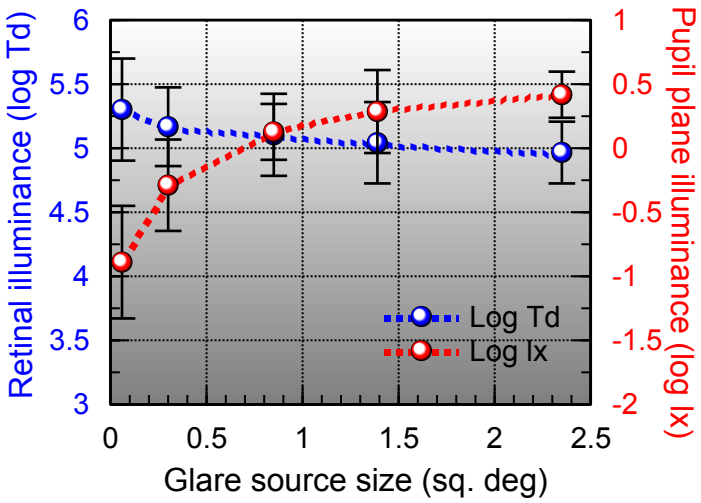

Figure 3-2 One person's discomfort glare thresholds at five different source sizes. Each point was the mean of six independent runs carried out on separate occasions, each run consisted of four interleaved staircases. The error bars represent ±2 SD.

Like the mean results from a group of 50 observers, there is also a significant main effect of glare source size in the individual data. Both retinal illuminance (log Td) and pupil plane illuminance (log lx) were used as dependent variables in a one-way repeated measures ANOVA. With glare source size as the factor, the one-way repeated measures ANOVA showed $F(4, 20) = 3.347$, $p < 0.05$ for retinal illuminance and $F(4, 20) = 62.227$, $p < 0.001$ for pupil plane illuminance. For the individual data, another one-way repeated measures ANOVA was carried out to compare 4 group mean thresholds except the threshold for the smallest source size. It shows that the effect of those four glare source sizes was not significantly different, $F(3, 15) = 1.974$, $p = 0.161$. Although the discomfort glare threshold for the smallest size (i.e. 0.28° in diameter) is slightly higher than those for the rest of the source sizes, the thresholds for discomfort glare described in terms of retinal illuminance (log Td) remain approximately constant. However, the

decreasing trend in retinal illuminance with the increasing source size can be attributed to other factors and will be examined in a later section.

As mentioned, the individual data presented in Figure 3-2 are also used to illustrate the within subject variability for each glare source size. The result shows that there is a low within subject variability. In contrast to the low variation of discomfort glare thresholds shown in the individual data, there is a high variation of discomfort glare thresholds between subjects at each particular glare source size. Figure 3-3 shows a histogram of the deviations between the mean thresholds for discomfort glare and each subject's discomfort glare threshold at each source size in terms of retinal illuminance (log Td). The deviations were calculated separately for each of five source sizes with the corresponding mean for that particular source size. It can be seen from Figure 3-3 that the frequency distribution is close to normal distribution when described in terms of log retinal illuminance. Moreover, the discomfort glare thresholds observed are within ±one log unit of the mean.

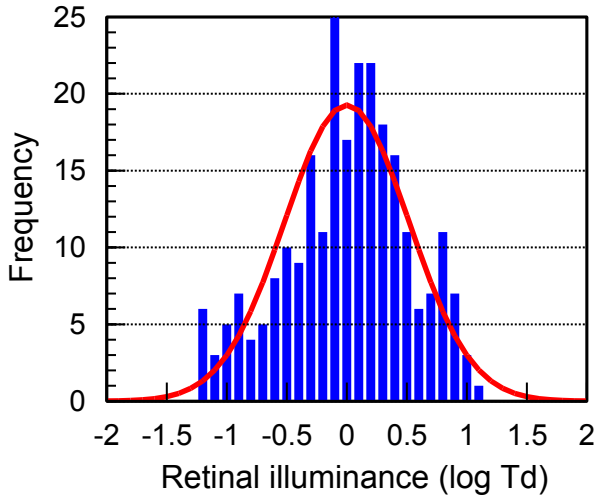

Figure 3-3 Histogram of the deviations from the mean data (shown in Figure 3-1). The deviations were calculated separately for each source size.

Although there is a large variation in discomfort glare thresholds between observers, many subjects show the same trend as the one presented in the mean data. This can be seen in Figure 3-4.

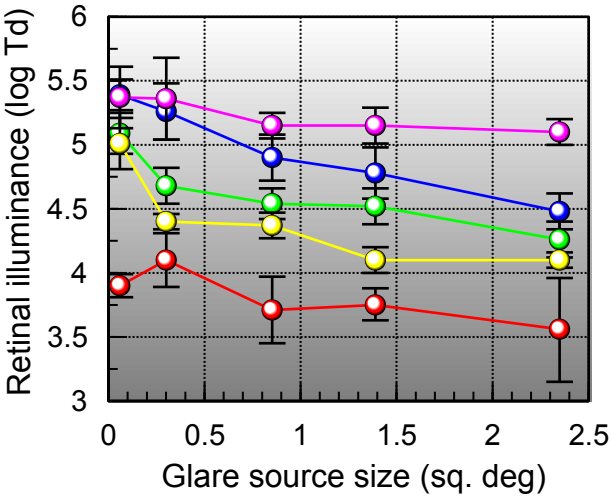

Figure 3-4 Inter-subject variation in discomfort glare thresholds. Five persons of the sample of 50, randomly selected are shown to illustrate the inter-subject variability. The error bars represent ±2 SD.

3.2.2 Discomfort glare thresholds and age

The effect of age on discomfort glare thresholds was investigated based on the same retinal illuminance data from a group of 50 participants. Those data

was binned into five age groups: 21-30, 31-40, 41-50, 51-60 and 61-80 years with 17, 8, 8, 11 and 6 subjects tested respectively. A one-way between subjects ANOVA with age as the factor was carried out on the binned data, showing that there is no main effect of age on thresholds for discomfort glare, $F(4, 45) = 0.563$, $p = 0.691$. Figure 3-5 shows the individual age data and Figure 3-6 shows the binned age data.

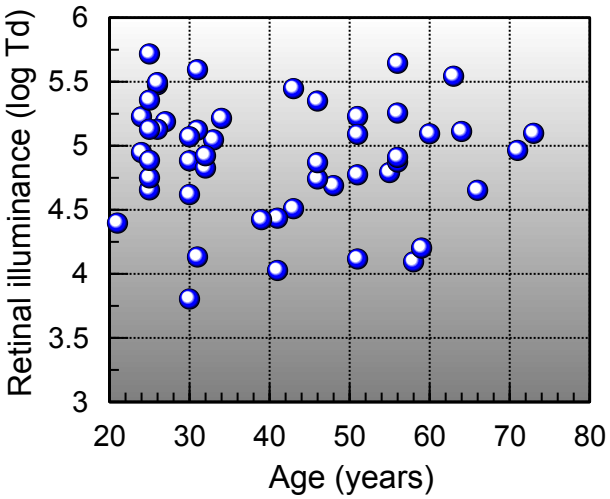

Figure 3-5 The discomfort glare thresholds for each participant were plotted as a function of age. Each point was the mean threshold of five sources sizes.

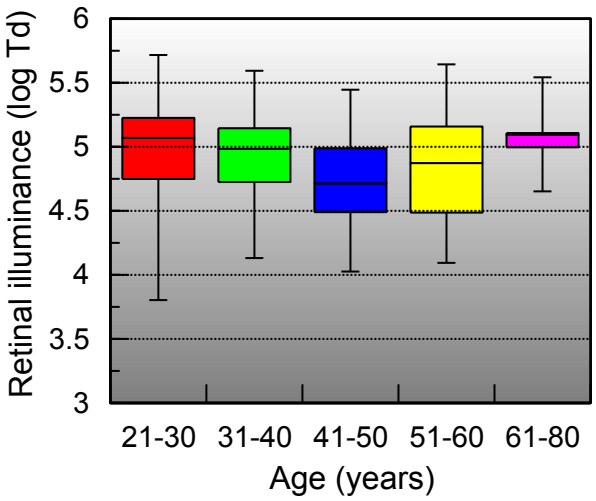

Figure 3-6 Boxplot of discomfort glare thresholds and age groups. Discomfort glare thresholds appeared to be independent of age. The bottoms and tops of each box were the first and third quartiles and the bands inside each box were the median. The ends of the whiskers were the minimum and maximum of all of the data for each age group.

3.2.3 Discomfort glare thresholds and gender

To examine the effect of gender on discomfort glare thresholds, the data set of 50 subjects were analysed into male and female groups. As mentioned in Section 2.8, there were 28 males and 22 females tested. Similar to the effect of age, there is no main effect of gender on the thresholds for discomfort glare in terms of retinal illuminance (log Td). This is confirmed by an independent-samples t-test, $t(48) = 0.318$, $p = 0.752$. To illustrate the effect of gender, a box-whisker plot is shown in Figure 3-7.

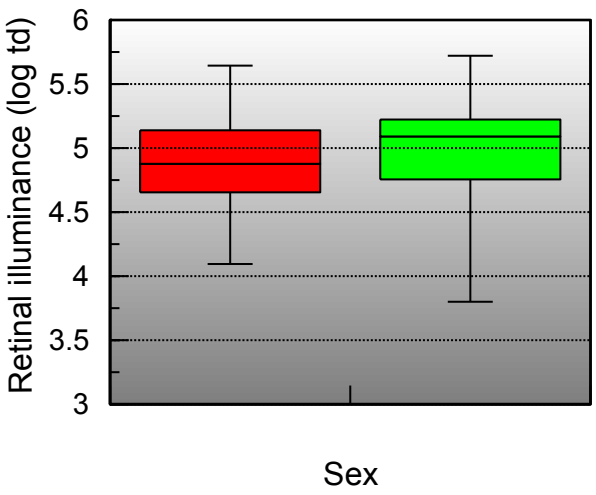

Figure 3-7 Box-whisker plot of discomfort glare thresholds and gender; red indicated male whereas green indicated female. The box showed the median and the interquartile range (first and third quartiles) and the whiskers represented the range of the data. Discomfort glare thresholds were the same for males and females.

3.2.4 Discomfort glare thresholds and eccentricity

To investigate the effect of glare source location in the retina on discomfort glare thresholds, the retinal illuminance (log Td) with the foveal fixation and three peripheral fixations were compared. The three peripheral locations included 3, 6 and 12 degrees horizontally from the centre. Figure 3-8 shows the effect of glare source eccentricity on the thresholds for discomfort glare. Each data point in this figure represents the mean discomfort glare threshold in terms of retinal illuminance (log Td) for 12 subjects.

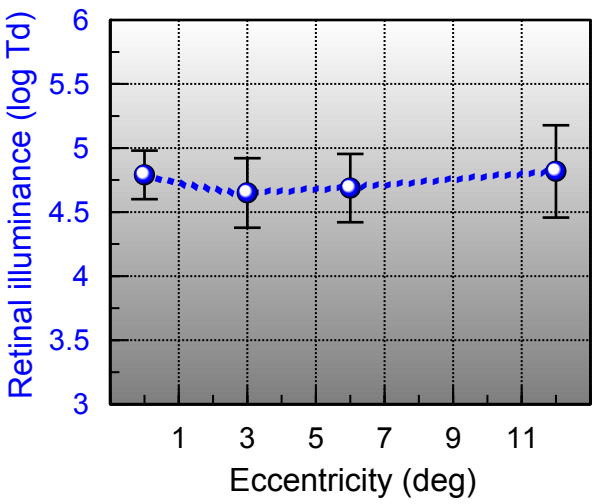

Figure 3-8 Mean discomfort glare thresholds from a sample of 12 participants were shown for a range of different eccentricities. The source size was 1.33° in diameter. The error bars represent ±2 SE. Measurements taken at the fovea and three peripheral (3°, 6° and 12°) locations show no change in thresholds with eccentricity.

A one-way repeated measures ANOVA with glare source eccentricity as the factor revealed that there is no significantly main effect of eccentricity, $F(3,33) = 0.760$, $p = 0.525$. The result suggested that for this range of eccentricities investigated in this study, the discomfort glare thresholds when described in terms of retinal illuminance (log Td) appear to be independent of eccentricity of the glare source.

3.2.5 Discomfort glare thresholds and background luminance

To examine the effect of background luminance on the thresholds for discomfort glare, the same 12 participants as those in the test for the effect of eccentricity were tested. Figure 3-9 reveals the effect of background luminance on discomfort glare thresholds. Similarly, each data point indicates the mean threshold for discomfort glare in terms of retinal illuminance (log Td).

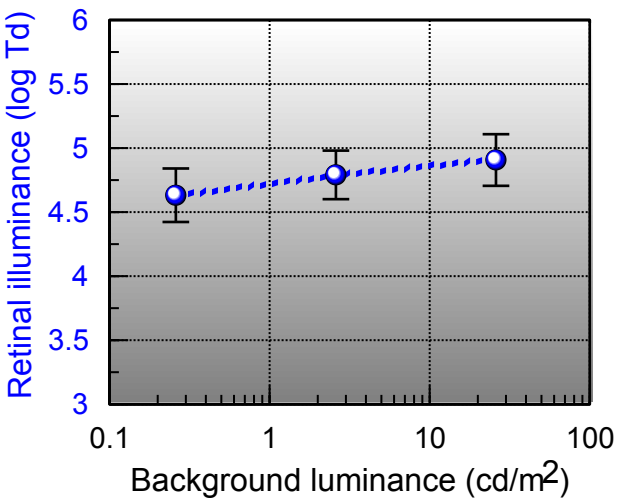

Figure 3-9 Mean discomfort glare thresholds from a sample of 12 participants were shown for a range of different background luminances. The source size was 1.33° in diameter. The error bars represent ±2 SE. Three background luminance levels were examined: 0.26, 2.6 and 26 cd/m². There was a significant increase in discomfort glare thresholds with background luminance.

A one-way repeated measures ANOVA with background luminance as the factor was carried out. Unlike the effect of eccentricity on discomfort glare thresholds, there is a significantly main effect of background luminance on the thresholds for discomfort glare, $F(2, 22) = 9.001$, $p < 0.01$. The mean discomfort glare thresholds in terms of retinal illuminance (log Td) increased with background luminance. However, the extent to which the mean thresholds increased with the increasing background levels is different. To investigate this, three independent-samples t-tests were conducted to compare discomfort glare thresholds in low mesopic and high mesopic (0.26 and 2.6 cd/m²), low mesopic and photopic (0.26 and 26 cd/m²) and high mesopic and photopic (2.6 and 26 cd/m²) conditions. Interestingly, no effect of background luminance on the thresholds for discomfort glare was detected between the low mesopic and high mesopic (0.26 and 2.6 cd/m²) conditions, $t(11) = 2.009$, $p = 0.070$. For the other two combinations, there is

a main effect of background luminance on discomfort glare thresholds, $t(11) = 4.272$, $p < 0.01$ for the combination between low mesopic and photopic (0.26 and 26 cd/m^2) conditions, and $t(11) = 2.412$, $p < 0.05$ for the combination between high mesopic and photopic (2.6 and 26 cd/m^2) conditions.

3.2.6 Light scatter and effective retinal illuminance

In addition to the experimental measurements of discomfort glare thresholds with a number of different variables, additional work was carried out to explain why the discomfort glare thresholds decrease as the source size is increased.

One of the reasons why the thresholds are size dependent is that the light from a glare source entering the pupil is scattered by the intraocular structures, which could cause a reduction in retinal contrast. This reduction in retinal illuminance is more pronounced for the smaller glare sources, because a higher proportion of the scattered light falls outside the region of the glare source for a smaller source. The higher proportion of the scattered light outside of the smaller light source moves the discomfort glare thresholds a little bit higher. Therefore, one could bear more visual discomfort from a smaller glare source since more light is scattered in comparison to a larger glare source. The measured discomfort glare threshold in terms of retinal illuminance from a smaller glare source consisted of the effective retinal illuminance and the contribution from the scattered light.

The actual retinal illuminance on the retina within the region of the target was estimated by convolving the Point Spread Function (PSF) of the human eye (van den Berg et al., 2010) with a simulated target image. This is described in Figure 3-10.

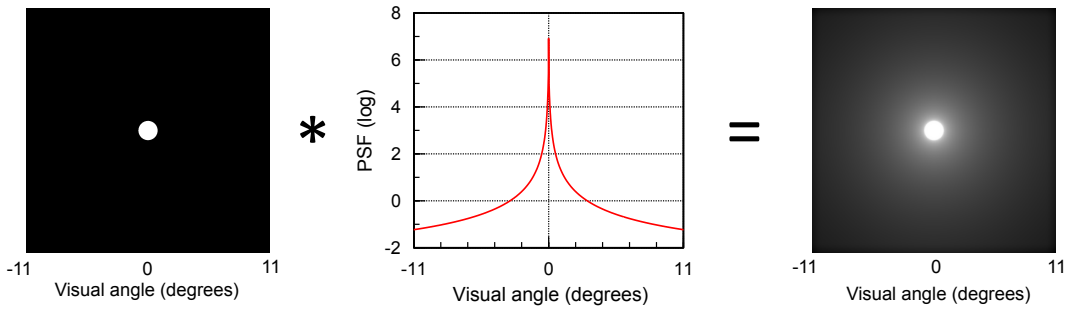

Figure 3-10 The actual retinal illuminance for each participant was estimated by convolving a simulated glare source with the point spread function of the eye. The left image shows an ideal simulated target before the convolution, and the right image shows an actual target after the convolution.

For the actual target region, presented in the right image of Figure 3-10, the horizontal target luminance profiles of the five source sizes used in this study were plotted, shown in Figure 3-11. It can be seen that within the target region, there is a larger reduction in target luminance for the smaller glare sources. It is necessary to take account of the effect of light scatter when the retinal illuminance is used to describe discomfort glare thresholds. Illustrated in Figure 3-12, the effective retinal illuminances are smaller than the measured retinal illuminances for each source size. In addition, the difference between the effective retinal illuminance and the measured retinal illuminance is larger for smaller source sizes. However, the significant trend of smaller source sizes having higher discomfort glare thresholds is still maintained. A one-way repeated measures ANOVA with glare source size as

the factor was carried out on the dependent variable of effective retinal illuminance (log Td) to show this trend, $F(4, 196) = 7.442$, $p < 0.001$.

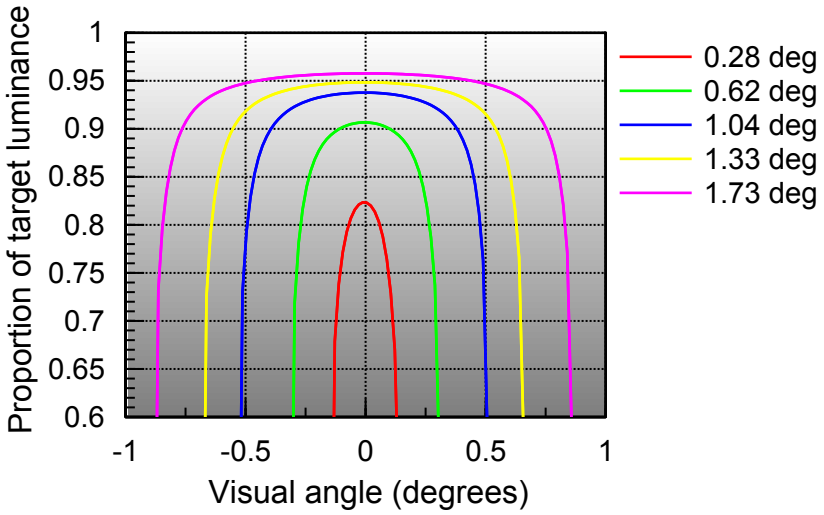

Figure 3-11 The horizontal luminance profile of the five source sizes tested after convolution. In the target region, smaller source sizes cause a larger reduction in retinal illuminance.

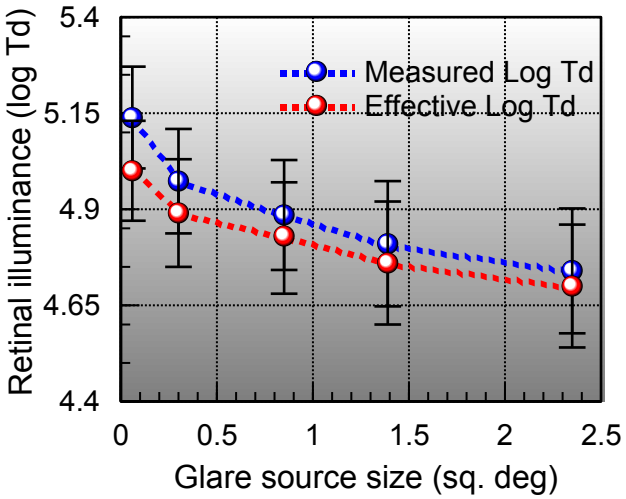

Figure 3-12 The threshold for discomfort glare was plotted in terms of the measured and effective retinal illuminance of the target. The thresholds are lower in terms of effective retinal illuminance, particularly for smaller sources sizes, however the significant trend of smaller source sizes having higher discomfort glare thresholds is still maintained.

In addition, the directional sensitivity of the cone photoreceptors (Stiles and Crawford, 1933) was considered in relation to the reduction of effective retinal illuminance for different source sizes. The impact of the Stiles-

Crawford effect on reducing the effective retinal illuminance for different source sizes, however, is not significant. Given that the mean pupil sizes were similar for each of the five tested source sizes, there was less than a 2% difference in effective retinal illuminance between the largest and smallest source size.

3.2.7 Mechanism to account for the size dependence of discomfort glare thresholds

It is worth noting that the thresholds for discomfort glare for each source size varied less in terms of effective retinal illuminance than in terms of pupil plane illuminance. The difference in thresholds for discomfort glare between the smallest and the largest source sizes was 0.30 log units in terms of effective retinal illuminance (see Figure 3-12); whereas the difference between the largest and the smallest source sizes was 1.25 log units in terms of pupil plane illuminance (see Figure 3-1). This suggests that the sensation of discomfort glare is more likely in relation to the spatial distribution of light on the retina, rather than the total amount of light entering the eye. This observation also implies a more important role for the processing of image contrast rather than total light flux entering the eye.

A simple model of contrast vision based on centre-surround ganglion cell receptive fields was examined. The model took into account both the saturation of a photoreceptor response and an edge response which was largely determined by the effective boundaries of the glare source.

The actual target was obtained by convolving an ideal target (a disc) with the Point Spread Function of the eye (van den Berg et al., 2010). The CIE 1999

total glare equation was employed in this model, which takes the average age of 41 years for a sample of 50 participants and the pigmentation factor of 0.5. The process can be illustrated in Figure 3-10.

A Michaelis-Menton function was modeled as a photoreceptor response function. The half-maximal response of the photoreceptor signals was set to 1.6 log Td; the response range was 3 log units. The photoreceptor response function is shown in Figure 3-13.

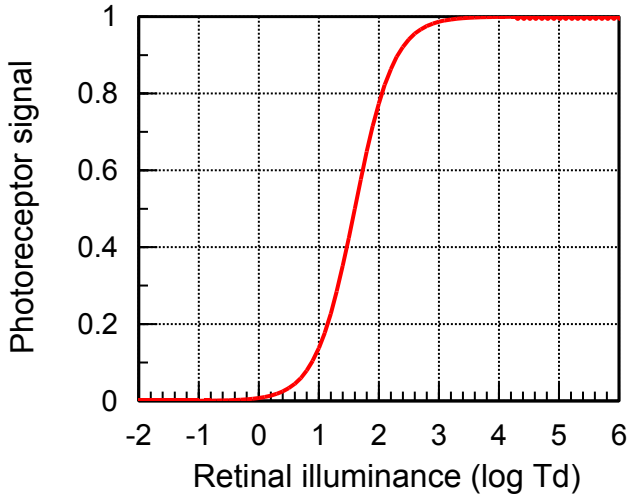

Figure 3-13 A photoreceptor response function with half-maximal response at 1.6 log Td and response range of 3 log units.

The edge response was taken as the circumference of a signal image weighted by the ganglion cell density. Obviously, different source sizes have different edge responses. The photoreceptor signal image was generated when the convolved target image was passed through the photoreceptor response function. The ganglion cell sampling density as a function of eccentricity is presented in Figure 3-14. It can be seen that more ganglion cells are concentrated in the fovea of the retina (Curcio and Allen, 1990).

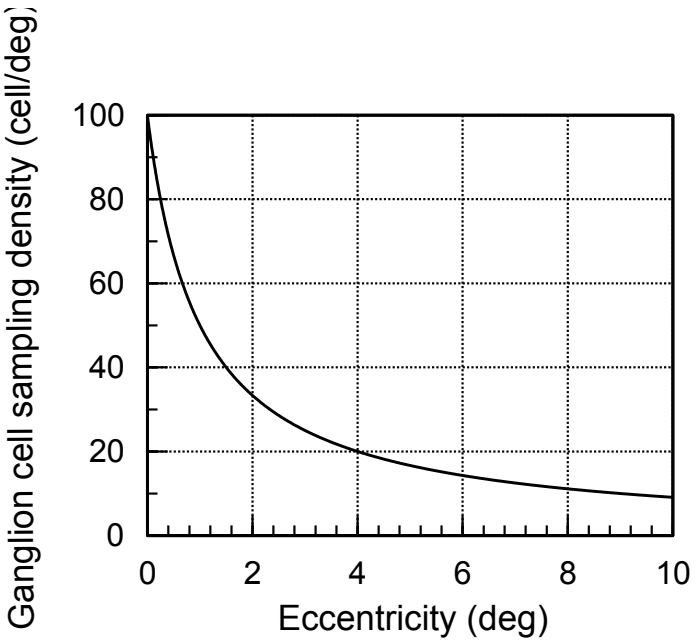

Figure 3-14 Ganglion cell sampling density as a function of eccentricity.

The model can predict the discomfort glare thresholds as a function of source size. The predicted thresholds for discomfort glare were then compared with the measured discomfort glare thresholds. The measured discomfort glare thresholds, in terms of retinal illuminance (log Td), are shown as the black line in Figure 3-15, which is the same as the blue line in Figure 3-1.

There are two model predictions. One prediction was based on the circumference of the glare source weighted by the retinal ganglion cell density, shown as the blue dashed line in Figure 3-15. The weighting was completed by multiplying the circumference of each of five source sizes by its retinal ganglion cell density at the eccentricity of its radius. The reciprocal of the weighted circumference for each source size was then scaled so that the overall mean of the predicted thresholds matched that of the measured discomfort glare thresholds. The other prediction was based on the effective circumference of the target in the photoreceptor signal image weighted by

the retinal ganglion cell density. The weighting process was carried out as the one in the first prediction. However, the circumference used in the second prediction was not the actual one of the glare source. It was calculated based on an effective edge in the photoreceptor signal image that was obtained from a convolved target image. The target image was set to 3.5 log Td, the retinal illuminance at which the photoreceptor response function saturates in this model. For each of five source sizes, the target radius in the photoreceptor signal image was taken as the radius where the photoreceptor signal was equal to 0.5. Therefore, the effective edge was extracted and circumferences used were based on these radii.

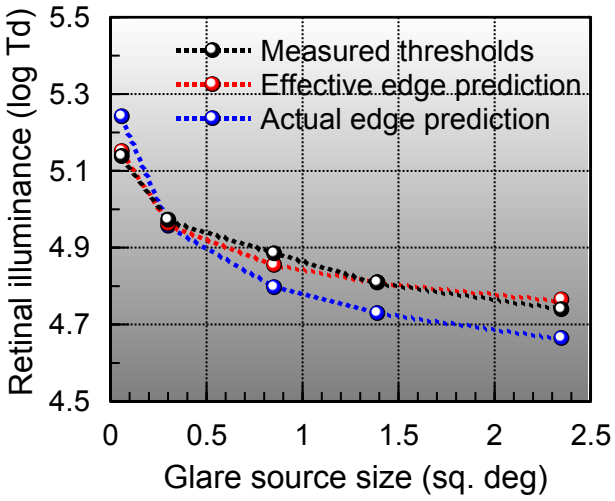

Figure 3-15 Model predictions of discomfort glare thresholds as a function of source size.

As stated in Section 3.4.6, the smaller source sizes have a higher proportion of scattered light outside the region of the target in comparison with the larger source sizes. This leads to a relatively larger radius in the photoreceptor signal image compared with the original target radius for the smaller source sizes. Therefore, the eccentricity of edge response as a

function of light level varies in a disproportionate way for different source sizes.

3.3 Discussion

A large number of studies of discomfort glare have focused on the effective evaluation of the level of visual discomfort for a given lighting fixture. An improvement in the ability to predict discomfort glare was sought (Vermeulen and de Boer, 1952, Vos, 2003b). A consensus on the issues that affect discomfort glare has been reached. This was confirmed by several research studies on glare. The UGR (CIE, 1995) mentioned in Section 3.2 consolidated much of what has been investigated about how the source size, source luminance, angular position and surrounding background luminance affect the ratings for discomfort glare. Nevertheless, little is known about the mechanisms underlying each component of the UGR model. In this study, it was found that it is the retinal illuminance, rather than the illuminance level at the plane of the observer's pupil, that was closely related to the discomfort glare for different source sizes investigated. Based on the saturation of photoreceptor responses and the edge response driven by the retinal ganglion cells, a simple model was able to predict the relative discomfort glare thresholds as a function of source size.

The results from this study are in good agreement with previous findings. It was found that the thresholds for discomfort glare were independent of age and gender, which replicated what has been found previously (Saur, 1969, Bennett, 1977). It is worth noting that unlike disability glare, no effect of observers' age on discomfort glare thresholds was found. Although light

scattering increases with age (Franssen and Coppens, 2007), it has been suggested there is no significant age effects when measuring discomfort glare thresholds. This is due to the fact that the reduction in the retinal illuminance of the glare source caused by the increased scattered light in the eye has a consequence to allow for an increase in the discomfort glare threshold needed to reach saturation. In addition, there was a large inter-subject variability in discomfort glare thresholds. The thresholds for discomfort glare differed a lot from one subject to another, agreeing with the previous work (Luckiesh and Guth, 1949, Saur, 1969). As for the effect of source size, the trend for smaller source sizes to be associated with slightly larger discomfort glare thresholds in terms of retinal illuminance (log Td) was found. This trend agrees with the finding in the early work of Luckiesh and Guth (L&G) in 1940s (Luckiesh and Guth, 1946, Luckiesh and Guth, 1949). Glare in the L&G experiment was measured in terms of BCD, described in Section 1.2.5.1. The BCD brightness is the luminance of a glare source that an observer reports is on the borderline between comfort and discomfort. In our study, the discomfort glare thresholds were measured in terms of retinal illuminance, taking into account pupil size. Despite the use of a different measure, the finding in our study was still in agreement with the trend found in L&G experiment. Also, it was found that the discomfort glare thresholds tended to increase with the increasing background luminance for a given range tested in this study, which is similar to what Guth and others observed (Luckiesh and Guth, 1949, Vermeulen and de Boer, 1952). When the background luminance was increased to 26 cd/m^2, the rods in the retina saturate and only cones continue to respond to the glare flash stimulus.

In order to explain the relationship between glare source size and the measured discomfort glare thresholds, the effect of forward light scatter in the human eye was first considered. Forward light scatter has been taken as the main cause of disability glare since it can reduce the contrast of the retinal image due to the introduction of a veiling luminance (Stiles, 1929c) from a peripheral glare source. However, in the area of discomfort glare, it could also play a significant role. The scattered light triggered by an external bright light source could stimulate the adjacent regions of the retina so that one may experience an expanded edge of the target that spreads out. Moreover, smaller sources lose more of the light from the target region than larger sources. Therefore, the effective retinal illuminance of a smaller source is proportionally lower in comparison with a larger source.

In a second attempt to explain the effect of glare source size on discomfort glare thresholds, the role of contrast vision was considered. It has been pointed out the discomfort glare thresholds for different source sizes are more likely related to the retinal illuminance rather than the pupil plane illuminance. Retinal illuminance is directly proportional to the amount of light per unit area on the retina, whereas the pupil plane illuminance is the total light flux entering the eye per unit area of the pupil. A two-stage model of contrast vision was employed to predict the relative discomfort glare thresholds for different source sizes. The model involved the saturation mechanism of photoreceptor responses followed by estimation of an edge response. The edge response was implemented by weighting the circumference of the glare source by the retinal ganglion cell density. Given

the simplicity and the possible practical utility, a simple version of the model was adopted. In fact, a similar result could be obtained using a more complex model, where the photoreceptor signal image is filtered through a difference-of-Gaussian filter (McCann et al., 2011). The two-stage model can also be used to account for the effect of background luminance on discomfort glare thresholds. The half-maximal response of the photoreceptor dynamic range would be set by the background luminance.

However, the model cannot predict the individual threshold for discomfort glare. Each subject could set their own criteria to what they mean by discomfort glare according to the extent to which saturation occurs. The variability of the criteria may account for the obtained inter-subject variability in thresholds for discomfort glare. In addition, a model based on the saturation mechanism may be accurate for the peripheral glare source. But the model based on the circumference of a glare source is not suitable for glare sources presented in the periphery. This is due to the properties of the peripheral retina that differ a lot in comparison with that of the foveal retina. A single retinal ganglion cell communicates with numerous photoreceptors as you go further into the peripheral retina; and also in the periphery, the density of rods is larger. Both of these effects in the peripheral retina make it difficult to detect the edge of an image. This may have a bias towards the fact that discomfort glare is more likely to be associated with retinal illuminance rather than luminance defined edges.

The findings reported in this chapter suggest that photoreceptor response saturation plays an important role in the determination of level of thresholds

for discomfort glare. Moreover, forward light scatter in the human eye is also critical as it reduces the contrast of the retinal image and extends the boundaries of the glare source. This is caused by the saturation of photoreceptor responses and the loss of spatial details in the adjacent area of the glare source. In addition, the reduction in the retinal illuminance of the glare source caused by the forward light scatter in the eye varies with source size. More light is scattered for the smaller glare sources. Consequently, an increase in discomfort glare thresholds in terms of retinal illuminance is needed to reach saturation. Therefore, a trend of the small but significant decrease in thresholds for discomfort glare with increasing source size is witnessed. This is also accounted for by the expected variation in the number of retinal ganglion cells which respond to the edges of the glare source. Despite the fact that discomfort glare thresholds are associated with photoreceptor signals saturation and the loss of spatial details, the measurement of thresholds for discomfort glare is a subjective perceptual experience which depends on the individual's response criterion. It, therefore, results in a two log unit range for the measured thresholds in terms of retinal illuminance. Although there is a variation in thresholds for discomfort glare, the relatively small source size dependence still plays a key part in the design of lighting installations, which will be described in Chapter 6.

If the hypotheses of saturation of photoreceptor responses and the forward light scatter in the eye that were put forward to account for the findings in this chapter are correct, they may also be reflected in the transient pupil responses to the onset of discomfort glare. If photoreceptor response

saturates, there is no longer a systematic increase in pupil constriction. This hypothesis follows from the explanation put forward for discomfort glare. In order to test this hypothesis, pupil responses to the discomfort glare were investigated which will be described in Chapter 4.

4 Transient pupil responses to the onset of discomfort glare

4.1 Summary

In order to account for the results of the measurement of discomfort glare thresholds, an explanation based on saturation of photoreceptor responses was put forward. This hypothesis also implies that pupil response amplitudes to light flux changes above the threshold for discomfort glare are also likely to saturate. This chapter describes the results of an experimental study that measured the constriction of the pupil as a function of the light flux / retinal illuminance generated by the glare source. In addition, a model for scattered light was also developed and applied to explain how pupil constriction amplitude may be affected by the light scattered outside the glare source.

4.2 Introduction

The pupil response plays an important role in clinical and laboratory tests which aim to evaluate the integrity of the retina and visual pathways (Kaufman et al., 2011).

The pupil light reflex (PLR) is a reflex that changes the size of the pupil in response to changes in light flux entering the eye, thus providing some limited control of retinal illuminance. A high light level causes the pupil to constrict (miosis), whereas a reduced light level causes the pupil to dilate (mydriasis). Therefore, the pupil light reflex modulates the total amount of light entering the eye.

It has been well established that the steady-state size of the pupil is largely determined by the ambient light level and a brisk pupil constriction is caused by a sudden increase in light flux on the retina. That transient pupil response is often described as the dynamic PLR response. The dynamic PLR response to the onset of discomfort glare was investigated in this study.

The transient pupil constriction in response to flashes of light requires a number of neurons with diverse properties, including limited spatial summation, band-pass temporal response characteristics and high contrast gain. A glare stimulus presented to the eye is likely to trigger both steady-state and transient components, but the relative contribution each component makes to the pupil constriction will depend on the size of the glare stimulus, its luminance contrast, location in the visual field and onset temporal characteristics. The sustained component also contributes to the transient pupil response since the neurons involved exhibit low-pass temporal response characteristics. However, the relative contribution that the sustained component makes is comparatively small (Barbur, 2004).

It has been shown that the pupil constriction is not simultaneous with the change in light flux. The pupil starts to constrict after a latent period in response to light (LÖWenstein and Friedman, 1942). During the latent period, pupil size remains unchanged. Once the pupil constriction starts, the pupil size decreases until it reaches a minimum value. As the redilatation begins, the pupil size increases until it recovers its initial size. The intensity of a light stimulus determines the length of the latency, the amplitude of the response and the velocity of the pupil constriction (Alpern et al., 1963). Further studies

confirmed these findings by showing that as the stimulus intensity increases, there is an increase in direct PLR amplitude, a decrease in pupil onset response latency and an increase in the maximum rate of pupil constriction (Ellis, 1981). Ellis also revealed that redilatation speed increases with increasing stimulus intensity.

Recent studies employed experiments to evaluate the effects of glare by means of assessing brightness reduction of a foveal stimulus. In these experiments, a glare source acted as a transient conditioning field located in the periphery. Evaluation of the pupil diameter and knowledge of the latency were required to determine the retinal illuminance. They were also of interest to explain the influences of the background luminance (Issolio and Colombo, 2006) and to investigate the time course of brightness under transient glare (Issolio et al., 2006).

A further study proposed a method to measure pupil size with the change in the amount of light reaching the retina caused by the presence of glare in the peripheral visual field (Colombo et al., 2007). The pupil diameter was measured under both steady-state and dynamic adaptation conditions. The dynamic condition was triggered by a transient glare source in the periphery with three different light levels. The results under steady-state condition showed that the pupil diameter varied between subjects and that on average, older subjects exhibited a smaller pupil size, in agreement with earlier studies (Bitsios et al., 1996) that examined how the PLR varied with age. As for the dynamic condition, it has been found that latent period was independent of age and illuminance level caused by glare. Other components

of the pupil response to light had also been examined. A series of flashes of increasing luminance contrast produced progressively larger response amplitudes, but when normalized for the difference in amplitude, showed complete absence of any significant difference in pupil response latency (Barbur, 2004).

In this chapter, we measured pupil constriction amplitudes as a function of retinal illuminance over a large dynamic range and put forward a model of pupil response to light flux increments to test the hypothesis that the pupil response amplitude would be expected to show some saturation for flash retinal illuminances above the thresholds for discomfort glare. The methodology for the measurement of pupil constriction amplitudes was detailed in Chapter 2.

4.3 Model of pupil response to light flux changes

A model for the dynamic pupil response was produced to predict how the pupil constriction amplitude in response to a uniform flash of light varied with the light flux entering the eye, both below and above the individual thresholds for discomfort glare.

4.3.1 Point spread function (PSF)

The study of image formation in the eye often involves predictions of retinal image quality using an approximation to the point spread function of the eye (PSF). The latter is a form of 2D impulse response function that captures the aberrations of the optics of the eye and can also account for forward light scatter in the eye. In an emmetropic eye with no aberrations, a point object

focused on the retina forms what is known as an Airy disc which represents the diffraction pattern caused by a circular aperture. The PSF in real eyes is however affected by diffraction, aberrations and scattered light. The function extends over a large visual angle, particularly when scattered light is involved. The central part is largely in relation to optical aberrations, whereas the peripheral parts are associated with light scattering that is an effect due to localised irregularities of refractive index of the ocular media, resulting in the spread of the light over the retina. Both the aberrations and light scattering contribute to the retinal image degradation. On the other hand, it has been shown that the interaction of scatter and aberration may yield an improved retinal image (Pérez et al., 2009). Of great interest, light scattering may have an important effect on the contrast of the retinal image when the subject's eye is exposed to a bright light source. For example, during night driving drivers are confronted with the glare from the headlamps of oncoming vehicles. Under such a visual environment, scattered light plays a significant role in reducing the contrast of retinal image.

The pupil model described in this chapter employed a PSF of the normal human eye based on the formula adopted by the CIE in 1999 (Vos and Van Den Berg, 1999). This is shown in Figure 4-1. When a point source is imaged onto the retina, the actual light distribution spreads out over a large age of the retina. Different portions of the distribution dominate different visual functions. In the central part, visual acuity plays a dominant role. The light distribution, however, continues to spread beyond this area. The area over 1° is called straylight, resulting from the effect of light scattering.

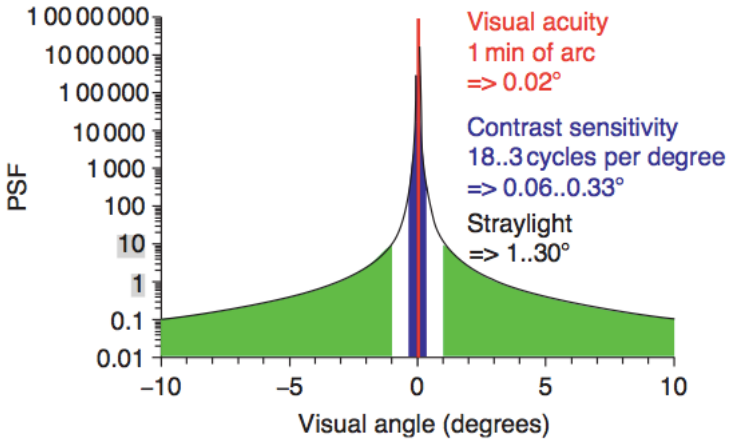

Figure 4-1 A PSF of a normal human eye according to CIE 1999 (van den Berg et al., 2010).

The complete PSF, taking into account the age and pigmentation factor of a subject, is given below. This is extracted from the total glare function proposed by Vos and Van den Berg (Vos and Van Den Berg, 1999).

$$PSF = [(1-0.08)(A/70)^4]\left[\frac{9.2\times10^6}{[1+(\theta/0.0046)^2]^{1.5}} + \frac{1.5\times10^5}{[1+(\theta/0.045)^2]^{1.5}}\right]$$

$$+[1+1.6(A/70)^4]\left\{\left[\frac{400}{1+(\theta/0.1)^2} + 3\times10^{-8}\times\theta^2\right]\right.$$

$$\left. + p\left[\frac{1300}{[1+(\theta/0.1)^2]^{1.5}} + \frac{0.8}{[1+(\theta/0.1)^2]^{0.5}}\right]\right\} + 2.5\times10^{-3}\times p$$

Where, θ, is the eccentricity in degrees, A is the age of subject in years and p is a pigmentation factor. p = 0 for a very dark eye, p = 1 for a bluish or greenish eye and p = 0.5 for a hazel eye.

As mentioned, one male subject, 27, and one female subject, 25, took part in the measurement of pupil constriction responses to the onset of discomfort glare. To predict the pupil constriction response using this model, the actual age and pigmentation factor for each individual were considered. The pigmentation factors for both were 1.0. The eccentricity was up to 57° with

an interval of 0.05°. The normalised point spread functions were very similar for the two subjects and are shown in Figure 4-2.

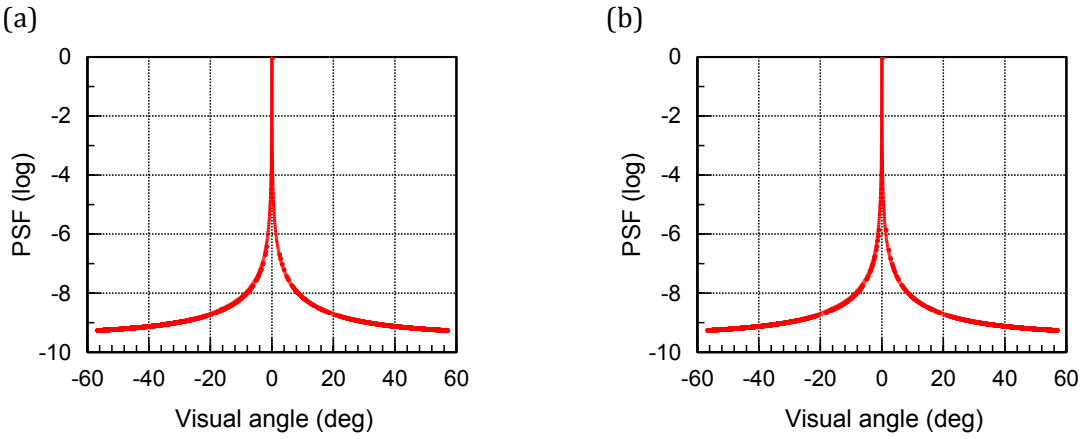

Figure 4-2 The normalised point spread functions of subjects (a) and (b). Subject (a) is 25 years old and subject (b) is 27 years old.

In order to evaluate the effect of the optics of the eye on quality of the retinal image, the glare source stimulus was convolved with the PSF of the subject's eye. This is shown in Figure 3-10. In this model, the visual field under consideration was extended up to 57° both nasally and temporally. The PSF used in the convolution was normalized to ensure that the integral of the PSF summed up to unity.

4.3.2 Photoreceptor saturation function

As described in Section 1.1.2.2, photoreceptors in the retina respond to a uniform flash of light. Their response signals increase with the increasing intensity of the flash until saturation occurs. If the photoreceptors, in terms of rods and cones, are stimulated by a number of light flashes with increasing intensity, the photoreceptor response increases in the beginning in a way that is proportional to the flash intensity, followed by a progressive saturation as the flash gets brighter (Baylor et al., 1979). It has been found

that a Michaelis-Menton equation approximately fits the relationship between the maximal response of photoreceptors and flash intensity.

The response of the photoreceptor signals as a function of retinal illuminance was approximated by a Michaelis-Menton equation of the form:

$$S(E) = \frac{E^n}{E^n + \sigma^n}$$

where E is the retinal illuminance in Trolands, n is a constant that affects the photoreceptor response range and σ is the retinal illuminance where half-maximal response occurs. In this case, the response range was set to 3 log units and at 1.6 log Td the half-maximal response occurred. The retinal illuminance where half response occurred was correlated with the adaptation background luminance. Figure 3-13 shows a photoreceptor signal function that was also used in this pupil model.

For each source size, the actual image after convolution with PSF was considered for a given range of light levels (3 to 7 log Td). Retinal illuminances both below and above the individual discomfort glare thresholds were employed. The convolved image at each light level was passed through the photoreceptor saturation function described above. Thus, a corresponding photoreceptor signal image was obtained.

4.3.3 Relationship between pupil constriction and total light flux

To establish how the amplitude of pupil constriction varies as a function of total light flux captured by the eye, two pupillometry tests were carried out with a P-SCAN system (See Section 2.3). One test was to measure the pupil

constriction amplitude with increasing light flux on the retina achieved by increasing systematically the area of the stimulus. The other one was to measure the pupil constriction amplitude as a function of luminance for a fixed target size. Although the variables differed between the two tests, the relationship between the pupil constriction amplitude and total light flux entering the eye were consistent. This is illustrated in Figures 4-3 and 4-4. The results from the tests show that the pupil constriction amplitude caused by a number of transient flashes was directly proportional to the total light flux entering the eye on the log scale.

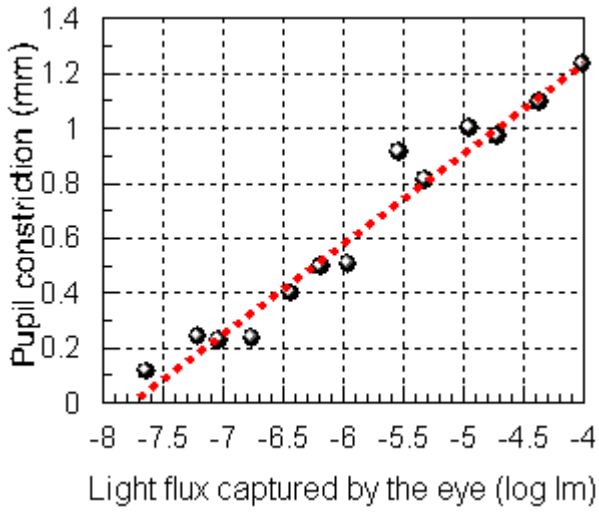

Figure 4-3 Data obtained on pupil constriction amplitude and the corresponding light flux captured by the eye. The light flux variations were accomplished by varying the area of the stimulus. The data was collected when testing subject (a).

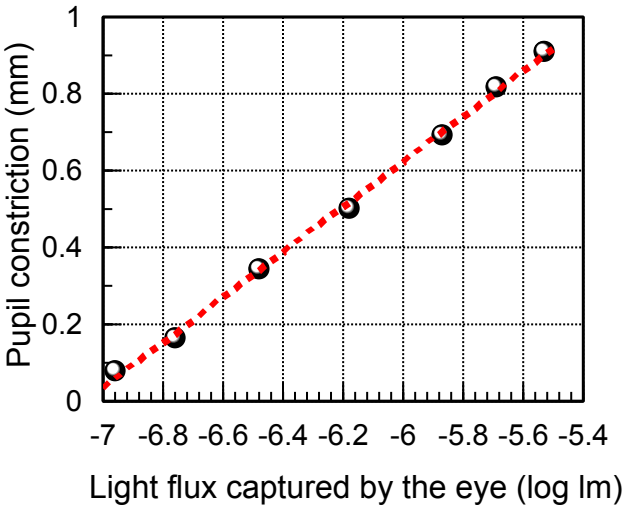

Figure 4-4 Data obtained on pupil constriction amplitude and the corresponding light flux captured by the eye. The light flux variations were achieved by increasing the target luminance. The data was collected with subject (a).

Once the relation between pupil constriction amplitude and light flux entering the eye was established, it could be used in the pupil model. The remaining problem was to decide on the slope and intercept of the fitted straight line needed to describe the relationship between pupil constriction amplitude and the total light flux entering the eye. The best approach was to use the measured pupil diameter changes for each subject from the measurement of pupil constriction described in Section 4.3. The light levels were extracted at which the measurements of pupil constriction were taken. At these light levels, the logarithms of light flux were simulated by the pupil model. Therefore, the measured pupil constriction amplitude as a function of the logarithm of light flux captured by the eye can be fitted into a straight line to obtain the slope and intercept. Thus, the predicted pupil constriction amplitude was achieved over a large range of light levels.

4.4 Results

As mentioned, the pupil constriction amplitudes in terms of pupil diameter changes were recorded for two individual subjects over a large range of light levels. The light levels described using retinal illuminance covered both below and above the individual discomfort glare thresholds. Figure 4-5 shows the results for the two subjects whose pupil constriction amplitudes were measured over three source sizes (0.62°, 1.33° and 1.73° in diameter).

The transient pupil response amplitudes to a uniform flash of light over a wide range of retinal illuminances are shown in Figure 4-5. The range investigated covered light levels both below and above the subjects' thresholds for discomfort glare. The properties of the stimulus in the measurement were identical to the main experiment that was used to measure the discomfort glare thresholds. Three different target source sizes were employed and their intensities covered a two log unit range in terms of retinal illuminance.

In addition, the trend of pupil constriction responses with a series of increasing flash intensities was predicted using the pupil model described in Section 4.4. It can be shown that a log-linear relationship between pupil constriction amplitudes and light levels in terms of retinal illuminance is also illustrated in Figure 4-5. This trend was maintained both below and above the discomfort glare thresholds. The black dashed line in Figure 4-5 indicates the corresponding discomfort glare thresholds for the specific subjects and employed source sizes; the red dashed line in Figure 4-5 indicates the log-linear trend for the pupil constriction amplitudes as a function of light levels.

The prediction represented by the red dashed line was calculated using the pupil model. As described in Section 4.4, for each of the full range of retinal illuminances, the target image (a uniform disc) was convolved with the PSF of the eye and was then passed through the Michaelis-Menton function. The log of the sum of this resulting image was transformed through a linear function to give the pupil signal. The linear function described in Section 4.4.3 was used. It can be seen from the separate experiment that the pupil constriction amplitude was found to be proportional to the log of the light flux of the target. As described, the slope and intercept of each linear function were based on the experimental data represented using black circles in Figure 4-5 for each source size and participant.

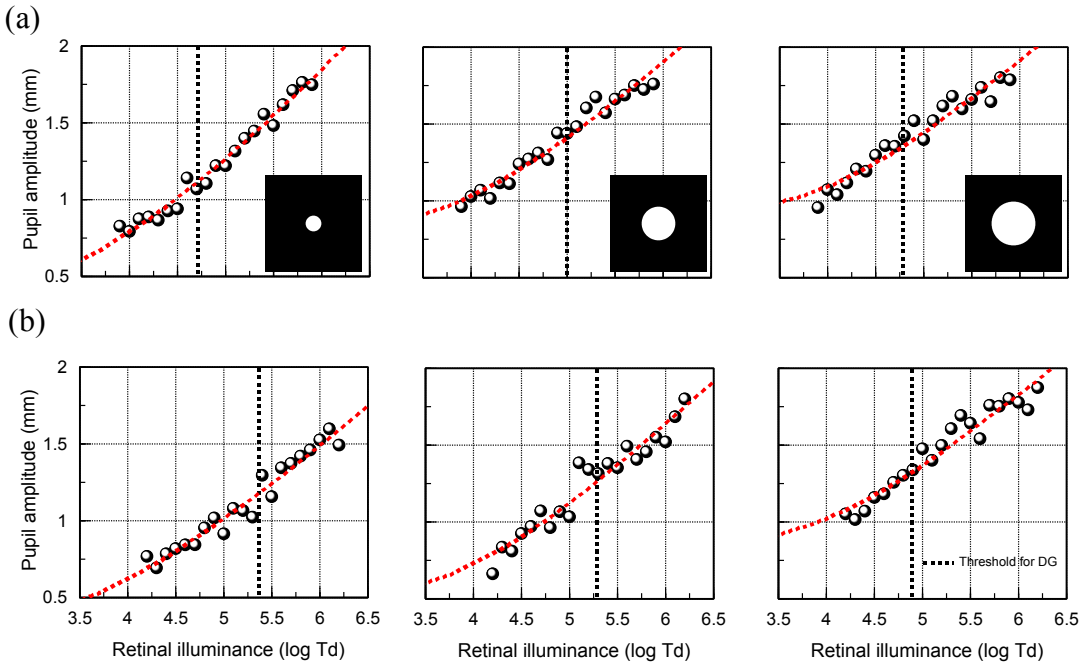

Figure 4-5 The pupil constriction responses to a number of uniform flashes of light were measured. The pupil constriction amplitude as a function of light level was also predicted. The black circles show the experimental data and the red dashed line show the predicted trend. The vertical black dotted line represents the corresponding discomfort glare threshold for specific individual and employed source size. Two subjects (a) and (b) were examined as indicated in Figure 4-2.

As presented in Figure 4-5, an approximately linear relationship was observed between the retinal illuminance of the light source on a log scale and the pupil constriction amplitudes. The predicted trend existed both below and above the discomfort glare thresholds. In addition, the expected saturation point of photoreceptor responses and ganglion cells is indicated. Based on the hypothesis put forward in the last part of Chapter 3, one would have expected a plateau in pupil constriction amplitudes as the light level increased above the discomfort glare thresholds. However, the results shown here indicate a continuous pupil response with the increasing light levels. Using the first two stages of the pupil model described in Section 4.4.1 and 4.4.2 and assuming a linear relationship between pupil constriction amplitude and the log of light flux of the target illustrated in Section 4.4.3, the continuous pupil response at high retinal illuminances could be accounted for by the scattered light in the eye driving the pupil.

4.5 Discussion

The pupil model described in this chapter was able to predict the transient pupil responses to the onset of discomfort glare both below and above the thresholds for discomfort glare. A log-linear relationship existed between the pupil constriction amplitudes and the retinal illuminance. The pupil model predicted that above the saturating point of the photoreceptor responses forward light scattering could drive the pupil to a certain degree so that the pupil continued to respond above the discomfort glare thresholds.

A number of earlier studies attributed discomfort glare to pupil fluctuation when examining the physiological origins of discomfort glare. It was known

that the sensation of discomfort glare appears to be associated with the pupillary response to light (Fry and King, 1975). The study investigating the role of the pupil constriction after brief exposures to light showed that the greater pupil constriction resulted in the greater visual discomfort (Fugate and Fry, 1956). However, their explanations were different to what has emerged from this study. They attributed the physiological origins underlying discomfort glare to pupil fluctuation. In fact, the findings in Chapter 3 and 4 reflect that this is not the case. Discomfort glare should be attributed to the saturation of photoreceptor responses, which has been illustrated using the measurement of discomfort glare thresholds in terms of retinal iluminance and the corresponding pupil model. The greater pupil constriction above the discomfort glare thresholds is caused by the effect of light scattering in the eye, rather than more visual discomfort.

To clarify that the pupil constriction responses above the individual discomfort glare thresholds are caused by light scatter in the eye, the employed pupil model was modified by removing the scatter light filtering. It is clearly shown from Figure 4-6 that without light scattering in the eye, the pupil constriction response reaches a plateau. The pupil constriction amplitude did however continue to increase above the discomfort glare threshold.

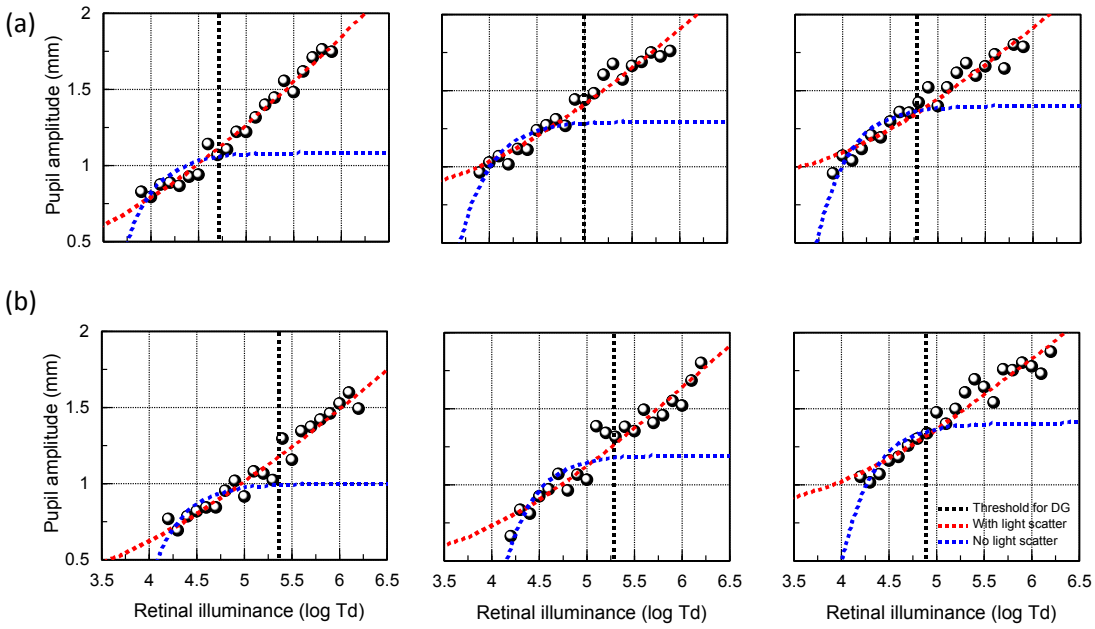

Figure 4-6 Two subjects were examined (a) and (b). The measured pupil constriction amplitudes (black circles) are fitted using saturating retinal mechanism with and without scatter light filtering. The predicted pupil signals with scatter effect are shown in red and without scatter effect in blue. Michaelis-Menton function is used to simulate the saturating mechanism with 3 log Td response range and a 1.6 log Td half response.

Other studies also investigated the pupil responses to discomfort glare. Howarth and his colleagues claimed that pupillary hippus is not a key factor in discomfort glare by showing no differences in fluctuation of pupil size with and without discomfort glare (Howarth et al., 1993). Their conclusion was in agreement with the findings in this chapter. The pupil response cannot easily be used to predict discomfort glare thresholds. The important observation that emerges from this study is that light scattered outside the area of the glare source is sufficient to drive the photoreceptors and to generate further increases in the pupil constriction amplitude, even when the glare source itself generates saturated signals.

5 Discussion and analysis

5.1 Introduction

The study of discomfort glare described in this thesis is part of a larger EPSRC funded project run in collaboration with Royal Holloway University and University College London. The whole project was concerned with street lighting glare, including both discomfort and disability glare. My principle investigation focused on the establishment of comfort/discomfort thresholds for various properties of the light source and different adaptation backgrounds using a series of laboratory experiments.

This chapter compares the measured thresholds for discomfort glare with the related findings from a number of other experiments carried out by other colleagues involved in the glare project. The apparatus and measurement techniques of the experiments carried out by others will be briefly introduced, followed by the comparison. A comparison of discomfort glare thresholds elicited with foveal and peripheral glare sources is presented in Section 5.2. Section 5.3 attempts to relate the measured discomfort glare thresholds with brain activity elicited under conditions of discomfort glare using fMRI neuroimaging techniques. Section 5.4 investigates and compares the measured discomfort glare thresholds and the corresponding scattered light in the eye measured in a separate study in the same subjects. Section 5.5 examines the measured discomfort glare thresholds in relation to estimates of functional contrast sensitivity in the same subjects.

The mechanisms and origins underlying discomfort glare have remained poorly understood in spite of significant progress in our understanding of disability glare. Through the comparisons of the corresponding findings related with discomfort glare, mechanisms that are reasonable and possible will be revealed, other than the retinal saturation mechanism mentioned in Chapter 3.

It has been generally suggested that visual distraction could be a key factor that causes discomfort glare (Lynes, 1977). When a light source in a room is considerably brighter with respect to the adaptation background luminance of the room, the bright light source can attract the point of regard. Discomfort glare is related with the brightness of the light source. The human eye pre-attentively struggles to avoid the discomfort glare; but at the same time, the discomfort glare is forced to transmit to the conscious mind as a complaint. Discomfort glare may disrupt the visual processing of complex visual tasks. However, it is not clear whether the discomfort glare presented in the fovea affects the visual processing of the tasks to the same extent as that presented in the periphery. The experiment that will be described in Section 5.2 measured the discomfort thresholds from peripheral glare. The results with respect to discomfort thresholds from peripheral glare will also be reviewed, along with the comparison between foveal and peripheral discomfort glare thresholds.

It has been suggested that functional magnetic resonance imaging (fMRI) could be useful as a new tool in the study of discomfort glare. fMRI has become a routine method for mapping neural activity in the human brain in

the presence of a certain form of visual stimulus. A previous fMRI study showed that the activity of cells in primary visual cortex increased with increasing luminance contrast of visual stimulus (Goodyear and Menon, 1998). The cortical areas with respect to visual perception were regarded as possible candidates for reflecting the strength of perceived discomfort glare. The fMRI study that will be introduced in Section 5.3 investigated the brain activity of two subject groups via fMRI while they undertook visual tasks with different light levels of discomfort glare. The subjects were divided according to their sensitivity to discomfort glare. The results will also be reviewed in Section 5.3, and certain patterns of brain activity that were related with the measured discomfort glare thresholds will be discussed.

It is well known that light scattered in the human eye affects the quality of the retinal image. Light scattering can cause a reduction in visual performance. Bright sources produce more scattered light and therefore one expects the effects of veiling glare to be more pronounced. The test that will be described in Section 5.4 assessed the properties of light scattering in the eye for a number of subjects. The results of the test will also be reviewed in Section 5.4, and the comparison between the measured discomfort glare thresholds and the intrinsic light scattering properties for the same subjects will be made.

In the study of discomfort glare, disability glare has to be mentioned. The difference between disability and discomfort glare is a matter of measurement. Disability glare measures what the subjects can do and their performances for a visual task, while discomfort glare measures how the

subjects feel and their appraisals. The introduction in Section 5.5 provided an assessment of functional contrast sensitivity under conditions of disability glare. The results will also be reviewed in Section 5.5 along with the comparison between discomfort glare in terms of the measured comfort/discomfort thresholds and disability glare in terms of the assessed functional contrast sensitivity.

Through the analysis and comparisons of a number of related findings, the properties of discomfort glare mechanism will be discussed further to improve our understanding of discomfort glare.

5.2 Comparison of foveal and peripheral discomfort glare thresholds

An element of the large study of disability and discomfort glare undertaken at City University, London included assessment of discomfort glare thresholds with peripheral glare sources. This study carried out largely by Dr Gary Bargary investigated what the discomfort threshold was when the glare was presented in the periphery.

In this experiment, the peripheral glare sources were mounted on a circular device. A screen was surrounded by the glare sources, shown in Figure 5-1. The glare stimulus consisted of four LED units produced by Perkin Elmer. As shown in Figure 5-1, the LED units were positioned at four different locations (0°, 90°, 180°, 270°). Each was 12° away from the centre of the screen horizontally and vertically. The screen employed in this experiment was an LCD 19'' display (Model: NEC SpectraView 1990SXi). Both the LCD monitor

and the LED units were calibrated with a spectroradiometer and a LMT 1009 luminance meter. The chromaticity of the peripheral glare stimulus and the LCD monitor was set to a neutral level with x = 0.305 and y = 0.323 according to CIE 1931 chromaticity space. The background luminance was set to constant at 5 cd/m^2.

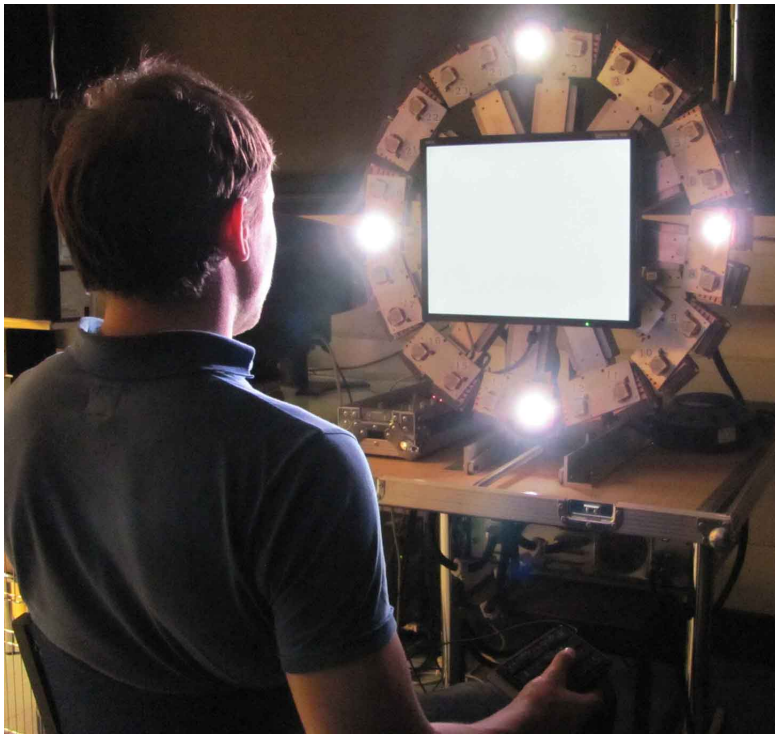

Figure 5-1 The apparatus used in the experiment measuring discomfort thresholds from peripheral glare. A screen presenting the Landolt C stimulus was surrounded by four LED units (Courtesy of Dr Gary Bargary).

In addition, a typical Landolt C stimulus was presented in the centre of the LCD monitor. Prior to the Landolt C stimulus, a fixation stimulus which was a cross subtending 1° was presented in the centre of the monitor to attract the subject's attention. All of these stimuli were accompanied by the peripheral LED lights.

The diameter of the Landolt ring was 20 minutes of arc. In order not to be accustomed to the presentation of the stimulus, the duration between the

disappearance of the fixation stimulus and the appearance of Landlot C stimulus was set to a random value, between 0.75 and 1.5 s. Each Landolt C stimulus was presented at a constant contrast of 300% and in one of the four different orientations (top-left, top-right, bottom-left and bottom-right). The subject was required to decide the position of the gap in the Landolt C. The contrast was calculated using Weber contrast, which is defined as $C = \frac{L - L_b}{L_b}$, where L and L_b represent the luminance of the target and the background, respectively. The background luminance of the LCD monitor was set to 24 cd/m^2. The viewing distance between the stimulus apparatus and the eyes of the participant was 1.5 m. Similar to the experiment of the measurement of pupil size described in Section 2.3, an infra-red camera was used to capture the video pupil image. The pupil size was recorded every 20 ms.

By method of adjustment, the discomfort glare thresholds were obtained in this experiment. Subjects could adjust the light level of the peripheral glare stimulus. Each subject was required to maintain fixation in the centre of the screen and simultaneously to adjust the luminance of four LED units in the periphery until the minimum visual discomfort was achieved. The peripheral glare was varied in terms of illuminance level at the plane of the pupil (lx). The step size was 1.5 lx and the increase and decrease of the brightness were controlled with two buttons. Each participant was asked to carry out ten repeats of the adjustment. However, the selected values from the last eight repeats were averaged to estimate the discomfort glare thresholds. The initial illuminance level (lx) for each out of ten repeats was varied randomly.

Once the appropriate glare source thresholds were determined by the subject for each of ten trials, the brightness of the peripheral glare was fixed and five Landolt C orientation discriminations were carried out. The Landolt C orientation discrimination lasted for 15 s. The reason why the behavioural assessment of discomfort glare thresholds was followed by the Landolt C orientation discrimination was that a longer steady glare stimulus was shown to the subjects so that they could tailor their criteria of the threshold judgment. Although the discomfort glare thresholds were obtained in terms of pupil plane illuminance (lx), the retinal illuminance (log Td) could be used to describe the discomfort glare threshold since the pupil size was measured throughout the test.

The behavioural assessment of discomfort thresholds from peripheral glare also provided the measured average threshold for an fMRI study (described in Section 5.3) which could be used as a baseline of light level to distinguish the high glare conditions from the low glare conditions. In addition, based on the results from this study, the participants were divided into two groups according to their sensitivity to glare.

Both this experiment and the one previously described measured the thresholds for discomfort glare. One major difference between this test and the primary one described in Chapter 2.2 is the position of the glare. In this test, glare was positioned in the periphery at four different locations, shown in Figure 5-2. Each LED unit was presented 12° away from the fovea. On the other hand, the primary experiment measuring the discomfort glare thresholds as a function of glare source size described in Chapter 2.2 used a

glare source presented in the fovea with varying source sizes. The background luminance surrounding the peripheral glare was set to 5 cd/m^2, while the ambient luminance employed in the measurement of discomfort glare thresholds as a function of glare source size was 2.6 cd/m^2.

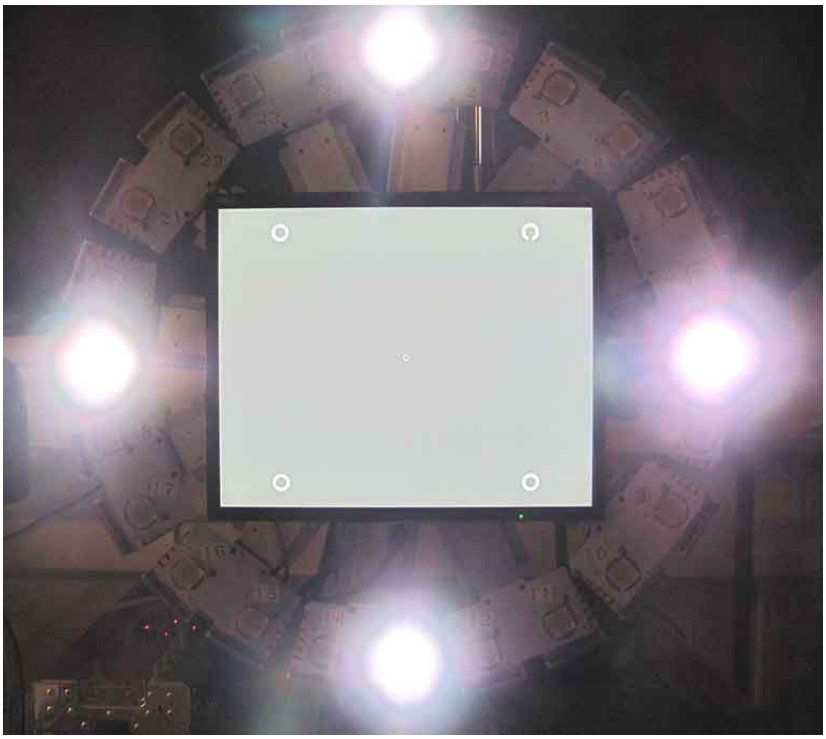

Figure 5-2 The position of peripheral glare. This set-up was used to measure the discomfort thresholds for peripheral glare (Courtesy of Dr Gary Bargary).

41 participants took part in the measurement of discomfort threshold from peripheral glare at City University London. The individual data are shown in Figure 5-3. As mentioned, the measurement variable in the test was pupil plane illuminance (lx). However, the final units were based on retinal illuminance (log Td) for the reason of comparison since the pupil diameter was measured throughout. It can be seen from Figure 5-3 that the discomfort threshold from peripheral glare varied from person to person within a two log-unit range. The average threshold for this sample of 41 participants was

4.95 log Td. This result is highly consistent with the finding shown in Figure 3-1 which was obtained from a sample of 50 observers.

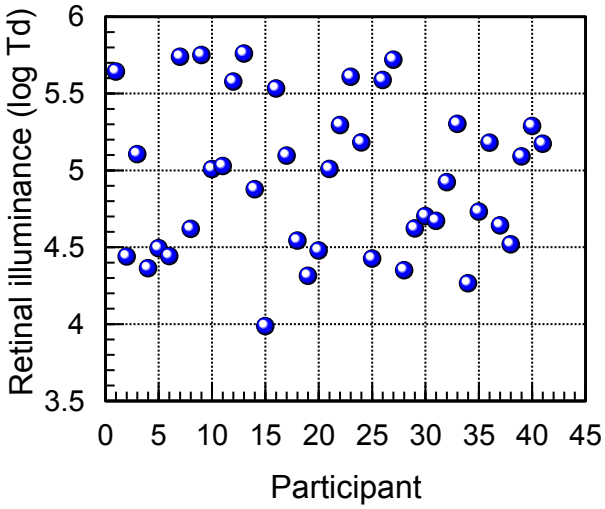

Figure 5-3 Discomfort glare thresholds measured for the peripheral glare. The average threshold was 4.95 log Td for a sample of 41 observers.

35 out of 41 participants carried out both my and Dr Bargary's tests at City University. The results for the measurement of discomfort thresholds from foveal glare took an average of five different source sizes for each individual. Figure 5-4 shows both sets of results on a single graph. The mean thresholds for discomfort glare in the fovea and in the periphery are 4.91 and 4.94 log Td respectively for this sample of 35 subjects. Although the average thresholds for both tests are pretty much the same, the subjects achieved a higher discomfort threshold when the glare was presented in the periphery. This is consistent with the previous findings (Guth, 1961, De Boer, 1967). With respect to individual data, a Pearson product-moment correlation was run to determine the relationship between an individual's discomfort threshold from foveal glare and that from peripheral glare. The data revealed little or no correlation between discomfort thresholds from foveal and

peripheral glare (r = 0.019, n = 35, p = 0.915), shown in Figure 5-5. This might be due to the high subjectivity of both tests. The same participant may change the criteria of the judgment of the presence of discomfort glare from time to time. In addition, the two tests were performed on two separate occasions by two different experimenters.

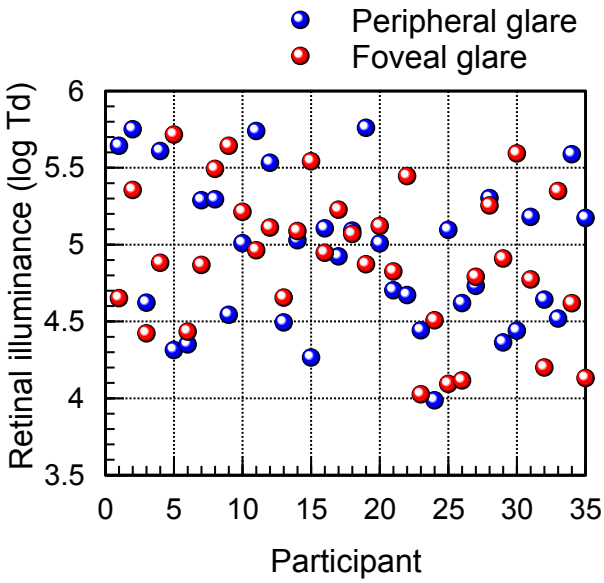

Figure 5-4 Foveal and peripheral discomfort glare thresholds plotted for each participant. The results show no significant correlation between two sets of thresholds in terms of retinal illuminance.

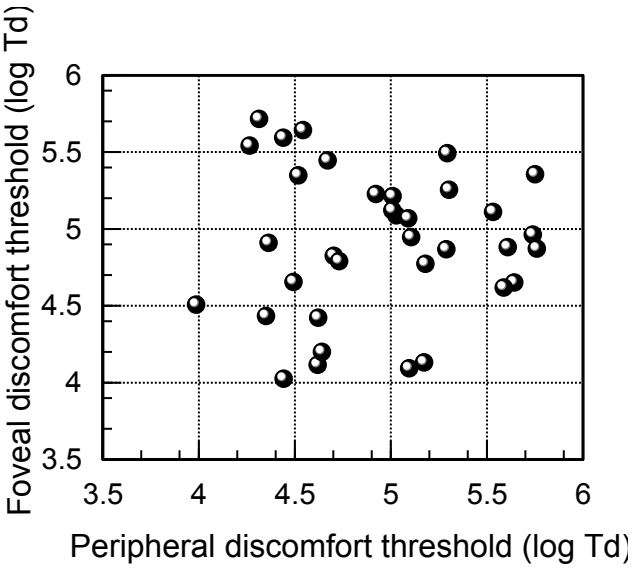

Figure 5-5 Discomfort thresholds in periphery versus fovea.

In summary, there was no significant correlation between foveal and peripheral discomfort glare thresholds. However, the distributions of discomfort glare thresholds both in periphery and fovea in terms of retinal illuminance (log Td) fell into a similar range from 4 to 6 log Td.

5.3 Comparison of discomfort glare thresholds with brain activity from fMRI neuroimaging

An fMRI experiment designed by the project team was implemented to investigate the neural mechanisms underlying discomfort glare. The analysis of fMRI data was carried out largely by Dr Michele Furlan at Royal Holloway College, University of London.

Through the behavioural assessment of discomfort glare thresholds carried out at City University, London (see Section 5.2), the mean threshold (4.95 log Td) for a population of 41 participants was achieved. Based on the mean value, three light levels with different glare conditions were established: 3.95, 4.95 and 5.95 log Td. The low glare condition, 3.95 log Td, was obtained using the mean discomfort glare threshold minus 1 log Td; whereas the high glare condition, 5.95 log Td, was obtained with the mean threshold plus 1 log Td. The fMRI test was carried out under these three different glare conditions. In addition, the participants were separated into two groups according to their sensitivity to discomfort glare. One subject group had lower thresholds for discomfort glare, while the other group had higher thresholds. All the participants involved in the fMRI test were ordered according to their thresholds for discomfort glare. The first 14 subjects with the thresholds lower than 5.10 log Td were attributed to lower threshold group. The

remaining 14 subjects with the thresholds higher than 5.10 log Td were attributed to higher threshold group. The results from the fMRI experiments were then compared between these two groups.

Similar to the preliminary behavioural assessment for discomfort glare thresholds described in Section 5.2, a screen surrounded by the glare sources was employed. Again, the glare sources consisted of four LED units produced by Perkin Elmer that were mounted on a circular device. However, the screen used in the fMRI experiment was a rear-projection screen. Therefore, in addition to the screen, a LCD projector was employed. The visual stimuli, including the fixation stimulus and the Landolt C stimulus, were projected by the projector onto the screen. The whole apparatus was placed at the end of the scanner bore, shown in Figure 5-6. The subject viewed both the projection screen and the glare sources via a mirror mounted on the head coil. The viewing distance was 1.5 m.

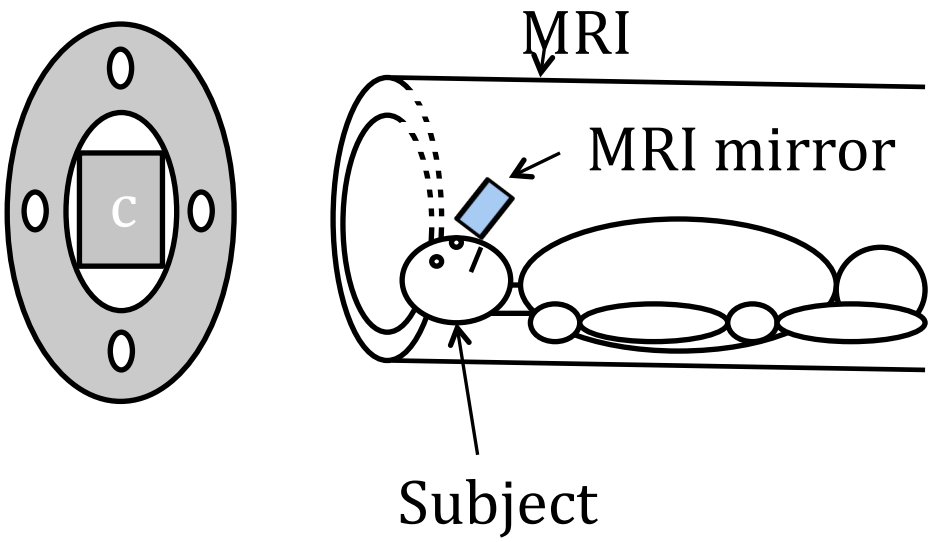

Figure 5-6 The apparatus in the fMRI experiment (Courtesy of Dr Michele Furlan).

The stimuli projected onto the projection screen were identical to those presented on the LCD monitor in the behavioural experiment. All visual stimuli were generated by a computer program using MATLAB. The glare source surrounding the projection screen in this experiment was set to three different light levels to produce three glare conditions as mentioned above. As in the behavioural assessment, the peripheral glare levels were changed in terms of illuminance level at the plane of the pupil (lx). All the subjects were required to complete the Landolt C orientation discrimination under all three glare conditions.

Simultaneously, the pupil images were captured throughout. Similarly, an infra-red video camera was positioned close to the eye to obtain the pupil image. The purpose for capturing the pupil image was to examine the extent to which the pupil size changed under different glare conditions. In addition to the infra-red camera, ViewPoint software produced by Arrington Inc. was used to track the pupil and measure its size at a sampling frequency of 60 Hz.

A block design was involved in the technique for fMRI neuroimaging in which two conditions are alternated in blocks: ON phase and OFF phase. ON phase indicates the condition where the peripheral glare is on at one of the three glare levels, while OFF phase indicates that the glare is completely off. Each scan run started with an OFF phase and each of the three different glare levels was repeated three times in a random order, which ended up with 9 ON phase blocks. An additional OFF phase block was introduced near the middle of each run in order to de-phase physiological noise.

During each scan run, the fixation stimulus was presented in the centre. This was followed by 4 Landolt C stimuli each presented for 200 ms. The interval time between two Landolt C stimuli varied between 750 and 1250 ms. After a period of 2 s without any Landolt C presentation, another series of 4 Landolt C stimuli were presented. The process of the stimuli presentations continued until the end of scan run. The subject was required to indicate the orientation of Landolt C by pressing one of the four buttons.

As introduced in Chapter 1, in addition to the human eye involved in the perception of the complex visual world, the human brain also plays an important role in accomplishing certain biologically relevant visual tasks. Using a combination of functional neuroimaging and psychophysical behavioural assessments, more information can be obtained to understand the underlying visual attributes of discomfort glare.

Some studies have claimed that a certain area of the human brain is involved in the processing of glare stimuli and the neural mechanisms related to discomfort glare should not be neglected. Stone proposed a theoretical model for the explanation of discomfort glare in the eye (Stone, 2009). He applied the gate control theory of pain to the trigeminal nucleus. It has been suggested that the eyes, facial muscles and extraocular muscles act as a linked system when responding to the lighting conditions. When the lighting conditions are excessive and inhibit the linked system to perceive as clear a retinal image as possible, strain is imposed, which initiates activity in the trigeminal nucleus. Stone's model proposed that some areas of the human

brain might be involved in the process of how the linked system responds to discomfort glare.

The fMRI test was designed to explore the functional organization of high-level human visual cortex under conditions of discomfort glare. From the fMRI scans, a certain pattern of brain activity related to the sensation of glare was revealed. This section will also uncover the results of fMRI neuroimaging under conditions of discomfort glare, followed by the comparison of discomfort glare thresholds with the associated brain activity.

During the functional MRI scan, the subjects were divided into two groups based on their sensitivity to discomfort glare. The differences in brain activity as measured in the fMRI study were manifested where the subjects with high and low discomfort glare thresholds were compared. The results showed that the subject group with lower discomfort glare thresholds had more neural activity in some regions of the brain, including bilateral lingual gyri, bilateral cunei and superior parietal lobule. For each of three glare levels examined, the differences in brain activity also existed when two subject groups were compared. It was suggested that the group with lower discomfort glare thresholds had significantly greater neural activity for every discomfort glare condition investigated.

Through the findings for the measurement of discomfort glare thresholds described in Chapter 3, the saturation of photoreceptor responses in the retina was suggested as one of the mechanisms underlying visual discomfort. Although the findings in Chapter 3 are more consistent with the retinal mechanism for discomfort glare due to the saturation of photoreceptor

signals, there could also be a cortical component involved as manifested in the differences in neural activity shown in the fMRI neuroimaging where the brain images for the high and low discomfort glare threshold groups were compared.

5.4 Comparison of discomfort glare thresholds with scattered light

The study involving the measurement of scattered light in the eye was conducted by Dr Emily J. Patterson as part of the larger investigation into light scatter and glare. It is of great interest to measure the scattered light in the eye for the same population of subjects whose discomfort glare thresholds were examined.

A psychophysical flicker nulling technique was employed to measure the scatter function of the human eye. Generally, a series of extended annuli were used to estimate the amount and angular distribution of scattered light in the eye for a number of participants. This technique was developed and implemented at City University, London and made available for this study. For the purposes of completeness, this scatter test is briefly summarized here but is described in full in Barbur's study (Barbur et al., 1993).

As for the evaluation of scatter function of the eye, the P-SCAN system illustrated in Section 2.3 was used to also enable the simultaneous measurements of pupil size and eye movements. During the measurement of scattered light, the subject viewed the centre of the visual display. The viewing distance was 0.7 m and a chin and forehead rest was used to locate

the subject's head. Over the rest, a hood was placed to reduce the amount of external light entering the eyes of the observer.

The scatter stimulus was presented on the screen, consisting of three concentric circles. A dark target disc was located in the centre; an extended annulus was placed outside; an isolation annulus was located in between, shown in Figure 5-7. The luminances of the display background and the isolation annulus were set to 5 cd/m^2 and 25 cd/m^2, with chromaticity coordinates of x = 0.169, y = 0.085 and x = 0.450, y = 0.450, respectively. An annular scatter source illustrated as the extended annulus was generated at different eccentricities. The central disc with the size of 0.8° formed the test target. The chromaticity coordinates for both the test target and the scatter source were x = 0.290, y = 0.317.

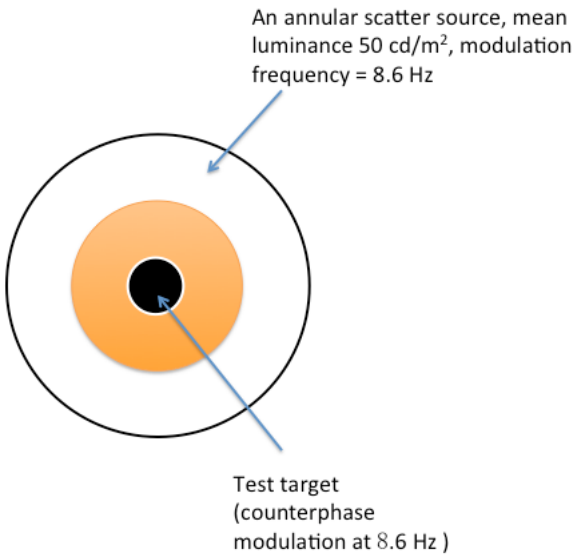

Figure 5-7 A schematic diagram showing the use of an extended annulus. It shows one of the five extended annuli employed in the scatter test.

The light scatter stimulus was modulated sinusoidally with a mean luminance of 50 cd/m^2 at a frequency of 8.6 Hz. The duration of a burst of

flicker was around 350 ms. The light scattered from the annulus source causes the central dark disc to flicker in phase with the scatter source. The luminance of the test target was then modulated in counterphase with the scatter source at the same frequency in order to cancel out the modulation of retinal illuminance caused by the scatter source. The mean luminance of the test target could be adjusted during the test, while the mean luminance of the scatter source remained unchanged.

Five different eccentricities of the scatter stimulus were used and the dimension of each extended annulus was adjusted to maintain a constant pupil plane illuminance. The effective radii of each extended annulus for each subject were calculated by the program. Once the flicker-null point was obtained for each annulus, the next would be presented in a random order. Five repeats for each of the five eccentricities were carried out in one run. Scatter parameters obtained were based on the mean values for each of the five eccentricities.

All the participants were given about three minutes to complete dark adaptation. Each subject was required to complete two runs and the obtained mean scatter parameters were used in the final analyses. During each flicker presentation, the subjects were asked to fixate on the central disc and to point out whether the central disc flickered or not. According to the feedback from the subjects, the experimenter would then increase or decrease the mean luminance of the test target in the centre. When the subjects were ready to carry on the test, the stimulus with the adjusted mean test target

luminance would be presented until the minimum perception of flicker at the test target was perceived.

The output of the scatter test consisted of three parameters: *n*, *k* and *k'*. *n* is a scatter index, describing the angular distribution of the scattered light. The straylight parameter, *k*, is proportional to the amount of scatter in a given eye. *k'* is then computed based on *n* and *k* according to an empirical scatter function (Barbur et al., 1993). The generated *k'* is an integrated straylight parameter, showing less variability in changes of scattered light. The scatter index, *n*, and the straylight parameter, *k*, were then used in Equation 5-1 to estimate the equivalent veiling luminance of the scatter source.

$$L_s = kE\theta^{-n} \tag{5-1}$$

In Equation 5-1, *E* is the illuminance level at the plane of the pupil produced by the scatter source, θ is the angular eccentricity of the scatter source, and L_s, known as the equivalent veiling luminance, is the luminance of an external source that produces the equivalent amount of retinal illuminance as that produced by the scattered light. In a test for the measurement of scattered light in the eye, the pupil plane illuminance, *E*, and the eccentricity of the annular scatter source, θ, are known. The straylight parameter, *k*, and the scatter index, *n*, can be obtained. Therefore, the equivalent veiling luminance that is the amount of light scattered by the annular source can be calculated based on Equation 5-1.

k' reflects a measure of the total amount of light scattered in the eye (Hennelly et al., 1997, Barbur et al., 1993), which can be illustrated as follows:

$$k' = \int_2^{\infty} kE\theta^{-n}\, d\theta \qquad (5\text{-}2)$$

In Equation 5-2, k is the straylight parameter that is proportional to the amount of scattered light; E is the illuminance level at the plane of the pupil; θ is the angular eccentricity of the scatter source; and n is the scatter index which determines angular distribution of scattered light.

The scatter graph of k' as a function of age is shown in Figure 5-8. The result is based on a sample of 40 participants. As mentioned in Section 2.4, although 53 participants were involved in the scatter test, the valid data was only from a sample of 40 subjects. It can be seen that the integrated straylight parameter, k', changes little with age for the subjects under 45 years. A rapid increase in the amount of scattered light follows above 45 years. This finding is consistent with the previous one revealing the effect of age on light scattering (Hennelly et al., 1998). The age-related increase in scattered light within the eye might be caused by increased inhomogeneity of the human lens (Boynton et al., 1954).

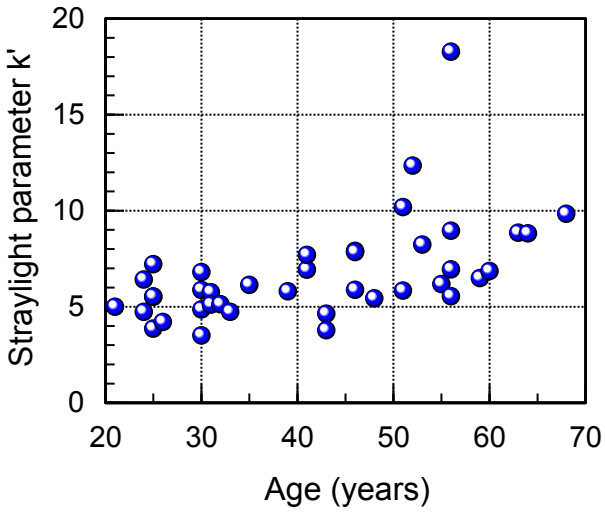

Figure 5-8 The integrated straylight parameter as a reference of age.

The measured discomfort glare thresholds in the fovea were valid for a sample of 36 subjects among those 40 participants. Both the integrated straylight parameters and discomfort glare thresholds for a population of 36 participants were plotted in Figure 5-9. It is clear that the integrated straylight parameter changed little with age for younger subjects, while it increased with age for older subjects. On the other hand, the measured discomfort glare thresholds in terms of retinal illuminance did not change significantly with age. It reveals that there was no main effect of age on discomfort glare thresholds, despite increased scatter with aging. The more forward scatter within the eye for older people causes a more pronounced decrease in the retinal illuminnace of the glare source. The consequence of the reduction is to allow for an increase in the retinal illuminance that was used for compensation so that the saturation could be reached. Therefore, the threshold for discomfort glare for an individual was not necessarily related to the amount of scattered light in his/her eyes. The correlation between the integrated straylight parameter and measured discomfort glare thresholds for those 36 participants is shown in Figure 5-10.

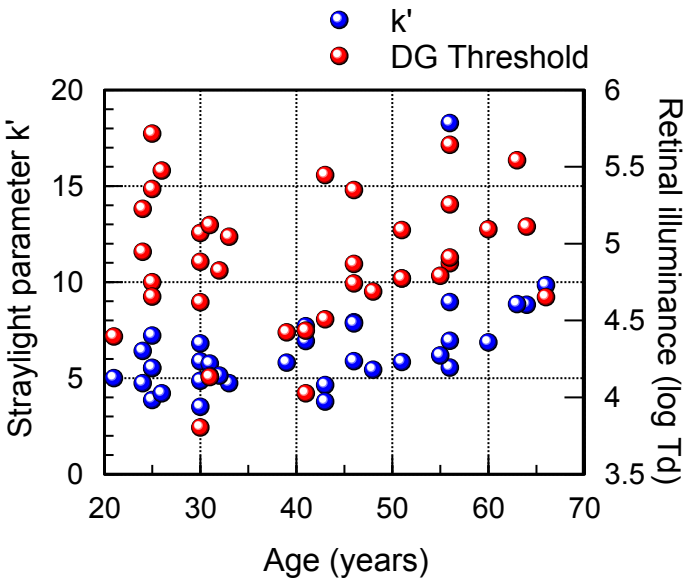

Figure 5-9 Comparison between integrated straylight parameter and discomfort glare threshold for a sample of 36 participants.

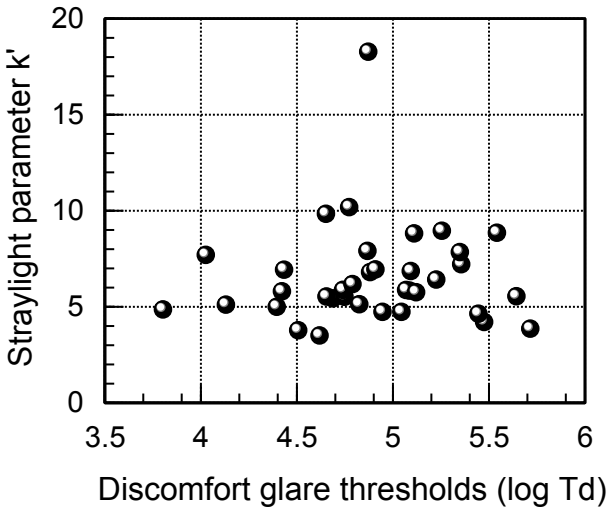

Figure 5-10 Correlation between integrated straylight parameter and discomfort glare thresholds for the same subjects as those in Figure 5-9.

5.5 Comparison of discomfort glare thresholds with contrast sensitivity thresholds under conditions of disability glare

Measurements of functional contrast sensitivity were carried out by Dr Emily J. Patterson as part of the larger study undertaken at City University, London. The assessment of functional contrast sensitivity employed the Contrast Acuity Assessment (CAA) test. For the purposes of completeness, this CAA test is briefly summarised here but is described in full in Chisholm's study (Chisholm et al., 2003).

In the assessment of functional contrast sensitivity, the visual display was an NEC CRT monitor operating at 120Hz (Model: NEC MultiSync FP2141SB). The P-SCAN system enabled the simultaneous binocular measurement of pupil sizes with a 50 Hz infra-red camera. A chin and forehead rest were used to position the subject's head. During the test, the subject was required to view the centre of the monitor through a large infra-red reflecting mirror. The viewing distance was 1.6 m. A black hood was placed over the forehead rest and the camera equipment, thus minimizing the amount of external light reaching the subject's eyes.

Two LED units produced by Perkin Elmer were used as a glare source in this experiment. Each consisted of four primary LEDs. The LED units were surrounded by black felt to reduce the dispersion of light, and two units were vertically stacked, which were located at 10° to the right of fixation horizontally. The chromaticity coordinates of the combined LED units was x= 0.278, y=0.286 according to CIE 1931 chromaticity space.

An example of one stimulus is shown in Figure 5-10. The spectral power distributions of both the target and background had a chromaticity of x=0.305, y=0.323. The Landolt C target was presented either at the centre of the screen or 5° to the left or right of fixation. Therefore, with respect to the glare source, the eccentricities of the target were 5°, 10° and 15°, since the glare source was placed at 10° to the right of fixation. The target presented in Figure 5-10 is positioned at 5° to the left of fixation along the horizontal meridian, thus having an eccentricity of 15° with respect to the glare source. The subjects were required to fixate the centre of the display throughout, regardless of the location of the target. The fixation stimulus in the centre was presented for 150 ms, followed by a delay of 800 ms, before the presentation of the Landolt C stimulus. The duration of Landolt C presentation lasted for 80 ms.

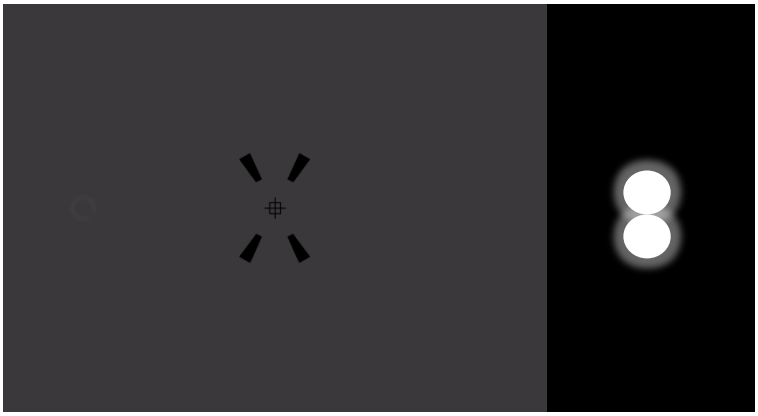

Figure 5-11 A schematic diagram of subjects' view of the experimental setup. The glare was placed to the right of the screen, 10° from fixation. The Landolt C stimulus was presented at 5° to the left of fixation, one of three locations. The gap size was set at 8' for this target. The background luminance was 2.6 cd/m² and the glare level was 1.35 lx. (Courtesy of Dr Emily J. Patterson).

The subject was asked to report the orientation of the gap in a Landolt C stimulus for each presentation. The contrast of the target was adjusted according to the subject's response until the contrast threshold was obtained.

Each run consisted of three interleaved staircases; each staircase was related to one target location. Therefore, three contrast thresholds at three different locations were obtained for each run.

The CAA test, illustrated in Figure 5-10, was carried out under the condition of one lighting combination with the background luminance at 2.6 cd/m^2 and the glare level at 1.35 lx. In addition, another two background levels, 1 cd/m^2 and 26 cd/m^2, and another two glare levels, 0 lx and 19.21 lx, were used in the measurements of functional contrast sensitivity. Consequently, the lighting conditions for the CAA test had nine combinations. The subject was required to complete the tests under nine lighting combinations in a random order.

Before the test, three minutes were required to complete dark adaptation for each participant, during which the instructions and practices were given. The background luminance and glare level were set to one lighting combination, and one experimental run for that lighting combination was completed. Then another luminance combination was set and another run was completed. Totally, 27 contrast thresholds were produced since each run for each of the nine combinations yielded three contrast thresholds for three target eccentricities.

Since the pupil size varied with the lighting conditions, one estimate of pupil diameter was produced for each of the nine lighting combinations. In total, nine estimates of pupil diameter were yielded through the monocular measurement of pupil size.

It has been generally accepted that under conditions of disability glare, the contrast of the retinal image is reduced and thus the visual performance is impaired. The factors that affect the impaired visual performance include the luminance, size and eccentricity of the glare source (van den Berg et al., 2013). These factors also have an impact on discomfort glare. The effects on discomfort glare have been established in Chapter 3.

For the reason of comparison between disability glare and discomfort glare, the obtained contrast thresholds in the fovea in the presence of high glare for the same background as that used in the study of discomfort glare were only concerned. The functional contrast thresholds for each individual for the concerned condition are shown in Figure 5-11. It shows that the functional contrast thresholds varied from person to person. The finding suggests that the visual performance under conditions of disability glare changed amongst a number of observers. In addition, it slightly depended on the age. Since the participants over 45 years were found to have an increasing amount of scattered light within the eye, a corresponding increase in functional contrast thresholds was expected. As shown in Figure 5-11, the subjects aged 45 years or above required higher minimum contrast that could be resolved than younger subjects.

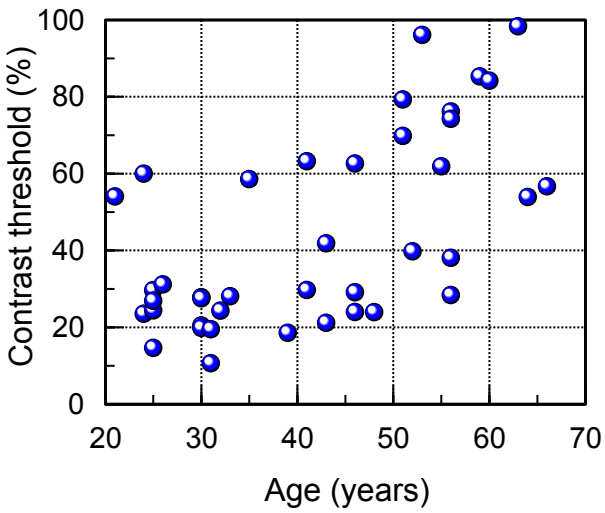

Figure 5-12 The individual's functional contrast thresholds as a function of age for a sample of 40 subjects. The Landolt C stimulus in the CAA test was presented in the fovea with the background luminance of 2.6 cd/m². The glare placed at 10° to the right of the centre was set to 19.21 lx.

The results of measured discomfort glare thresholds in the fovea from 36 out of those 40 participants were obtained. The comparison of discomfort glare thresholds and functional contrast thresholds under condition of disability glare is illustrated in Figure 5-13. The corresponding correlation is shown in Figure 5-14.

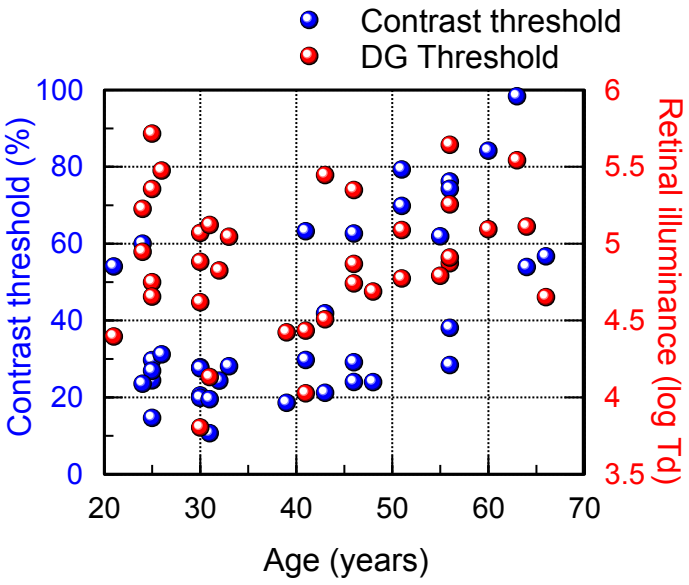

Figure 5-13 Comparison between functional contrast threshold and discomfort glare threshold for a sample of 36 participants. The Landolt C stimulus in the CAA test was presented in the fovea with the background luminance of 2.6 cd/m². The disability glare placed at 10° to the right of the centre was set to 19.21 lx.

As shown in Figure 5-13, the assessed functional contrast threshold under the condition of disability glare depends on the age, while there is no effect of age on the measured discomfort glare thresholds. A lot of individual differences are involved in the susceptibility to discomfort glare due to the subjective measurement. However, the severity of disability glare depends on the age. Through the comparison, it is clear that the mechanisms underlying disability glare are not always the same as those behind discomfort glare.

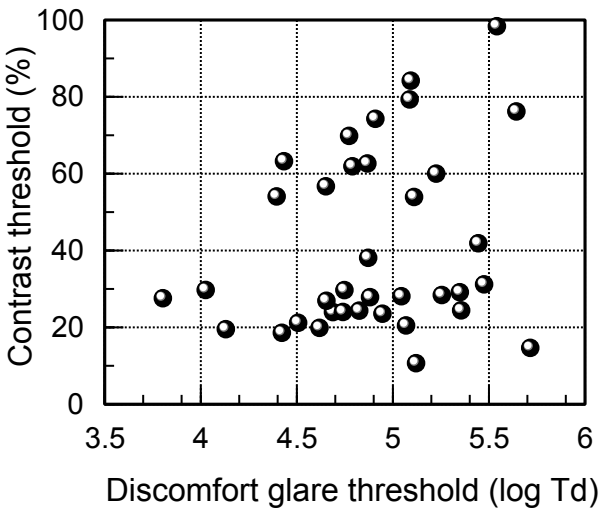

Figure 5-14 Correlation between functional contrast threshold and discomfort glare threshold for the same subjects as those in Figure 5-13.

6 Summary and conclusions

This thesis describes a number of techniques designed and carried out to investigate various aspects of discomfort glare with the principal aim of identifying the key mechanisms involved. The way discomfort glare thresholds were affected by surround luminance and glare source parameters was investigated and the results provided useful information on the design of lighting installations that produce sufficient horizontal illumination with minimum discomfort glare.

6.1 Mechanisms for discomfort glare

This study of discomfort glare is timely since the mechanisms underlying discomfort glare are poorly understood by comparison with those that cause disability glare and the recent advances in lighting technology through the introduction of LEDs have tended to increase glare from lighting installations. The findings described in this thesis are discussed in relation to the properties of plausible retinal and central mechanisms that may cause discomfort glare.

The findings from this study suggest that retinal mechanisms play a key part in discomfort glare. We propose that the saturation of photoreceptor responses and the corresponding changes in the retinal representation of bright glare source images play a critical role in the determination of discomfort glare thresholds. Once saturation occurs, the photoreceptors in the retina can no longer signal the increase in retinal illuminance and this causes the complete loss of spatial detail over the glare source and the spreading of its boundaries and edges through increased amounts of

scattered light. In addition, the intrinsically photosensitive retinal ganglion cells (ipRGCs) may also be involved since the light levels involved are sufficiently high to drive melanopsin (Provencio et al., 1998). There are other side effects that may be linked to discomfort glare. The intrinsic photoactivation of melanopsin and the saturation of protoreceptor signals that feed into ipRGCs may exacerbate light-induced migraine (Tatsumoto et al., 2013).

It is generally accepted that up to 30% of the light entering the eye is scattered by intraocular structures and does not contribute to image formation at the retina (Chou, 2012). The forward light scatter creates a veiling effect that reduces the contrast of the retinal image. This is the principal factor that causes disability glare. Similarly, scattered light may also play an important role in the study of discomfort glare. Scattered light generated by a sudden increase in retinal illuminance stimulates adjacent regions of the retina and causes significant loss of spatial detail and broadening of stimulus boundaries. This is because scattered light extends the edges of the glare source and causes loss of spatial detail over the target that precedes photoreceptor saturation.

Scattered light in the eye also causes a reduction in retinal illuminance over the glare stimulus and this reduction varies with glare source size. As a result, saturation of photoreceptor responses will require a higher retinal illuminance and hence an increase in discomfort glare thresholds. This factor and the increased light scatter with age may well account for the relatively unchanged discomfort glare thresholds as a function of age.

The fact that the measured discomfort glare thresholds are size dependent can be accounted for by the variation in the number of ganglion cells that is related to the corresponding edges of the glare source. Discomfort glare thresholds reflect the saturation of photoreceptor responses and the loss of spatial details within and around the glare sources. In addition, the thresholds also reflect the subject's subjective perceptual experience and this aspect can be significantly affected by disability glare. The latter may also contribute to increased variability by affecting the subject's response criterion over time. It is not, therefore, surprising that discomfort glare thresholds, in terms of retinal illuminance, vary by as much as 1 log unit from the mean.

The findings from the measurement of discomfort glare thresholds and pupil constriction amplitudes provided the data needed to put together a model of the pupil response to light flux increments on the retina. The model predicts well the experimental findings and reinforces the conclusions of the study. The model predicts the transient pupil response to the onset of the glare stimulus over a range of retinal illuminance both above and below the discomfort glare threshold. It was found that there is a log-linear relationship between the pupil constriction amplitudes and the retinal illuminance both below and above the discomfort glare thresholds. The fact that the pupil continues to respond even above the threshold for discomfort glare was predicted by the pupil model, which is a new observation of great interest. These findings suggest that the scattered light above the discomfort glare threshold continues to drive the dynamic pupil response. Although this

conclusion is supported by the model, the possibility remains that above the discomfort glare threshold, the continued increase in pupil response amplitude with increasing retinal illuminance is driven by melanopsin through ipRGCs. Further studies are needed to distinguish between these two hypotheses, both of which can account for the observed experimental findings.

The study of discomfort glare using fMRI imaging of the brain conducted at the Royal Holloway College provides some evidence for the existence of cortical mechanism that respond selectively to visual stimuli above the discomfort glare threshold. The neural activity in the visual cortex with and without discomfort glare was measured in the fMRI study. It was found that there were differences in neural activity between the high and low glare-sensitive participants. The findings in the fMRI study showed that the high glare-sensitive subjects had more neural activity by comparison with the low glare-sensitive ones. Although the findings from the measurement of discomfort glare thresholds revealed retinal component of mechanisms for discomfort glare due to the saturation of photoreceptor signals in the retina, there could also be a cortical component involved as manifested in the differences in neural activity measured in the fMRI study.

In summary, the findings from this study suggest that discomfort glare can be attributed to both retinal and cortical mechanisms.

6.2 Application of discomfort glare study

The findings reported in this thesis suggest that one may be able to control discomfort glare in lighting installations without having to reduce horizontal

illuminance to a level that no longer supports adequate vision. These findings may have numerous applications.

In street lighting, discomfort glare has been shown to be a great disadvantage to motorists and pedestrians. This is due to the fact that discomfort glare from street lighting including street lamps and vehicle headlamps can cause distraction and fatigue for both motorists and pedestrians and this can lead to accidents. The presence of adverse street lighting conditions may increase the possibility of road traffic accidents. The findings from this study suggest that street lighting can be improved without exceeding the thresholds for discomfort glare.

The main experiment described in this thesis is the measurement of discomfort glare thresholds in terms of retinal illuminance for a number of parameters including glare source size, eccentricity and background luminance. The most effective method to control discomfort glare is to manipulate the glare source size. Although the results from the primary experiment show that the discomfort glare thresholds vary with the glare source size, the relatively slight dependence on glare source size may have critical implications in the design of street lighting. The main findings suggest that the desired levels of horizontal pavement illuminance could be achieved without changing the level of discomfort by using the appropriate source size of the street lamp.

6.3 Limitations

There are a number of issues that limit the findings of the measured discomfort glare thresholds. Therefore, the variability in thresholds for

discomfort glare is comparatively larger than that was expected. One of these matters is that the chromaticity of the glare source was fixed. The currently used glare source contained four LEDs that were equally driven. That resulted in a pinkish light source, rather than a white source. In addition, the glare stimulus was presented as a brief flash. The length of the flash was also fixed. That may be the source of the large inter-subject variability in thresholds.

6.4 Future work

This thesis has investigated discomfort glare by employing a number of measurements and by developing corresponding models. Further studies are needed to improve the accuracy with which discomfort glare thresholds can be measured and to account for the large inter subject variability.

The chromaticity of the glare source could be varied. This could be accomplished by an additional experiment that varies the chromaticity of the glare source to investigate the effect of spectral power distribution of the glare on discomfort glare thresholds.

The glare stimulus employed in the main experiment measuring the discomfort glare thresholds was brief in order to minimize light adaptation, i.e., a 300 ms flash. The onset of pupil constriction followed the onset of the glare stimulus. It remains of interest to establish how discomfort glare thresholds may change for stimuli that are viewed continuously.

The current findings also suggest that when the background luminance was set to mesopic light levels, there is little effect of background on discomfort

glare thresholds. To account for the results, a number of additional mesopic light levels could be chosen as the local background luminance. The measurement of discomfort glare thresholds could be carried out with a range of mesopic background light levels to reveal how the mesopic vision affects the perception of discomfort glare.

Further experiments and modeling work is also needed to establish whether the continued increase in pupil response amplitude well above the threshold for discomfort glare can be attributed to melanopsin signals or simply to scattered light that falls outside the stimulus area.

References

ADRIAN, W. 2003. Spectral sensitivity of the pupillary system. *Clinical and Experimental Optometry,* 86**,** 235-238.

ALPERN, M., MCCREADY, D. W. & BARR, L. 1963. The dependence of the photopupil response on flash duration and intensity. *The Journal of general physiology,* 47**,** 265-278.

BARBUR, J. L. 2004. Learning from the pupil-studies of basic mechanisms and clinical applications. *The visual neurosciences,* 1**,** 641-656.

BARBUR, J. L., DE CUNHA, D., HARLOW, A. & WOODWARD, E. G. 1993. Methods for the measurement and analysis of light scattered in the human eye. *Non-invasive Assessment of the Visual System (Technical Digest Series).* J. Opt. Soc. Am.

BARBUR, J. L. & STOCKMAN, A. 2010. Photopic, Mesopic and Scotopic Vision and Changes in Visual Performance. *Encyclopedia of Eye,* 3**,** 323-31.

BARBUR, J. L., THOMSON, W. D. & FORSYTH, P. M. 1987. A new system for the simultaneous measurement of pupil size and two-dimensional eye-movements. Pergamon-Elsevier Science Ltd the Boulevard, Langford Lane, Kidlington, Oxford, England OX5 1GB.

BAYLOR, D. A., LAMB, T. D. & YAU, K. W. 1979. The membrane current of single rod outer segments. *The Journal of physiology,* 288**,** 589-611.

BAYLOR, D. A., NUNN, B. J. & SCHNAPF, J. L. 1984. The photocurrent, noise and spectral sensitivity of rods of the monkey Macaca fascicularis. *J Physiol,* 357**,** 575-607.

BENNETT, C. A. 1977. Discomfort glare: concentrated sources—parametric study of angularly small sources. *Journal of the Illuminating Engineering Society,* 7**,** 2-15.

BERMAN, S. M., BULLIMORE, M. A., BAILEY, I. L. & JACOBS, R. J. 1996. The influence of spectral composition on discomfort glare for large-size sources. *Journal of the Illuminating Engineering Society,* 25**,** 34-41.

BERMAN, S. M., BULLIMORE, M. A., JACOBS, R. J., BAILEY, I. L. & GANDHI, N. 1994. An Objective Measure of Discomfort Glare. *J Illum Eng Soc***,** 40-49.

BINDER, S. C. 2003. *Evaluation of Discomfort Glare and Pavement Marking Material Visibility for Eleven Headlamp Configurations.* Virginia Polytechnic Institute and State University.

BITSIOS, P., PRETTYMAN, R. & SZABADI, E. 1996. Changes in autonomic function with age: a study of pupillary kinetics in healthy young and old people. *Age and ageing,* 25**,** 432-438.
BODMANN, H. W., SOLLNER, G. & SENGER, E. 1966. A simple glare evaluation system. *Illum Eng,* 61**,** 347-352.
BOYCE, P. R. 2003. *Human factors in lighting*, Crc Press.
BOYNTON, R. M., ENOCH, J. M. & BUSH, W. R. 1954. Physical measures of stray light in excised eyes. *Josa,* 44**,** 879-886.
BULLOUGH, J., BRONS, J., QI, R. & REA, M. 2008. Predicting discomfort glare from outdoor lighting installations. *Lighting Research and Technology,* 40**,** 225-242.
CHISHOLM, C. M., EVANS, A. D. B., HARLOW, J. A. & BARBUR, J. L. 2003. New test to assess pilot's vision following refractive surgery. *Aviation, space, and environmental medicine,* 74**,** 551-559.
CHOU, B. R. 2012. The Eye and Visual System: A Brief Introduction. *Environmental Impact of Light Pollution and its Abatement***,** 3.
CIE 1983. *Discomfort Glare in the Interior Working Environment*, CIE.
CIE 1994. *Glare Evaluation System for Use Within Outdoor Sports and Area Lighting*, CIE.
CIE 1995. *Discomfort Glare in Interior Lighting*, Commission Internationale de l'Éclairage.
CLEAR, R. D. 2013. Discomfort glare: What do we actually know? *Lighting Research and Technology,* 45**,** 141-158.
COLOMBO, E., COMASTRI, S. A., ISSOLIO, L. & ECHARRI, R. 2007. Pupil light reflex produced by glare under mesopic adaptation. *Journal of Light & Visual Environment,* 31**,** 70-79.
COWEY, A. & STOERIG, P. 1995. Blindsight in monkeys. *Nature,* 373**,** 247-249.
CURCIO, C. A. & ALLEN, K. A. 1990. Topography of ganglion cells in human retina. *Journal of Comparative Neurology,* 300**,** 5-25.
DE BOER, J. B. 1967. Visual perception in road traffic and the field of vision of the motorist. *Public lighting***,** 11-96.
DE WAARD, P. W., IJSPEERT, J. K., VAN DEN BERG, T. J. & DE JONG, P. T. 1992. Intraocular light scattering in age-related cataracts. *Investigative Ophthalmology & Visual Science,* 33**,** 618-625.
DEYOE, E. A. & VAN ESSEN, D. C. 1988. Concurrent processing streams in monkey visual cortex. *Trends in neurosciences,* 11**,** 219-226.

EINHORN, H. D. 1969. A new method for the assessment of discomfort glare. *Lighting Research and Technology,* 1**,** 235-247.
EINHORN, H. D. 1979. Discomfort glare: a formula to bridge differences. *Lighting Research and Technology,* 11**,** 90-94.
ELLIS, C. J. 1981. The pupillary light reflex in normal subjects. *The British journal of ophthalmology,* 65**,** 754-759.
FISHER, A. J. & CHRISTIE, A. W. 1965. A note on disability glare. *Vision Research,* 5**,** 565-571.
FRANSSEN, L. & COPPENS, J. E. 2007. *Straylight at the retina: scattered papers*.
FRY, G. & KING, V. 1975. The pupillary response and discomfort glare. *Journal of the Illuminating Engineering Society,* 4**,** 307.
FUGATE, J. M. & FRY, G. A. 1956. Relation of changes in pupil size to visual discomfort. *Illum Eng,* 51**,** 537.
GELLATLY, A. W. & WEINTRAUB, D. J. 1990. User reconfigurations of the de Boer rating scale for discomfort glare. Ann Arbor, Michigan 48109-2150 U.S.A.: The University of Michigan, Transportation Research Institute.
GOODYEAR, B. G. & MENON, R. S. 1998. Effect of luminance contrast on BOLD fMRI response in human primary visual areas. *Journal of Neurophysiology,* 79**,** 2204-2207.
GUTH, S. K. 1951. Subjective appraisal of comfortable brightness relationships. *Am J Optom Arch Am Acad Optom,* 28**,** 468-483.
GUTH, S. K. 1952. BCD brightness ratings in lighting practice. *Illum Eng,* 47**,** 184.
GUTH, S. K. 1961. Discomfort glare. *Am J Optom Arch Am Acad Optom,* 38**,** 247-59.
GUTH, S. K. 1963. A method for the evaluation of discomfort glare. *Illum Eng,* 58**,** 351-364.
GUTH, S. K. & MCNELIS, J. F. 1961. Further data on discomfort glare from multiple sources. *Illum Eng,* 56**,** 46-47.
HAHNEMANN, D. & BEATTY, J. 1967. Pupillary responses in a pitch-discrimination task. *Perception & Psychophysics,* 2**,** 101-105.
HENNELLY, M. L., BARBUR, J. L., EDGAR, D. F. & WOODWARD, E. G. Factors affecting the integrated straylight parameter in the normal human eye. Investigative Ophthalmology & Visual Science, 1997. LIPPINCOTT-RAVEN PUBL 227 EAST WASHINGTON SQ, PHILADELPHIA, PA 19106, 4721-4721.

HENNELLY, M. L., BARBUR, J. L., EDGAR, D. F. & WOODWARD, E. G. 1998. The effect of age on the light scattering characteristics of the eye. *Ophthalmic and Physiological Optics,* 18**,** 197-203.
HOLLADAY, L. L. 1926. The fundamentals of glare and visibility. *JOSA,* 12**,** 271-319.
HOLLADAY, L. L. 1927. Action of a light-source in the field of view in lowering visibility. *JOSA,* 14**,** 1-1.
HOLLINS, M. & ALPERN, M. 1973. Dark adaptation and visual pigment regeneration in human cones. *The Journal of general physiology,* 62**,** 430-447.
HOOD, D. C., FINKELSTEIN, M. A. & BUCKINGHAM, E. 1979. Psychophysical tests of models of the response function. *Vision Research,* 19**,** 401-406.
HOPKINSON, R. G. 1956. Glare discomfort and pupil diameter. *JOSA,* 46**,** 649-656.
HOPKINSON, R. G. 1957. Evaluation of glare. *Illum Eng,* 52**,** 329-336.
HOPKINSON, R. G. 1963. *Architectural physics: lighting*, H. M. Stationery Off.
HOWARTH, P. A., HERONS, G., GREENHOUSE, D. S., BAILEY, I. L. & BERMAN, S. M. 1993. Discomfort from glare: The role of pupillary hippus. *Lighting Research and Technology***,** 37-42.
ISSOLIO, L. A., BARRAZA, J. F. & COLOMBO, E. M. 2006. Time course of brightness under transient glare condition. *JOSA A,* 23**,** 233-238.
ISSOLIO, L. A. & COLOMBO, E. M. 2006. Brightness for different surround conditions: The effect of transient glare. *Perception & Psychophysics,* 68**,** 702-709.
KAUFMAN, P. L., ADLER, F. H., LEVIN, L. A. & ALM, A. 2011. *Adler's Physiology of the Eye*, Saunders/Elsevier.
KOLB, H. *Gross Anatomy of the Eye* [Online]. Available: http://webvision.med.utah.edu/book/part-i-foundations/gross-anatomy-of-the-ey/.
KOOI, F. L. 2004. Yellow lessens discomfort glare: physiological mechanism (s). DTIC Document.
LINBERG, K. A. & FISHER, S. K. 1986. An ultrastructural study of interplexiform cell synapses in the human retina. *Journal of Comparative Neurology,* 243**,** 561-576.
LINDSAY, P. H. & NORMAN, D. A. 1977. *Human information processing: An introduction to psychology*, Academic Press.

LÖWENSTEIN, O. & FRIEDMAN, E. D. 1942. Pupillographic studies: I. Present state of pupillography; its method and diagnostic significance. *Archives of Ophthalmology,* 27**,** 969-993.
LUCKIESH, M. & GUTH, S. K. 1946. Discomfort glare and angular distance of glaresource. *Illum Eng,* 41**,** 485-492.
LUCKIESH, M. & GUTH, S. K. 1949. Brightnesses in Visual Field at Borderline Between Comfort and Discomfort (BCD). *Illum Eng,* 44**,** 650-667.
LUCKIESH, M. & HOLLADAY, L. L. 1925. Glare and visibility. *Transactions of the Illuminating engineering Society,* 20**,** 221-252.
LUCKIESH, M. & MOSS, F. K. 1942. Intrinsic brightness as a factor in discomfort from glare. *JOSA,* 32**,** 6-6.
LYNES, J. 1977. Discomfort glare and visual distraction. *Lighting Research and Technology,* 9**,** 51-52.
MAINSTER, M. A. & TURNER, P. L. 2012. Glare's causes, consequences, and clinical challenges after a century of ophthalmic study. *American journal of ophthalmology,* 153**,** 587-593.
MCCANN, B. C., HAYHOE, M. M. & GEISLER, W. S. 2011. Decoding natural signals from the peripheral retina. *Journal of vision,* 11**,** 19.
MURRAY, I. J., PLAINIS, S. & CARDEN, D. 2002. The ocular stress monitor: a new device for measuring discomfort glare. *Lighting Research and Technology,* 34**,** 231-239.
NAKA, K.-I. & RUSHTON, W. A. H. 1966. S-potentials from luminosity units in the retina of fish (Cyprinidae). *The Journal of physiology,* 185**,** 587-599.
OGAWA, S., LEE, T. M., KAY, A. R. & TANK, D. W. 1990. Brain magnetic resonance imaging with contrast dependent on blood oxygenation. *Proceedings of the National Academy of Sciences,* 87**,** 9868-9872.
OSTERBERG, G. 1935. *Topography of the layer of rods and cones in the human retina*, Nyt Nordisk Forlag.
PALMER, S. 1999. *Vision science: photons to phenomenology*, Massachusetts Institute of Technology.
PARSONS, J. H. 1910. Glare, its causes and effects. *Illum Eng***,** 99-103.
PÉREZ, G. M., MANZANERA, S. & ARTAL, P. 2009. Impact of scattering and spherical aberration in contrast sensitivity. *Journal of Vision,* 9**,** 19.

PROVENCIO, I., JIANG, G., WILLEM, J., HAYES, W. P. & ROLLAG, M. D. 1998. Melanopsin: An opsin in melanophores, brain, and eye. *Proceedings of the National Academy of Sciences,* 95**,** 340-345.

RAYNHAM, P., OSTERHAUS, W. & DAVIES, M. 2007. Mapping of Brain Functions and Spatial Luminance Distributions as Innovative Tools for Assessing Discomfort Glare in the Built Environment. *Enquiry/The ARCC Journal of Architectural Research,* 4.

REA, M. S. 2000. The IESNA lighting handbook: reference & application.

ROY, C. S. & SHERRINGTON, C. S. 1890. On the regulation of the blood-supply of the brain. *The Journal of physiology,* 11**,** 85.

RUBIÑO, M., CRUZ, A., GARCIA, J. A. & HITA, E. 1994. Discomfort glare indices: a comparative study. *Applied optics,* 33**,** 8001-8008.

RUSHTON, W. H. 1972. Visual Pigments in Man. *In:* DARTNALL, H. A. (ed.) *Photochemistry of Vision.* Springer Berlin Heidelberg.

SAENZ, M. 2007. *The Human Visual System* [Online]. Available: http://www.klab.caltech.edu/~saenz/mindscience/notes.html.

SAUR, R. L. 1969. Influence of physiological factors on discomfort glare level. *Am J Optom Arch Am Acad Optom,* 46**,** 352-7.

SCHNAPF, J. L., KRAFT, T. W. & BAYLOR, D. A. 1987. Spectral sensitivity of human cone photoreceptors. *Nature,* 325**,** 439-41.

SCHREUDER, D. A. 2008. The human observer; visual performance aspects. *Outdoor Lighting: Physics, Vision and Perception.*

SCHWARTZ, S. H. 2010. *Visual perception: A clinical orientation*, The McGraw-Hill Companies, Inc. .

STILES, W. S. 1929a. The effect of glare on the brightness difference threshold. *Proceedings of the Royal Society of London. Series B, Containing Papers of a Biological Character***,** 322-351.

STILES, W. S. 1929b. The nature and effects of glare. *Illum Eng,* 22**,** 304-312.

STILES, W. S. 1929c. The scattering theory of the effect of glare on the brightness difference threshold. *Proceedings of the Royal Society of London. Series B, Containing Papers of a Biological Character***,** 131-146.

STILES, W. S. & CRAWFORD, B. H. 1933. The luminous efficiency of rays entering the eye pupil at different points. *Proceedings of the Royal Society of London. Series B, Containing Papers of a Biological Character***,** 428-450.

STONE, P. T. 2009. A model for the explanation of discomfort and pain in the eye caused by light. *Lighting Research and Technology,* 41**,** 109-121.

STRINGHAM, J. M., GARCIA, P. V., SMITH, P. A., MCLIN, L. N. & FOUTCH, B. K. 2011. Macular pigment and visual performance in glare: benefits for photostress recovery, disability glare, and visual discomfort. *Investigative Ophthalmology & Visual Science,* 52**,** 7406-7415.

TATSUMOTO, M., EDA, T., ISHIKAWA, T., AYAMA, M. & HIRATA, K. Light of Intrinsically Photosensitive Retinal Ganglion Cell (ipRGC) Causing Migraine Headache Exacerbation. Cephalalgia, 2013. SAGE PUBLICATIONS LTD 1 OLIVERS YARD, 55 CITY ROAD, LONDON EC1Y 1SP, ENGLAND, 2-2.

THEEUWES, J., ALFERDINCK, J. W. & PEREL, M. 2002. Relation between glare and driving performance. *Hum Factors,* 44**,** 95-107.

VAN DEN BERG, T. J. T. P., FRANSSEN, L. & COPPENS, J. E. 2010. Ocular media clarity and straylight. *Encyclopedia of Eye,* 3**,** 173-183.

VAN DEN BERG, T. J. T. P., FRANSSEN, L., KRUIJT, B. & COPPENS, J. E. 2013. History of ocular straylight measurement: a review. *Zeitschrift für Medizinische Physik,* 23**,** 6-20.

VERMEULEN, D. & DE BOER, J. B. 1952. On the admissible brightness of lighting fixtures. *Applied Scientific Research, Section B,* 2**,** 85-107.

VOS, J. J. 1999. Glare today in historical perspective: Towards a new CIE glare observer and a new glare nomenclature. *Publications-commission internationale de l eclairage cie,* 133**,** 38-42.

VOS, J. J. 2003a. On the cause of disability glare and its dependence on glare angle, age and ocular pigmentation. *Clinical and Experimental Optometry,* 86**,** 363-370.

VOS, J. J. 2003b. Reflections on glare. *Lighting Research and Technology,* 35**,** 163-176.

VOS, J. J. & VAN DEN BERG, T. 1999. Report on disability glare. *CIE collection,* 135**,** 1-9.

WORDENWEBER, B., WALLASCHEK, J., BOYCE, P. & HOFFMAN, D. 2010. Automotive Lighting and Human Vision. Berlin: Springer-Verlag.